Universidade do Minho
Escola de Medicina

Ricardo Filipe Bastos Gonçalves

Investigating the neuronal ensembles encoding valence in the Laterodorsal Tegmentum

janeiro de 2023

Investigating the neuronal ensembles encoding valence in the Laterodorsal Tegmentum
Ricardo Filipe Bastos Gonçalves
UMinho | 2023

Universidade do Minho
Escola de Medicina

Ricardo Filipe Bastos Gonçalves

Investigating the neuronal ensembles encoding valence in the Laterodorsal Tegmentum

Dissertação de Mestrado
Mestrado em Ciências da Saúde

Trabalho efetuado sob a orientação da
Doutora Bárbara Guimarães Salazar Coimbra
e da
Doutora Ana João Gomes Rodrigues

janeiro de 2023

DIREITOS DE AUTOR E CONDIÇÕES DE UTILIZAÇÃO DO TRABALHO POR TERCEIROS

Este é um trabalho académico que pode ser utilizado por terceiros desde que respeitadas as regras e boas práticas internacionalmente aceites, no que concerne aos direitos de autor e direitos conexos.
Assim, o presente trabalho pode ser utilizado nos termos previstos na licença abaixo indicada.
Caso o utilizador necessite de permissão para poder fazer um uso do trabalho em condições não previstas no licenciamento indicado, deverá contactar o autor, através do RepositóriUM da Universidade do Minho.

Licença concedida aos utilizadores deste trabalho



Atribuição-NãoComercial-SemDerivações

CC BY-NC-ND

https://creativecommons.org/licenses/by-nc-nd/4.0/

Agradecimentos

Primeiramente à Doutora Bárbara Coimbra, minha orientadora, agradeço por todos os ensinamentos que me transmitiu, pelo auxílio, disponibilidade, conselhos e, acima de tudo, pela sua paciência.

À Doutora Ana João Rodrigues, minha orientadora, agradeço por me proporcionar todos os meios necessários para realizar esta dissertação. Obrigado por todo o interesse demonstrado, ideias e sugestões, pelo conhecimento partilhado e pela oportunidade de trabalhar na sua equipa.

À Carina, à Verónica, à Catarina, à Marcelina, à Natacha e a todos os meus colegas de equipa, por todos os conselhos, companhia e disponibilidade demonstrado ao longo deste ano.

Ao Carlos e às minhas amigas e colegas de mestrado, Carolina, Margarida, Sara, Rita, Patrícia e Alexandra pelos almoços prolongados, convívio e apoio durante os períodos "menos bons".

Ao grupo C2B e às pessoas da comunidade da Escola de Medicina que de alguma forma contribuíram para completar esta etapa.

Por último, obrigado aos meus pais, irmã e ao meu afilhado pelo apoio e por mostrarem interesse no meu trabalho.

O trabalho apresentado nesta tese foi realizado no Instituto de Investigação em Ciências da Vida e Saúde (ICVS), da Universidade do Minho. O apoio financeiro foi prestado através de bolsas da Fundação Bial através do projeto 175/20; do Fundo Europeu de Desenvolvimento Regional (FEDER), no âmbito do projeto PTDC/MED-NEU/29071/2017 (REWSTRESS), através do COMPETE 2020; o projeto recebeu financiamento do Conselho de investigação Europeu (ERC) sob o programa de Investigação e Inovação da União Europeia Horizonte 2020 (acordo de financiamento No 101003187); o projeto que resultou nestes resultados recebeu financiamento da Fundação "La Caixa" (ID100010434) sob o acordo LCF/PR/HR20/52400020; o projeto foi financiado por Fundos Nacionais, por meio da Fundação para a Ciência e Tecnologia (FCT) no âmbito dos projetos PTDC/MED-NEU/4804/2020, PTDC/SAL-TOX/6802/2020 (REMIND), UIDB/50026/2020 e UIDP/50026/2020; da Plataforma de Microscopia Científica do ICVS, membro da *PPBI - Portuguese Platform of Bioimaging* (PPBI -POCI-01-0145-FEDER-022122).





















STATEMENT OF INTEGRITY

I hereby declare having conducted this academic work with integrity. I confirm that I have not used plagiarism or any form of undue use of information or falsification of results along the process leading to its elaboration.

I further declare that I have fully acknowledged the Code of Ethical Conduct of the University of Minho.

Resumo

Diariamente, os indivíduos filtram a informação sensorial do ambiente que os rodeia. A atribuição de valência permite aos mamíferos concentrarem-se em estímulos salientes ao determinar se estes são recompensadores e devem ser abordados ou se são aversivos, e devem ser evitados, de forma a prosperarem e sobrevirem. O processo ativo de codificação de valência é gerado pelo sistema límbico que o traduz numa reação fisiológica e/ou comportamental. Uma pequena estrutura do tronco cerebral, o núcleo tegmental dorso-lateral (LDT), tem ganho atenção devido ao seu papel em diversos comportamentos relacionados com recompensa e aversão. O LDT é um núcleo heterogéneo sendo composto maioritariamente por células glutamatérgicas, colinérgicas e GABAérgicas. O seu papel no circuito de recompensa/aversão foi inicialmente associado ao controlo de células dopaminérgicas da área tegmental ventral (VTA). Recentemente, o nosso grupo descobriu projeções para outro elemento importante deste circuito, o núcleo accumbens (NAc). Há algumas evidências que o LDT responde a vários estímulos de valência positiva e negativa. Contudo, não se sabe ao certo que populações codificam valência e se estas populações apresentam um baixo ou alto grau de sobreposição/segregação.

Nesta dissertação, avaliámos a ativação neuronal no LDT, através de marcação de c-Fos, associados a estímulos de valência negativa (choque na pata) ou positiva (cocaína ou sacarose). Depois, usando o modelo de murganho TRAP2 (*Fos* $^{2A\text{-}iCreERT2}$), comparamos os grupos neuronais recrutados por dois eventos com valência temporalmente distintos no LDT. Utilizando o modelo, também realizamos ativação optogenética de neurónios do LDT responsivos a estímulos positivos ou negativos. Adicionalmente, analisamos anatomicamente a inervação do NAc pelas populações neuronais responsivas a estímulos provenientes do LDT.

Os nossos dados mostram que o LDT contém populações neuronais que respondem ao choque, cocaína ou sacarose, medido por uma maior densidade de células c-Fos+. Comparando os grupos neuronais, verificamos que o choque e a cocaína recrutaram maioritariamente populações celulares distintas no LDT. Adicionalmente, a ativação optogenética dos neurónios do LDT ativados por choque ou cocaína nos testes de *real time place preference* (RTPP) ou *conditioned place preference* (CPP) foi inconclusiva. Por último, as células do LDT responsivas a cocaína não mostraram inervação preferencial para nenhuma das sub-regiões do NAc. No entanto, as células do LDT responsivas a choque projetaram preferencialmente para a sub-região posterior do NAc *shell*.

Estes resultados demonstram que o LDT é um participante ativo na atribuição de sinais de valência que podem revelar princípios fundamentais sobre o processamento emocional.

Palavras-chave: ativação neuronal, estímulo negativo, estímulo positivo, núcleo tegmental dorso-lateral

Abstract

Individuals must filter the overwhelming environmental sensory information that every day surrounds them. Assigning affective valence allows mammalians to focus on salient stimuli by determining whether they are rewarding and should be approached or are aversive and should be avoided, in order to thrive and survive. The active process of valence encoding is generated by the brain's limbic system that translates it, ultimately, in a physiological and/or behavioral reaction. A small brainstem structure, the laterodorsal tegmental nucleus (LDT), has gained much attention in recent years due to its prominent role in a myriad of reward- and aversion-related behaviors. The LDT is a heterogeneous nucleus, being mainly composed by glutamatergic, cholinergic and GABAergic cells. Its role in the reward/aversion circuitry was initially attributed to the influence of this region on midbrain dopaminergic cells of the ventral tegmental area (VTA). However, recently, our group found direct projections from the LDT to another important player of the circuit, the nucleus accumbens (NAc). Moreover, there is sparse evidence showing that the LDT responds to several positive- and negative-valence stimuli. However, it is not known which neuronal populations encode valence and if these populations are segregated or overlap.

In this thesis we studied cell activation following negative- (footshock) and positive-valence stimuli (cocaine and sucrose) in the LDT using c-Fos immunolabelling. Then, using the TRAP2 (*Fos* $^{2A\text{-}iCreERT2}$) mouse model, we evaluated in the same subject the neuronal ensembles activated by temporally distinct valence-containing events. Using this model, we also performed optogenetic activation of positive or negative stimulus-responsive neurons in the LDT. Furthermore, we analyzed the pattern of NAc innervation of these LDT responsive ensembles.

Our data shows that the LDT contains neuronal populations that respond to shock, cocaine or sucrose, measured by a higher c-Fos+ cell density in comparison to controls. Analyzing the responsive ensembles, we verified that shock and cocaine recruited mainly distinct cell populations in the LDT. The assessment of behavioral phenotype in the real time place preference (RTPP) or conditioned place preference (CPP) tasks to optogenetic activation of footshock- or cocaine-responsive neurons in the LDT was inconclusive. The NAc innervation analysis revealed that cocaine-responsive cells do not appear preferentially innervate different subregions of the NAc. Conversely, shock-responsive LDT cells projected preferentially to the posterior shell subregion of the NAc.

These results provide evidence that the LDT is an active participant in assignment of valence signals that could reveal fundamental principles about emotional processing.

Key words: laterodorsal tegmentum, negative stimulus, neuronal activation, positive stimulus

Table of contents

DIREITOS DE AUTOR E CONDIÇÕES DE UTILIZAÇÃO DO TRABALHO POR TERCEIROS i
Agradecimentos ii
STATEMENT OF INTEGRITY iii
Resumo iv
Abstract v
List of abbreviations and acronyms viii
List of figures xii
List of tables xiii
1. Introduction 1
1.1. Affective valence 3
1.2. Reward: natural and drugs of abuse 4
1.3. Aversion: fear, anxiety and disgust 5
1.4. Studying the brain's valence circuitry 5
1.5. Laterodorsal Tegmentum (LDT) 9
1.5.1. Neuroanatomy 9
1.5.2. LDT connectivity 11
1.5.3. LDT in reward and aversive behaviors 12
1.5.3.1. LDT in Reward-related behaviors 16
1.5.3.1.1. Lesion and pharmacological studies 17
1.5.3.1.2. Optogenetic/chemogenetic studies 18
1.5.3.2. LDT in Aversion-related behaviors 20
1.6. Open questions in the field 22
2. Objectives 23
3. Materials and Methods 24
3.1. Animals 24
3.2. Drug treatments 24
3.3. Stereotaxic surgery: LDT viral injection and cannula implantation 25
3.4. Behavior 25
3.4.1. Apparatus 25
3.4.2. LDT recruitment by positive and negative valence stimuli 26
3.4.2.1. Endogenous c-Fos neural labelling experiment 26

3.4.2.2. TRAPing and neural labelling of two distinct stimuli experiment 27
3.4.3. Optogenetic manipulation of valence-responsive LDT ensembles 27
3.4.3.1. Real Time Place Preference 28
3.4.3.2. Conditioned Place Preference 28
3.4.3.3. Optical stimulation 29
3.5. Histology 29
3.5.1. Sacrifice and sectioning 29
3.5.2. Immunofluorescence (IF) 30
3.5.3. Image acquisition and analysis 30
3.6. Statistical analysis 32
4. Results 33
4.1. Identification of Reward- or Aversion-responsive LDT neuronal ensembles 33
4.2. Overlap/segregation of LDT ensembles representing distinct valence events 36
4.2.1. Positive control for valence encoding: Amygdala 39
4.2.2. TRAPing of LDT ensembles responsive to negative- and positive-valence stimuli 41
4.2.3. LDT ensembles representing distinct valence events 45
4.3. Optogenetic modulation of LDT-responsive ensembles 47
4.4. NAc innervation of LDT ensembles responsive to valence stimuli 49
5. Discussion, conclusion and future perspectives 58
5.1. Discussion 58
5.1.1. Recruitment of LDT ensembles upon exposure to negative vs. positive valence stimuli 58
5.1.2. Overlap of LDT ensembles responsive to negative and positive valence stimuli 61
5.1.3. Optogenetic stimulation of LDT shock- or cocaine-responsive ensembles 63
5.1.4. NAc innervation by LDT shock- or cocaine-responsive ensembles 65
5.2. Conclusion 66
5.3. Future perspectives 68
6. References 69
7. Annexes 105

List of abbreviations and acronyms

4-OHT: 4-hydroxytamoxifen

AAV5: Adeno-associated virus 5

ACC: anterior cingulate cortex

ACh: acetylcholine

AMPA: α-amino-3-hydroxy-5-methyl-4-isoxazolepropionic acid

Amy: amygdala

ANOVA: analysis of variation

AP: anterior-posterior

Bar: Barrington's nucleus

BLA: basolateral amygdala

CA1: cornu ammonis 1

CeA: central amygdaloid nucleus

CFC: context fear conditioning

Ch6: cholinergic group 6

ChAT: choline acetyltransferase

ChR2: channelrhodopsin-2

CnF: cuneiforme nucleus

CPA: conditioned place aversion

CPP: conditioned place preference

CreER: Cre-recombinase

CRH: corticotropin-releasing hormone

DA: dopamine

DAPI: 4',6-diamidino-2-phenylindole

DBB: Diagonal Band of Broca

DG: dentate gyrus

DGAV: Direção-Geral de Alimentação e Veterinária

Dox: doxycycline

DREADDS: designer receptors exclusively activated by designer drugs

DRN: dorsal raphe nucleus

DTg: dorsal tegmental nucleus

DV: dorsal-ventral

EF1: elongation factor 1

EPM: elevated plus maze

ER: estrogen receptor

FBS: fetal bovine serum

FELASA: Federation of European Laboratory Animal Science Associations

fMRI: functional magnetic resonance imaging

GABA: gama-aminobutyric acid

GAD: glutamic acid decarboxylase

GFP: green fluorescent protein

Gi: gigantocellular reticular

GLP-1: glucagon-like peptide 1

GLP-1R: glucagon-like peptide receptor 1

GP: globus pallidus

Hb: habenula

HYP: hypothalamus

i.p.: intra peritoneal

IC: inferior colliculus

iCreERT2: tamoxifen-inducible Cre recombinase

ICSS: intracranial self-stimulation

ICVS: Life and Health Sciences Research Institute

IEG: immediate early gene

IF: immunofluorescence

IPN: interpeduncular nucleus

LC: locus coeruleus

LDT: laterodorsal tegmentum

LHb: lateral habenula

M2/4: muscarinic type 2/4

mAChRs: muscarinic acetylcholine receptors

MDD: major depressive disorder

ML: medial-lateral

MnPO: median preoptic nucleus

mPFC: medial prefrontral cortex

MS: medial septum

NAc: nucleus accumbens

nAChRs: nicotinic acetylcholine receptors

NMDA: N-methyl-D-aspartate

NpHR: halorhodopsin

NTS: nucleus tractus solitarius

OFC: orbitofrontal cortex

OP: open field

PAG: periaqueductal gray

PBS-T: phosphate buffered saline with 0.3 % Triton-X100

PBS: phosphate buffered saline

PCG: pontine central grey

PFA: paraformaldehyde

PFC: prefrontal cortex

Pn: pontine reticular

PPE: personal protection equipment

PPN: pedunculopontine Tegmentum

PR: progressive ratio

PV+: parvalbumin-positive

RAS: reticular activating system

REM: rapid eye-movement

RT: room temperature

RTPP: real-time place preference

SC: superior colliculus

SEM: standard error of the mean

SN: substantia nigra

SOM+: somatostatin-positive

STN: subthalamic nucleus

SUD: substance use disorder

TetTag: tetracycline-controlled transcriptional activation

TH: thalamus

TRAP: targeted recombination in active populations

TRE: tetracycline inducible expression

tTA: tetracycline-controlled transactivator

UNC: university of North Carolina

US: unconditioned stimuli

V4: fourth ventricule

vGluT2: vesicular glutamate transporter 2

VP: ventral pallidum

VTA: ventral tegmental area

WT: wild-type

YFP: yellow fluorescent protein

List of figures

Figure 1- Affective valence 1
Figure 2- Simplified valence circuitry 8
Figure 3- LDT cells are recruited in negative and positive valence events 35
Figure 4- TRAP system 37
Figure 5- Experimental design of the TRAPing and overlap of LDT ensembles representing distinct valence events experiment 38
Figure 6- Amygdala recruitment for negative and positive stimuli is detected by TRAPing 40
Figure 7- LDT recruitment for negative and positive events is detected by TRAPing 42
Figure 8- LDT recruitment for negative and positive events - endogenous c-Fos 44
Figure 9- Shock and cocaine mainly recruit segregated ensembles in the LDT 46
Figure 10- Optogenetic manipulation of LDT shock- and cocaine-responsive ensembles 48
Figure 11- Quantification of innervation of the NAc by LDT positive and negative-responsive cells 52

List of tables

Table 1- Summary of main findings implicating the LDT in valence-associated behaviors. 13

Table 2 - Antibody information for all immunofluorescence protocols used. 30

Table 3 - Mixed effects models statistical report. 52

Table 4 - Summary of the main results obtained by evaluating neuronal activation after exposure to negative- and positive-valence stimuli via c-Fos labelling or TRAPing, overlap of shock- and cocaine-ensembles and NAc innervation by these two ensembles. 67

1. Introduction

Every day individuals are overwhelmed with sensory information. Remarkably, we can filter the information by focusing on stimuli that predict something good or bad. Organisms do so by assigning affective valence to stimuli and rapidly respond to the dynamic surroundings in an adaptive manner (Tye, 2018). Valence refers to the degree of which an emotional experience is rewarding/pleasurable (positive valence) or aversive/unpleasant (negative valence). In other words, it is the quality of a stimulus or event of being perceived as 'good' or 'bad' by an individual (Berridge, 2019; Tye, 2018). Valence has both a hedonic (pleasure vs displeasure state) and motivational aspects, such that, rewarding stimuli support approach-motivated behaviors (behavior repetition) whereas aversive ones support avoidance-motivated behaviors (behavior extinction) (**Figure 1**) (Guitart-Masip *et al.*, 2014; Tye, 2018). Some environmental stimuli have innate valence, meaning that, no prior experience is required to elicit a behavior output/response to them (Tye, 2018) while others, are initially neutral and require learning to form associations between the stimuli and their motivationally significant outcomes (Mori and Sakano, 2022; Pavlov (1927), 2010).

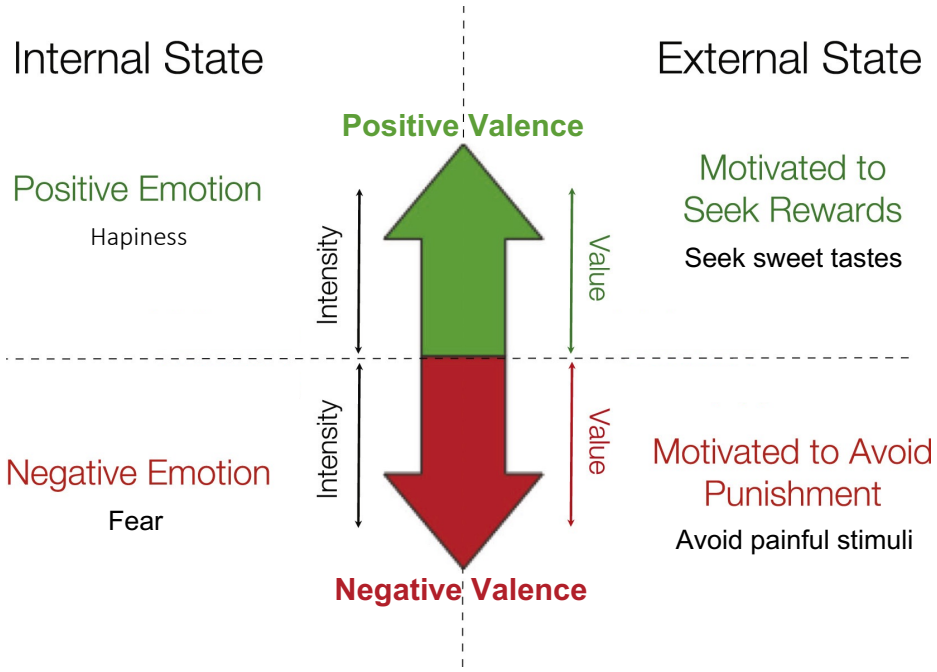


Figure 1- Affective valence. Affective valence refers to the "sign" of the internal state, either positive (depicted as green) representing rewarding states that support approach behavior, or negative (depicted as red) representing aversive ones that support avoidance behavior. Value tracks the worth of external stimuli (salience) and intensity indicates the absolute value of the strength of an internal state (arousal). Based on (Tye, 2018).

Dysfunction in valence encoding has been associated with neuropsychiatric disorders characterized by low hedonic tone (low capacity to experience pleasure) and motivational deficits/dysregulation, such as major depressive disorder (MDD) and substance use disorder (SUD) (Bressan and Crippa, 2005;

Cooper *et al.*, 2017; Heshmati and Russo, 2015; Russo and Nestler, 2013; Scheres *et al.*, 2007; Sternat and Katzman, 2016; Wang *et al.*, 2021). It is, therefore, of utmost importance to study the brain circuits, regions and cellular mechanisms involved in valence encoding to better understand the pathophysiology of these affective disorders to potentially reveal new therapeutic targets (Heshmati and Russo, 2015; Schlaepfer *et al.*, 2014).

Classically, the so called dopamine (DA) mesoaccumbal pathway, also known as the reward pathway (projections from the ventral tegmental area (VTA) to Nucleus Accumbens (NAc)), has been shown to be crucial for the processing of behaviorally-relevant stimuli, by assigning reward/aversive properties to them, and for motivated behaviors (Joshua *et al.*, 2009; Montague *et al.*, 2004; Schultz, 2013; Tsai *et al.*, 2009; Wise, 2004; Yokel and Wise, 1975).

In recent years, the valence brain circuitry is being dissected by taking advantage of electrophysiological, optogenetic/chemogenetic and brain imaging techniques paired with new transgenic models and viral approaches. Several brain regions have shown to causally respond to rewarding (natural or drugs of abuse) and/or aversive events, such as the NAc (Bobadilla *et al.*, 2020; Roitman *et al.*, 2005)), VTA (Brischoux *et al.*, 2009; Coizet *et al.*, 2006), prefrontal cortex (PFC); (Coley *et al.*, 2021; Ye *et al.*, 2016) and the amygdala (Amy); (Gore *et al.*, 2015; Grewe *et al.*, 2017; Zhang and Li, 2018). Furthermore, artificial manipulation of general or population/type-specific projections to/from these regions has shown to modulate different modalities of valence encoding (Al-Hasani *et al.*, 2021; Coimbra *et al.*, 2021; Lammel *et al.*, 2012; Soares-Cunha *et al.*, 2022, 2020).

The laterodorsal tegmentum (LDT), also known as laterodorsal tegmental nucleus, appears to be an important player in rewarding/aversive behaviors, though this brain region has been overlooked in the field. First, LDT sends modulatory inputs to the VTA (Lammel *et al.*, 2012; Lester *et al.*, 2008; Lodge and Grace, 2006; Nelson *et al.*, 2007). Second, recently the LDT was also shown to directly project to the NAc, influencing positive reinforcement and motivated behaviors (Coimbra *et al.*, 2019; Dautan *et al.*, 2014). In addition to positive valence, the LDT has been implicated in negative valence processing (Wolfman *et al.*, 2018; Yang *et al.*, 2016). Lastly, according to its connectivity to several regions of the valence circuitry, namely PFC, VTA and NAc, it is on a privileged position to potentially modulate several components of this circuit.

In the following sections, we will briefly focus on valence encoding in different brain regions that have shown connections to the LDT and then explore the current knowledge about the LDT and its role in rewarding/aversive behaviors.

1.1. Affective valence

A fundamental task of the mammalian brain is to assign emotional/motivational valence to environmental stimuli by determining whether they are rewarding and should be approached or are aversive and should be avoided. Valence must be actively generated by the brain's limbic system and translated into hedonic, emotional and/or motivational reactions (i.e. valence processing/encoding) that can result, ultimately, in an affective physiological and/or behavioral reaction (Berridge, 2019, 2018). In an evolutionary point of view, valence encoding allowed animals to survive, thrive and adapt in an ever-changing environment, supporting primal behaviors like pursuing food or reproduction (Anderson and Adolphs, 2014; Berridge and Kringelbach, 2008) or avoiding dangerous circumstances/engage in defensive behaviors due to predation or harmful stimuli (Tovote *et al.*, 2015). In fact, similar basic emotional mechanisms (with an objective/external response) are conserved across animal species, including humans (Adolphs and Anderson, 2018; Anderson and Adolphs, 2014). However, in humans, a more subjective, intangible component of emotion can be found (Anderson and Adolphs, 2014), remaining the question if emotions are experienced in the same way by humans and other animals (Tye, 2018).

For the scope of this dissertation, we will not go further into emotion theories, and emotions will be regarded as 'an internal state that is caused by external or internal stimuli and that underlies a specific set of measurable (i.e. can be studied), behavioral, physiological, hormonal and autonomic reactions' (Tye, 2018). Nevertheless, other concepts, like salience and arousal, often present in those theories (Adolphs and Anderson, 2018), must be explained, as they are necessary to characterize the properties of stimuli and their influence on the individuals.

Salience is considered as the intensity of perception of a stimulus, meaning its property to be recognized as motivationally-relevant and induce an affective response in an individual (Uddin, 2015), whereas arousal is associated with increased activation and awareness of the individual to a given event /stimulus (Critchley *et al.*, 2013), being able to influence salience (Lee *et al.*, 2020). Important to note that both rewarding and aversive stimuli can be salient and have the capacity to arouse (Lang, 1995; Tye, 2018).

Valence involves both innate and learned aspects. Some stimuli, called unconditioned stimuli (US), have innate valence because with no prior exposure, they can elicit an affective responses (Adolphs and Anderson, 2018; Pavlov (1927), 2010). Bitter tastants, like quinine, generally signal toxicity, triggering disgust, whereas shadows overhead may signal a predator approaching, triggering fear and defensive responses (Adolphs and Anderson, 2018). In addition, previously neutral stimulus can acquire

valence when presented/paired with a negative or positive outcome, the so-called Pavlovian conditioning (Anderson and Adolphs, 2014; Pavlov (1927), 2010), for example licking in response to a light repeatedly combined with food reward presentation.

Importantly, valence is flexible, as affective reactions can be modified by factors that alter the hedonic impact of a certain stimulus, including physiological factors (such as hunger and/or satiety states), psychological factors (learned preferences and/or aversions) and neurobiological manipulations (such as neural inhibition or stimulation) (Berridge and Kringelbach, 2015).

1.2. Reward: natural and drugs of abuse

It is important to note that reward, commonly used as a synonym of a pleasant stimulus, is complex and is composed of several components that correspond to distinguishable neurobiological mechanisms that have been shown to be mediated by partly dissociable brain substrates (Berridge and Kringelbach, 2008). 'Liking' represents the actual pleasure component or hedonic impact of a reward, 'wanting' the motivation for reward and learning corresponds to associations, representations and predictions about future rewards based on past experiences (Berridge and Kringelbach, 2008; Morales and Berridge, 2020; Olney *et al.*, 2018). Understanding how different brain systems play distinct roles in the composite of reward may have important implications in designing specialized therapeutic strategies to reverse or compensate particular types of psychopathological dysfunction found in psychiatric disorders (Berridge and Kringelbach, 2008; Olney *et al.*, 2018).

Food is one of the most universal pleasant stimuli and one of the most accessible experimental methods to study the neuroscience of reward processing (Adolphs and Anderson, 2018; Kringelbach, 2005; Peciña *et al.*, 2006; Small *et al.*, 2001). Beyond food, sexual and social interactions are another natural reward (Berridge and Kringelbach, 2008; Prieto-Garcia *et al.*, 2015; Vestlund and Jerlhag, 2020). All of these are somehow related to the evolutionary need to survive and propagate the individual's genetic information.

Drugs of abuse are, however, other types of reward that are viewed as usurpers of the brain systems that evolved to respond to natural rewards (Berridge and Kringelbach, 2008). In drug addiction, reward seeking becomes maladaptive, in the sense that subjects lose control over drug use and expend considerable amounts of time and energy directed toward attaining and using the drug of abuse, sacrificing their well-being and, therefore, endangering survival (Koob, 2009; Roberts *et al.*, 2007). While drug and natural rewards involve overlapping brain nuclei (Hadad and Knackstedt, 2014; Pfarr *et al.*, 2018; Volkow and Morales, 2015), differences in cell or circuit recruitment for drugs of abuse *versus*

natural reward-related behaviors, like reward-seeking, may be found in animal studies (Bobadilla *et al.*, 2020; Cameron and Carelli, 2012; Carelli *et al.*, 2000; Kane *et al.*, 2020; Nall *et al.*, 2021).

1.3. Aversion: fear, anxiety and disgust

Animals evolved to avoid stimuli that are potentially harmful to the body, including toxins, predators and mechanical stressors. Therefore, the brain has dedicated systems to allow the animal to recognize environments and respond to stimuli that may expose one to such harmful agents (LeDoux, 2012). Such events, elicit negative internal states like fear, anxiety and disgust (Russell, 1980), that underlie a specific set of measurable behavioral (like freezing, fleeing/escape and vocalizations), physiological, hormonal and autonomic responses (Da *et al.*, 2019; De Franceschi *et al.*, 2016; Tovote *et al.*, 2015). Fear is elicited upon factual, acute sensory perception of a threat, whereas anxiety can be evoked by potential, circumstantial and anticipated threats, *i.e.* in the absence of an immediate threat (for example, open and well illuminated spaces in where animals might be more vulnerable) (Davis *et al.*, 2010; Grupe and Nitschke, 2013; LeDoux, 2014). Evidence suggests that the central mechanisms underlying fear and anxiety states are mediated by partially overlapping neuronal substrates (Tovote *et al.*, 2015). In addition, disgust, which can be elicited by bitter-tasting substances (Tanaka *et al.*, 2021a), is primarily related to contamination and represents a possible danger of contracting disease (Cisler *et al.*, 2009; Oaten *et al.*, 2009). Several studies have demonstrated that fear and disgust exert different effects on brain functions like sensory perception, attention and memory and on physiological or autonomic functions (Carretié *et al.*, 2011; Chapman *et al.*, 2013; Cisler *et al.*, 2009; Xu *et al.*, 2015).

While some responses to noxious stimuli are innate (Fanselow, 2018), others are developed through learning like aversive/negative Pavlovian conditioning and instrumental aversive learning (positive punishment learning and active avoidance and escape learning) (Jean-Richard-Dit-Bressel *et al.*, 2018; LeDoux and Daw, 2018). A punishment refers to an adverse outcome of an action (commonly used punishers include footshock, airpuff and quinine), and it suppresses the future expression of that behavior. In contrast, during active avoidance and escape learning, an animal learns to take an action in order to avoid an aversive stimulus, thus the behavior frequency increases (also known as negative reinforcement) (Jean-Richard-Dit-Bressel *et al.*, 2018).

1.4. Studying the brain's valence circuitry

To study valence encoding, researchers have been using different strategies for characterizing neuronal activity patterns in response to positive or negative valence stimuli, cues predicting those stimuli and changes in stimuli-associations contingency. The development of optogenetics/chemogenetics and

new transgenic models, allowed to casually link the activity of specific neuronal ensembles with rewarding or aversive responses. More recently, the use of calcium and neurotransmitter imaging has been enabling the alignment of neuronal activity and/or neurotransmitter signaling with valence-related behaviors.

It is important to note that, to study reward and aversion in rodent models, behavioral tasks have been developed. Place preference tests are typical paradigms used to evaluate the rewarding or aversive properties of stimuli. The conditioned place preference (CPP) test is based on passive Pavlovian/classical conditioning, in which animals learn to associate a specific chamber/context with an emotionally relevant stimuli, such as a drug or optogenetic manipulation of a given brain region (*i.e.* the context acquires incentive value). After training/conditioning, depending on whether the manipulation was rewarding or aversive, the context itself, in the absence of the stimulus, can elicit either approach or avoidance from the environment, respectively (Bardo and Bevins, 2000; Tzschentke, 2007). On the other hand, the real-time place preference (RTPP) paradigm measures place preference on an immediate timeframe and in a contingent manner, in which the subject can trigger and stop stimulation, allowing to assay if a specific neuronal stimulation is perceived acutely as rewarding or aversive (Bimpisidis *et al.*, 2020). In addition, operant conditioning, in which the subject must learn that a contingent action, like lever-pressing, leads to a certain outcome, is also widely used to study the reinforcing/motivating properties of stimuli. Operant training has been expanded to include instrumental learning for optogenetic or pharmacological self-stimulation (Carlezon and Chartoff, 2007; Negus and Miller, 2014).

Over the years, several brain regions have been associated with valence representation/encoding, including the NAc (Bobadilla *et al.*, 2020; Castro *et al.*, 2021; Nieh *et al.*, 2016; Roitman *et al.*, 2005), VTA (Brischoux *et al.*, 2009; Cohen *et al.*, 2012; Coizet *et al.*, 2006; Del Arco *et al.*, 2020; Matsumoto and Hikosaka, 2009; Nieh *et al.*, 2016), PFC (Coley *et al.*, 2021; Del Arco *et al.*, 2020; K Namboodiri *et al.*, 2021; Niedringhaus and West, 2022; Rawls and Lamm, 2021; Schoenbaum *et al.*, 1999; Ye *et al.*, 2016), Amy (Fadok *et al.*, 2018; Gore *et al.*, 2015; Grewe *et al.*, 2017; Mori and Sakano, 2022; Paton *et al.*, 2006; Shabel and Janak, 2009; Zhang *et al.*, 2021; Zhang and Li, 2018), hippocampus (Herbst *et al.*, 2022; Jarzebowski *et al.*, 2022; Jimenez *et al.*, 2020; Kim and Cho, 2020), ventral pallidum (VP; (Stephenson-Jones *et al.*, 2020)), lateral Habenula (LHb; (Lecca *et al.*, 2020; Stamatakis and Stuber, 2012)), interpeduncular nucleus (IPN; (McLaughlin *et al.*, 2017; Sherafat *et al.*, 2020)), locus coeruleus (LC; (Bouret and Richmond, 2015; Hofmeister and Sterpenich, 2015; McCall *et al.*, 2015)), dorsal raphe nucleus (DRN; (Cohen *et al.*, 2015)) and the LDT (Baur *et al.*, 2018; Ishibashi *et al.*, 2009; José Lança *et al.*, 2000; Lambert *et al.*, 2017; Liu *et al.*, 2009; Yang *et al.*, 2016), amongst others (**Figure 2**).

The VTA and NAc, two key regions of the valence circuitry, have long been known to play a fundamental role in assignment of reward to stimuli and positive reinforcement of behaviors (reward learning) required for the continuation of the species, such as sex (Damsma *et al.*, 1992), social interactions (Hansen *et al.*, 1993), and consumption of food (Castro *et al.*, 2021; Kiyatkin and Gratton, 1994). In previous studies, the mesoaccumbal pathway had already been implicated in assigning reward to drugs of abuse (Yokel and Wise, 1975). In fact, the majority of drugs of abuse was shown to increase the levels of DA in the NAc (Di Chiara and Imperato, 1988). This and other studies manipulating DA signaling from VTA to NAc, lead researchers to propose the activation of DA neurons of the VTA, with subsequent release of DA in downstream targets, like the NAc, as a central mechanism for the rewarding/reinforcing effects of drugs of abuse (Di Chiara and Imperato, 1988; Druhan *et al.*, 1990; Pascoli *et al.*, 2015; Pierce and Kumaresan, 2006; Robledo *et al.*, 1992; Tsai *et al.*, 2009; White *et al.*, 1991). In addition, these two regions are also engaged in negative stimuli and aversion related-processes (Al-Hasani *et al.*, 2015; Badrinarayan *et al.*, 2012; Brischoux *et al.*, 2009; Lammel *et al.*, 2012; Soares-Cunha *et al.*, 2020; Tan *et al.*, 2012; Xiu *et al.*, 2014). The amygdala, a structure extensively studied in emotional processing, is also known to react to both positive and negative valence stimuli, being associated with reward-related mechanisms, like reward learning, as well as fear processing and aversive learning (Gore *et al.*, 2015; Kim and Cho, 2020; Schoenbaum *et al.*, 1999; Zhang and Li, 2018). Likewise, other areas like the PFC (Cummings *et al.*, 2022; Kamii *et al.*, 2017; Vander Weele *et al.*, 2018; Ye *et al.*, 2016) and LC (Bouret and Richmond, 2015; McCall *et al.*, 2015) have shown to mediate both reward and aversion as well.

Thus, positive and negative valence appear to be represented concurrently in some brain regions and whether these brain regions contain a largely distinct or overlapping populations of neurons representing the opposite valences is a current subject of investigation. Recently, efforts are being made to understand if these co-existing neuron populations are distinguishable in terms of genetics, anatomy (*i.e.* connectivity or spatial organization) or functionality/activity in response to stimuli (nicely reviewed in (Namburi *et al.*, 2016)).

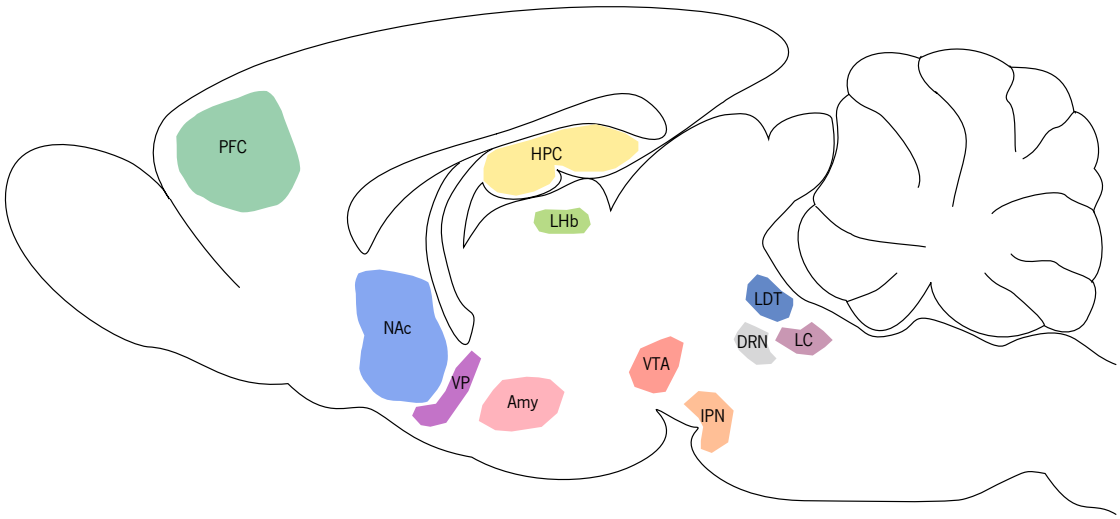


Figure 2- Simplified valence circuitry. Schematic sagittal representation of the main regions involved in valence and reward/aversion. Localization across the mediolateral axis, size and shape are adjusted for simplicity and representation purposes. Amy – Amygdala; DRN – Dorsal Raphe Nucleus; HPC – Hippocampus; IPN – Interpeduncular Nucleus; LC – Locus Coeruleus; LDT - Laterodorsal Tegmental Nucleus; LHb – Lateral Habenulla; NAc – Nucleus Accumbens; PFC – Prefrontal Cortex; VP – Ventral Pallidum; VTA – Ventral Tegmental Area. Adapted from (Paxinos and Franklin, 2001).

1.5. Laterodorsal Tegmentum (LDT)

The LDT is a heterogeneous pontine nucleus, conventionally defined by the outline of the cholinergic neuron population and known as the cholinergic group 6 (Ch6) (Mesulam *et al.*, 1983). Together with the Pedunculopontine Tegmentum (PPN), a neighboring and similar structure, they form the brainstem cholinergic system (Kobayashi *et al.*, 2003). LDT neurons expressing choline acetyltransferase (ChAT), which synthetizes acetylcholine (ACh), are found in humans (Mesulam *et al.*, 1989), non-human primates (Calvey *et al.*, 2015; Satoh and Fibiger, 1985; Williams *et al.*, 2022), cats (Jones and Beaudet, 1987; Vincent and Reiner, 1987), rodents (Armstrong *et al.*, 1983) and other animals (Bux *et al.*, 2010; Mahady *et al.*, 2017; Marcos and Coveñas, 2021). However, this nucleus also contains glutamate- and gama-aminobutyric acid (GABA)-expressing neurons (Luquin *et al.*, 2018; Wang and Morales, 2009). Classically, this nucleus has been implicated in rapid eye-movement (REM) sleep, sleep-wake cycle and states of arousal however, more recently, has been involved in rewarding/aversive behaviors (Coimbra *et al.*, 2019; Kohlmeier, 2013; Kohlmeier and Polli, 2020; Lammel *et al.*, 2012; Nelson *et al.*, 2007; Steidl *et al.*, 2017b).

1.5.1. Neuroanatomy

The LDT is a small nucleus borded dorsally by the fourth ventricule (V4) and ventrally by the cerebropontine formation and its positioned caudally to the PPN, in the pontine central gray (Cornwall *et al.*, 1990; Maley *et al.*, 1988; Mesulam *et al.*, 1983), forming an continuum of cholinergic neurons that extends from the caudal border of the substantia nigra (SN) to the lateral part of the central gray matter, in the periventricular area near the border of V4 (Armstrong *et al.*, 1983). At the caudal end, the LDT is located medially by the Dorsal Tegmental Nucleus (DTg) and laterally by the Barrington's nucleus (Bar) and the LC (Paxinos and Franklin, 2001).

Curiously, although the LDT is known as a cholinergic structure, it contains, in higher number, glutamatergic (Clements and Grant, 1990; Lavoie and Parent, 1994a) and GABAergic cells (Ford *et al.*, 1995), intermingled among each other. Vesicular glutamate transporter 2 (vGluT2)- and glutamic acid decarboxylase (GAD; synthesizes GABA)-positive populations represent, respectively, 40 % and 38 %, while ChAT+ cells represent 22 % of total cells (Wang and Morales, 2009). More recent stereological estimations point to 46 % of total cells to be GABAergic, 32 % glutamatergic and 22 % cholinergic cells (Luquin *et al.*, 2018; Pereira *et al.*, 2020). Moreover, an antero-posterior distribution of the most prevalent population was reported: the rostral portion was more concentrated in vGluT2+ cells, the medial, despite showing the highest concentration of ChAT+ cells of the three subdivisions, had a similar proportion of the three

populations, and the caudal end presented more GAD+ cells (Wang and Morales, 2009). Contributing to this heterogeneity, evidence suggests that, within the same neurochemical population there may be different expression profiles of neurotransmitter receptors, hinting potentially distinct functional roles, as it is the case of GABAA and GABAB receptors (Luquin *et al.*, 2022).

Initial studies claimed that GABA or glutamate could co-express in a subset of the population of cholinergic LDT cells (Clements *et al.*, 1991; Jia *et al.*, 2003; Lavoie and Parent, 1994b) and, in fact, cholinergic neurons from different brain regions are suggested to corelease either glutamate or GABA together with ACh (Allen *et al.*, 2006; Kljakic *et al.*, 2017; Ren *et al.*, 2011; Saunders *et al.*, 2015). However, more recent data has questioned this and it is currently believed that the GABAergic, glutamatergic and cholinergic neurons represent mostly distinct populations, as only around 2-5 % of ChAT+ LDT cells co-expressed either vGluT2 or GAD (Luquin *et al.*, 2018; Steinkellner *et al.*, 2019; Wang & Morales, 2009). Interestingly, using a genetic fate-mapping strategy, it was found that around 90 % of cholinergic LDT cells expressed VGluT2 at some point during development (Steinkellner *et al.*, 2019).

1.5.2. LDT connectivity

With the use of tracers and viral tracing strategies, the connectivity of the laterodorsal tegmentum has been identified, revealing an extensive connectivity with numerous brain regions including the cortex, basal ganglia, forebrain, thalamus, hypothalamus, midbrain, and upper and lower brainstem.

Afferents have been identified originating in the cortex, namely the medial prefrontral cortex (mPFC), orbital frontal (OFC), anterior cingulate (ACC) and motor cortices, and sourcing in the basal ganglia, specifically the NAc, substantia nigra (SN), VP and also in the VTA (Bueno *et al.*, 2019; Cornwall *et al.*, 1990; Hoover and Vertes, 2011; Huerta-Ocampo *et al.*, 2021; Satoh and Fibiger, 1986; Semba and Fibiger, 1992; Souza *et al.*, 2022; Takagishi and Chiba, 1991; Terreberry and Neafsey, 1987; Vertes, 2004; Wang *et al.*, 2019; Zhao *et al.*, 2022). Other areas that project to the LDT include the Amy, Thalamus (TH), Hypothalamus (HYP), Habenula (Hb), Superior and Inferior colliculi (SC and IC, respectively), Cuneiforme Nucleus (CnF) and Periaqueductal gray (PAG) (Bueno *et al.*, 2019; Huerta-Ocampo *et al.*, 2021; Satoh and Fibiger, 1985; Semba and Fibiger, 1992; Wang *et al.*, 2019; Zhao *et al.*, 2022). The LDT also receives inputs from the Raphe Nucleus, LC, IPN, DTg, PPN, Pontine Central grey (PCG), Pontine reticular (Pn), Gigantocellular reticular (Gi), Vestibular nuclei and Nucleus Tractus Solitarius (NTS) (Bueno *et al.*, 2019; Hernandez *et al.*, 2021; Huerta-Ocampo *et al.*, 2021; Shi *et al.*, 2021; Wang *et al.*, 2019; Zhao *et al.*, 2022). These findings suggest that the LDT is a link for relaying signals from basal ganglia and sensory structures, possibly influencing thalamic circuits that transmit feed-forward information to basal ganglia and cortical circuits. Noteworthy, cell-type afferent-specificity has been demonstrated, for instance, cortical areas were found to preferentially project to glutamatergic LDT cells, the amygdala innervated more intensely the somatostatin-positive (SOM+) GABAergic cells, while the hypothalamus projected more to glutamatergic and parvalbumin-positive (PV+) GABAergic cells. In addition, all cell types of the LDT receive local innervation, being particularly evident for PV+ GABAergic cells (Wang *et al.*, 2019).

The LDT neurons send rich ascending and descending fibers to the whole brain. The LDT has shown to project to the PFC and basal ganglia, namely dorsal striatum and NAc, VP, SN, Globus Pallidus (GP), Subthalamic nucleus (STN) and also to VTA (Bolam *et al.*, 1991; Clarke *et al.*, 1987; Coimbra *et al.*, 2019; Cornwall *et al.*, 1990; Dautan *et al.*, 2020, 2016a, 2016b, 2014; Gould *et al.*, 1989; Holmstrand *et al.*, 2010; Holmstrand and Sesack, 2011; Oakman *et al.*, 1995; Satoh and Fibiger, 1986; Woolf and Butcher, 1986; Zhao *et al.*, 2022). Importantly, the LDT, together with the PPN, is the only source of acetylcholine input to the VTA, and thus, to the mesoaccumbal pathway (Dautan *et al.*, 2016b). However, only the LDT was shown to modulate the activity of mesoaccumbal/NAc-projecting neurons (DA

and non-DA neurons) (Dautan *et al.*, 2016b). Other areas that receive LDT innervation include TH, Amy, HYP, Medial Septum (MS), Diagonal Band of Broca (DBB), Hb, SC, LC, IPN and Raphe nucleus (Bueno *et al.*, 2019; Cornwall *et al.*, 1990; Huerta-Ocampo *et al.*, 2021, 2020; Parent and Descarries, 2008; Steriade *et al.*, 1988; Woolf and Butcher, 1986; Zhao *et al.*, 2022). Thus, the pattern of connectivity seems to point the LDT to target circuits associated with limbic functions, for example, besides having direct projections to the Accumbens, the LDT influences the ventral striatum activity indirectly via VTA, and, potentially, via thalamostriatal projections. Moreover, NAc-projecting cholinergic LDT neurons give rise to collaterals that innervate the VTA and Thalamus (Dautan *et al.*, 2014).

Importantly, a recent report using resting-state functional magnetic resonance imaging (fMRI) in humans, confirmed LDT connectivity previously identified in other species. Specifically, to frontal cortex, basal ganglia (VTA, dorsal and ventral striatum and SN) and the limbic system (thalamus, hippocampus and amygdala) (Singh *et al.*, 2022).

1.5.3. LDT in reward and aversive behaviors

Initial lesion studies of the 1960s revealed the role of the LDT in controlling states of sleep and wakefulness. Follow up work, validated the cholinergic cells as the main contributor for these vital functions (reviewed in (Kohlmeier and Polli, 2020)). The LDT cholinergic cells are part of the reticular activating system (RAS), that comprises several brainstem nuclei that, collectively project to the thalamus, participating in the gating (*i.e.* controlling, either by suppressing or facilitating, the flow of information) of cortical activity underlying states of wakefulness, arousal, and the stages of sleep (Baghdoyan *et al.*, 1987; Steriade *et al.*, 1990). Specifically, the LDT has shown a relevant role in gating and controlling REM sleep. Cholinergic cells were shown to be maximally active during REM sleep and during sleep-waking transition, whereas GABAergic and glutamatergic cells displayed a wider array of discharging profiles during those phases (Boucetta *et al.*, 2014; Cissé *et al.*, 2018).

However, the multiplicity of sites that the LDT projects to, including cortical, sensorial, and limbic structures, as referred before, suggested a role beyond state control. A role that started to be brought to light in the late 1990s and continues to be explored in the current days. The **Table 1** summarizes the main findings with behavioral outputs that have, to this date, implicated the LDT in valence-associated behaviors.

Table 1- Summary of main findings implicating the LDT in valence-associated behaviors.

Region/circuit (cell type)	Tool(s)	Behavioral Task	Valence-related effect	Reference
		Reward		
Pharmacological studies				
LDT	Muscarinic type 2/4 (M2/4) receptor agonist	Cocaine and food self-administration on a PR reinforcement	Reduced the reinforcing properties (motivational drive)	(Shabani *et al.*, 2010)
LDT	Ionotropic glutamate receptor AMPA antagonist	Cocaine reinstatement	Attenuated the reinstatement of lever-pressing for cocaine self-administration	(Schmidt *et al.*, 2009)
LDT	NMDA and AMPA receptor antagonists or M2/4 receptor agonist	Cocaine CPP	Suppressed acquisition of cocaine place preference	(Shinohara *et al.*, 2014)
LDT	GLP-1R agonist	Cocaine reinstatement	Attenuated the reinstatement of lever-pressing for cocaine self-administration	(Hernandez *et al.*, 2021)
LDT	Amylin and calcitonin receptor agonist	Cocaine locomotion and 2-bottle (alcohol/water) free choice	Attenuated cocaine-induced locomotion and decreased alcohol intake	(Kalafateli *et al.*, 2021a, 2021b)
LDT	Ghrelin receptor agonist (or antagonist)	2-bottle (alcohol/water) free choice	Increased alcohol intake (reduced alcohol intake)	(Jerlhag *et al.*, 2009)
LDT	GLP-1R agonist (or antagonist)	Alcohol locomotion and 2-bottle (alcohol/water) free choice	Attenuated alcohol-induced locomotion and reduced alcohol intake	(Vallöf *et al.*, 2019)
		Sexual interaction test and food consumption	Decreased sexual interactions and food intake (antagonism increased food intake)	(Reiner *et al.*, 2018; Vestlund and Jerlhag, 2020)
LDT	Ghrelin receptor agonist (or antagonist)	Sexual motivation test and sexual interaction test	Increased sexual behaviors (antagonism decreased sexual behaviors)	(Prieto-Garcia *et al.*, 2015)
LDT	Amylin and calcitonin receptor agonist	Food consumption and sucrose PR reinforcement	Reduced food intake and motivated feeding behaviors	(Reiner *et al.*, 2017)
	Amylin and calcitonin agonist + GABA receptors antagonists	Food consumption	Reversed the food intake suppressive effects	

Optogenetic/chemogenetic studies				
LDT (glutamatergic)	NpHR	Cocaine locomotor sensitization	Prevented the development of sensitization	(Puranik *et al.*, 2022)
NTS-LDT	DREADDS (excitatory)	Cocaine reinstatement	Attenuated the reinstatement of lever-pressing for cocaine self-administration	(Hernandez *et al.*, 2021)
LDT-VTA	ChR2	ICSS and CPP	Reinforced lever-pressing and elicited place preference	(Coimbra *et al.*, 2021; Lammel *et al.*, 2012; Steidl and Veverka, 2015)
	ChR2 + intra-NAc D1/D2 antagonism	ICSS and CPP	Attenuated operant responding and place preference	(Steidl *et al.*, 2017a)
	ChR2 (NpHR)	Food Progressive ratio and two choice lever press	Increased motivational drive and shifted preference to laser-associated lever (opposite when inhibiting)	(Coimbra *et al.*, 2021)
LDT-VTA (cholinergic)	ChR2	CPP	Elicited place preference	(Steidl *et al.*, 2017a; Xiao *et al.*, 2016)
	ChR2	Sugar lever pressing extinction	Delayed extinction of lever pressing	(Dautan *et al.*, 2016b)
LDT-VTA (glutamatergic)	ChR2	RTPP-like paradigm	No effect on place preference but increased the entries to the stimulation-paired chamber	(Steidl *et al.*, 2017b)
	NpHR	Cocaine locomotor sensitization	Prevented the development of sensitization	(Puranik *et al.*, 2022)
LDT-VTA (GABAergic)	DREADDS (excitatory)	Cocaine reinstatement	Attenuated the reinstatement of lever-pressing for cocaine self-administration	(Hernandez *et al.*, 2021)
LDT-NAc	ChR2	Progressive ratio, two-choice lever, CPP and RTPP	Enhanced the motivational drive, increased the value of a food reward, and induces place preference	(Coimbra *et al.*, 2019)
	NpHR	Progressive ratio and two-choice lever	Decreased the motivational drive and decreased the value of a food reward	
LDT-NAc (cholinergic)	ChR2	Progressive ratio, two-choice, CPP and RTPP	Enhanced the motivational drive, increased the value of a	(Coimbra *et al.*, 2019)

			food reward, and induces place preference	
LDT-NAc (glutamatergic)	ChR2	Progressive ratio and two-choice	Enhanced the motivational drive and increased the value of a food reward	(Coimbra *et al.*, 2019)
LDT-NAc (GABAergic)	ChR2	Progressive ratio and two-choice	Decreased the motivational drive and decreased the value of a food reward	(Coimbra *et al.*, 2019)
Aversion				
LDT	DREADDS (inhibitory)	Fear paradigm	Reduced freezing responses to footshocks	(Broussot *et al.*, 2022)
LDT (GABAergic)	DREADDS (inhibitory)	Fear paradigm	Reduced freezing responses to footshocks	(Broussot *et al.*, 2022)
LDT (parvabulmin+)	ChR2	Fear conditioning	Induced fear- and anxiety-like behaviors	(Yang *et al.*, 2016)
LDT (CRH+)	ChR2	OP and EPM	Increased anxiety-like behaviors	(Tang *et al.*, 2021)
LDT (CFC-responsive cells)	c-Fos-tTA + TRE-ChR2 virus	Fear conditioning	Induced fear-like behavior	(Roy *et al.*, 2022)
IPN-LDT	ChR2	RTPP	Elicited place avoidance	(Wolfman *et al.*, 2018)
	NpHR	CPA	Attenuated the nicotine place avoidance	
LDT-VTA	NpHR	RTPP	Elicited place avoidance	(Coimbra *et al.*, 2021)
	DREADDS (excitatory or inhibitory)	Fear paradigm	Activation induced stronger freezing responses to footshocks, whereas inhibition reduced	(Broussot *et al.*, 2022)
LDT-Thalamus (cholinergic)	Chr2	EPM	Increased anxiety-like behaviors	(Zhao *et al.*, 2022)
LDT-NAc (glutamatergic)	ChR2	RTPP	Elicited place avoidance	(Coimbra *et al.*, 2019)
LDT-VTA (GABAergic)	ChR2	Fear paradigm	Induced freezing responses/immobility in the absence footshocks	(Broussot *et al.*, 2022)
	NpHR	CPA	Attenuated the nicotine place avoidance	(Liu *et al.*, 2022)
	DREADDS (inhibitory)	Fear paradigm	Reduced freezing responses to footshocks	(Broussot *et al.*, 2022)

Abbreviations: AMPA, α-amino-3-hydroxy-5-methyl-4-isoxazolepropionic acid; CFC, context fear conditioning; ChR2, channelrhodopsin-2; CPA, conditioned place aversion; CPP, conditioned place preference; DREADDS, designer receptors

exclusively activated by designer drugs; EPM, elevated plus maze; GABA, γ-Aminobutyric acid; GLP-1R, glucagon-like peptide receptor 1; ICSS, intracranial self-stimulation; IPN, interpeduncular nucleus; NAc, nucleus accumbens; NMDA, N-methyl-D-aspartate; NpHR, halorhodopsin; OP, open field; PR, progressive ratio; RTPP, real time place preference; TRE, tetracycline responsive element; tTA, tetracycline transactivator; VTA, ventral tegmental area.

1.5.3.1. LDT in Reward-related behaviors

From early on, the VTA was known to be important in goal-directed behaviors, thus the LDT projections to the mesoaccumbal pathway were speculated to involve the LDT in motivated and salience-related behaviors (Cornwall *et al.*, 1990; Oakman *et al.*, 1995). Electrical stimulation of the LDT was shown to result in a phasic rise of DA in the NAc (Forster and Blaha, 2000). A previous work had already revealed the involvement of the LDT cholinergic population in the DA rise, by pharmacologically stimulating cholinergic signaling in VTA, which elicits similar DA rise, that is impacted by specific lesioning of the LDT (Blaha *et al.*, 1996). Additionally, the researchers proved that LDT glutamatergic input to VTA was involved in the dopamine rises as well (Forster and Blaha, 2000; Lester *et al.*, 2008). Structural investigations showed that the LDT provides glutamatergic, cholinergic and even GABAergic inputs to the VTA (Omelchenko and Sesack, 2005). Subsequential work revealed that the LDT innervates preferentially NAc-projecting VTA DA neurons and that the LDT excitatory input (glutamatergic and cholinergic) has a crucial role in regulating and enabling/gating burst firing of VTA dopaminergic neurons (Dautan *et al.*, 2016b; Lammel *et al.*, 2012; Lodge and Grace, 2006). A change to phasic activity of VTA DA neurons produces synchronous bursts (Joshua *et al.*, 2009), leading to DA release in NAc (Floresco *et al.*, 2003), which is thought to encode a prediction error signal important for motivational salience (Schultz, 2013), turning an organism toward, or away, from repetition of behaviors. Thus, the switch in the firing mode of DA neurons, triggered by excitatory drive, is critical for the expression of goal-directed behaviors (Tsai *et al.*, 2009).

Therefore, the functionality of the LDT-VTA pathway in reward behaviors has led to an increasing interest for the LDT for the past decade. More recently, direct projections from the LDT to the NAc have been discovered and demonstrated to have a role in reward-behaviors as well (Coimbra *et al.*, 2019; Dautan *et al.*, 2016a, 2014). Moreover, the LDT has been implicated for some time in addiction-related behaviors (Kohlmeier, 2013; Laviolette *et al.*, 2000; Nelson *et al.*, 2007), contributing to further potentiate the interest in this nucleus.

1.5.3.1.1. Lesion and pharmacological studies

Lesions of the LDT have shown to modulate drug-induced locomotion (Alderson *et al.*, 2005; Dobbs and Cunningham, 2014; Forster *et al.*, 2002; Laviolette *et al.*, 2000). Stereotypical behaviors, including orofacial movements, were increased in LDT-lesioned animals after exposition to amphetamine however, the lesion decreased stereotypy in response to morphine (Forster *et al.*, 2002). Interestingly, after lesioning, the peaks of drug-elicited NAc DA release were increased in the case of amphetamine but decreased in morphine (Forster *et al.*, 2002). Specific cholinergic lesioning of the LDT, after operant self-administration training, increased the latencies for rats to initiate cocaine operant self-administration resulting in reduced cocaine intake however, once the response was initiated or with priming, animals responded similarly to pre-lesion conditions (Steidl *et al.*, 2015). Which suggests that the LDT is necessary for the responsiveness to cocaine-predictive stimuli/cues, which trigger drug-seeking behavior.

The LDT stimulation-evoked increase DA release in NAc was shown to be potentiated by intra peritoneal (i.p.) injections of cocaine, but failed to do so when an muscarinic acetylcholine receptors (mAChRs) antagonist was also injected into the VTA (Lester *et al.*, 2010). Rise in acetylcholine levels within the VTA of mice after i.p. administration of methamphetamine (Dobbs and Mark, 2008) are attenuated by intra-LDT microinjections of mAChR agonist, however not having an effect on drug-induced NAc DA rise (Dobbs and Mark, 2012). LDT administration of a mAChR agonist, which attenuated ACh output, was able to decrease lever-pressing for cocaine self-administration in a progressed ratio schedule and breakpoint for cocaine responding (Shabani *et al.*, 2010). Blockade of glutamatergic AMPA receptors in the LDT, which should inhibit LDT excitability, was shown to attenuate lever-pressing in reinstatement of drug seeking behavior induced by priming cocaine injection, an effect also observed after intra-VTA blockage of AMPA, nicotinic acetylcholine receptors (nAChRs) and mAChRs, suggesting that ACh output from the LDT was involved, with perhaps a contribution of glutamatergic LDT input and output (Schmidt *et al.*, 2009). These studies indicate that the LDT and LDT-VTA pathway have an important role in regulating the reinforcing value of drug reward and reward seeking motivated behaviors.

Intra-LDT pharmacological blockade of glutamate receptors or blockade of AChRs in the VTA attenuated cocaine CPP acquisition. This attenuation reached its maximum effect following intra-LDT application of an mAChR agonist that hyperpolarizes the LDT neurons, leading to profound inhibition (Shinohara *et al.*, 2014). Additionally, cholinergic antagonism in the VTA right before posttest session of CPP, reduced the cocaine CPP (Shinohara *et al.*, 2014). Thus, these data suggests that LDT activity and glutamatergic input to the LDT are necessary for cocaine CPP formation whereas, cholinergic input to the VTA is crucial for cocaine CPP acquisition and expression, which points out a role of cholinergic signaling

in cocaine-related memory retrieval. In accordance, burst firings of the VTA DA neurons are critical for cocaine CPP acquisition and was shown to be sufficient to produce place preference (Tsai *et al.*, 2009; Zweifel *et al.*, 2008), indicating that burst firing is sufficient for acquisition of behavioral conditioning. Together, these results suggest that the acquisition of cocaine CPP requires enhanced DA neuronal activity through activation of LDT cholinergic neurons, not excluding a potential role for glutamatergic projections.

Regarding natural rewards, intra-LDT administration of mAChR agonist that inhibits the LDT, attenuated lever-pressing for food pellets self-administration (Shabani *et al.*, 2010). Interestingly, in recent years several classical energy balance-regulating peptides have been implicated in reward-related behaviors. LDT treatment with glucagon-like peptide 1 (GLP-1) agonist has shown to decrease the sexual interaction behaviors in sexually naïve male mice and decrease food intake, whereas antagonism increased food intake (Reiner *et al.*, 2018; Vestlund and Jerlhag, 2020). Likewise, ghrelin signaling in the LDT regulates sexual reward and sexual behavior in mice (Prieto-Garcia *et al.*, 2015). Furthermore, this peptide administered to the LDT modulated accumbal dopamine through nAChRs in the VTA (Jerlhag *et al.*, 2012). An agonist of amylin and calcitonin, locally administered in the LDT reduced hedonic feeding behaviors in male rats, likely through the LDT GABAergic population (Reiner *et al.*, 2017). Nevertheless, these peptides have also shown to regulate drug-related behaviors for example, GLP-1 signaling in the LDT, coming from the NTS, recruits GABAergic cells and attenuates the reinstatement of cocaine seeking self-administration (Hernandez *et al.*, 2021). These peptides also modulate, via LDT, the alcohol intake, alcohol-induce locomotion, alcohol-elicited NAc DA release and cocaine locomotor stimulation (Jerlhag *et al.*, 2009; Kalafateli *et al.*, 2021a, 2021b; Reiner *et al.*, 2018; Vallöf *et al.*, 2019). Altogether, these data suggests that endogenous appetite-regulatory peptides in the LDT might modulate sexual and food reward and drug-associated behaviors, indicating a possible neurochemical overlap between the hedonic reward system and those regulating energy balance.

1.5.3.1.2. Optogenetic/chemogenetic studies

Although the previous studies have provided a body of evidence of the role of the LDT in reward processes, they are technically limited by their inability to demonstrate LDT direct actions in the VTA or other specific targets, since effects following nucleus-specific manipulations, including intra-nucleus injections, could have been indirect or included players beyond those intended. Optogenetics and chemogenetics have provided an elegant way of modulating neuronal activity with cell specificity and

temporal control that previous tools were unable to, allowing to infer causality of activating/inhibiting a specific neuronal population/projections with a particular behavioral outcome.

Non-selective optogenetic activation of all LDT-VTA terminals was found to be reinforcing since it can elicit operant behavior for a lever-associated with laser stimulation (Steidl and Veverka, 2015) and produces CPP (Coimbra *et al.*, 2021; Lammel *et al.*, 2012). Later it was shown that the operant responding for optogenetic excitation of LDT inputs to the VTA increases NAc DA levels and both the operant responding and CPP, elicited by LDT-NAc activation, are attenuated with intra-NAc D1/D2 receptors antagonists injection (Lammel *et al.*, 2012; Steidl *et al.*, 2017a). Thus, DA release into the NAc seems to be critical to the reinforcing/rewarding effects of activation of LDT terminals in the VTA. Recently, our lab demonstrated that LDT-VTA activation can increase value of a stimulation-paired food reward in a two-choice lever, as it shifts preference to the laser-paired pellet in comparison to an otherwise equal reward, whereas the opposite was observed with LDT-VTA inputs inhibition. Furthermore, photoactivation enhanced motivational drive, that is, the willingness to work to get the reward associated with LDT-VTA stimulation in a progressive ratio task (the reverse happens when inhibiting) (Coimbra *et al.*, 2021). Specific photoexcitation of the cholinergic LDT terminals in the VTA triggered positive reinforcement (Steidl *et al.*, 2017b; Xiao *et al.*, 2016). Interestingly, in a operant place preference paradigm, activation of glutamatergic LDT-VTA neurons resulted in significantly more entries into the stimulation-paired chamber, but very short chamber visit durations, resulting in overall low amounts of time spent in the light-paired chamber. This may indicate a differential contribution of the two excitatory sources, in which activation of glutamatergic axons may reinforce chamber entries while activation of cholinergic axons may be more important for the rewarding effects of chamber stays (Steidl *et al.*, 2017b). Moreover, chemogenetic activation of NTS-to-LDT circuit or LDT-VTA GABA projections was sufficient to attenuate the reinstatement of cocaine seeking after a cocaine priming injection (Hernandez *et al.*, 2021).

Our lab has shown that non-selective optogenetic activation of all LDT-NAc projections enhances motivational drive, shifts preference to an otherwise equal reward in a two-choice task, whereas inhibition induces the opposite outcomes, and induces place preference (Coimbra *et al.*, 2019). Targeting specifically the main populations of the LDT, we demonstrated that activation of cholinergic inputs to NAc is sufficient to recapitulate the effects of general stimulation. Glutamatergic projections activation also enhanced preference for the laser-associated reward and increased motivation, while GABAergic inputs activation decreased the value of the laser-paired reward and decreased motivation (Coimbra *et al.*, 2019).

Thus, this data points out that the LDT appears to be uniquely positioned to exercise a modulatory role of reward-motivated behaviors, not only through the control of burst firing and increase in dopamine release via the projections to the mesoaccumbens pathway, but also via its direct connections to the NAc.

1.5.3.2. LDT in Aversion-related behaviors

Although the preponderance of studies has shown a role of the LDT in reinforcement of relevant stimuli, indicative of a positive valence, activity in the LDT has also been shown to be involved in coding negative valence underlying aversion. LDT is activated by different aversion-inducing stimuli like inescapable or conditioned shock (Liu *et al.*, 2009, 2003), predator odorant (Yang *et al.*, 2016), acute restraint (Tang *et al.*, 2021), and even social defeat stress (Fernandez *et al.*, 2018). Although caution in making conclusions was noted, due to small number of cells recorded, stimulation of cholinergic afferents to VTA was found to enhance the firing of DA-VTA neurons that were excited by an noxious paw pinch (Dautan *et al.*, 2016b).

General stimulation of IPN terminals in the LDT was shown to elicit avoidance behavior in a RTPP paradigm, suggesting that these projections contribute to aversion (Wolfman *et al.*, 2018). Furthermore, in the same study, these projections were implicated in the aversive effects of high doses of nicotine, as photoinhibition blocked the conditioned place aversion elicited by high concentrations of the stimulant (Wolfman *et al.*, 2018). Recently, inhibition of LDT GABAergic terminals in the VTA prevented nicotine aversion (Liu *et al.*, 2022). Optical inhibition of LDT to VTA projections or LDT-NAc glutamatergic inputs activation induced avoidance in a RTPP task (Coimbra *et al.*, 2021, 2019). Selectively stimulating LDT PV+ GABAergic (but not SOM+) cells induces fear- and anxiety-like responses including freezing, accelerated heart rate and increased serum corticosterone. Likewise, activation of LHb glutamatergic inputs to the LDT interneurons generated fear-like responses (Yang *et al.*, 2016). Chemogenetically silencing LDT neurons or LDT-VTA projections prior to administration of electrical footshocks reduced the freezing responses to the aversive stimulant, whereas LDT-VTA chemogenetical activation induced strong freezing responses (Broussot *et al.*, 2022). Selective inhibition of LDT-VTA GABA terminals, but not other populations, dampened freezing responses and optogenetic activation induced freezing and bradycardia, a hallmark of freezing, in the absence of shock (Broussot *et al.*, 2022). Furthermore, optical activation of LDT cholinergic projections to the ventral posterior complex of the Thalamus during the elevated plus maze (EPM) led to a significant decrease in time spent in the open arms, meaning that the circuit induces more anxiety in the animals, indicative of an internal negative state (Zhao *et al.*, 2022). Photostimulation of corticotropin-releasing hormone (CRH)-positive LDT neurons during an open-field test resulted in less

time and shorter distances exploring the center of the arena, and during EPM, resulted in fewer entries and less time and distance exploring in the open arm, suggesting that transient activation of LDT CRH neurons induces an internal aversive state (Tang *et al.*, 2021).

Finally, there is evidence that LDT neurons participate in the induction of 22-kHz ultrasonic vocalizations in rodents, a well-known manifestation of a negative-affective state for example, during harmful situations (Brudzynski, 2021, 2007; Brudzynski *et al.*, 2011).

1.6. Open questions in the field

Overall, with the strong associations of the LDT with behaviors, it is still puzzling how the different LDT cell populations are capable of coordinating so many diverse behaviors, especially those like reward- and aversion-related. Importantly, it is unknown if this brain region contains a largely distinct or overlapping populations of neurons representing opposite valences and thus, distinguishable or common properties of these populations are to be determined. In addition, the brain areas associated with high-order functions, including prefrontal cortical areas may also be involved in the regulation of these basic innate behaviors through their projections to the LDT, acting via a top-down mechanism.

How cholinergic, glutamatergic and GABAergic output from the LDT to likely different population of DA, and non-DA, cells of the VTA can be involved in encoding both positive and negative valence remains an open question. Furthermore, the newly discovered LDT-NAc projections raised the complexity by which the LDT can control the mesoaccumbal pathway, but how this circuit works to drive positive or negative motivated-behaviors remains unclear.

2. Objectives

The aim of the present dissertation was to study LDT neuronal ensembles representing/encoding valence, to better understand the role of the LDT in the valence circuitry. In addition, a focus was made on the LDT-NAc projections since these remain greatly understudied.

This thesis was subdivided in four main objectives:

1. Identify neuronal ensembles encoding positive and negative valence by evaluating LDT cells responsive to negative stimulus (foot shock) or positive stimuli (sucrose and cocaine), using endogenous c-Fos marker.

2. Determine the degree of overlap/segregation of LDT ensembles representing distinct valence stimuli using the targeted recombination in active populations (TRAP2) mouse model; this approach allows permanent labelling (TRAPing) of cells that are active during one stimulus and combine with endogenous c-Fos labelling in response to other stimulus.

3. Optogenetically activate LDT ensembles encoding valence-related events and observe their impact in behavior, in a real time place preference and a conditioned place preference paradigms.

4. Characterize the pattern of innervation in the NAc of projections of positive- or negative-valence stimuli responsive LDT ensembles.

3. Materials and Methods

3.1. Animals

Male and female C57Bl6/J mice were used in the c-Fos neural labelling experiment (Charles River Laboratories, Barcelona, Spain). Male and female Fos-TRAP homozygous (*Fos* $^{2A\text{-}iCreER/2A\text{-}iCreER}$) and *R26* $^{AI14/AI14}$ mice were obtained from Jackson Labs (stock #030323 and stock #007914, respectively). The two mouse lines were crossed to obtain F1 double heterozygous TRAP2;Ai14 mice (*Fos* $^{2A\text{-}iCreER/+}$; *R26* $^{AI14/+}$) used in the double neural labelling experiment. Fos-TRAP homozygous mice were crossed with wildtype C57Bl6/J mice (Charles River Laboratories, Barcelona, Spain) to obtain TRAP2 mice (*Fos* $^{2A\text{-}iCreER/+}$) used in the anatomical projections analysis and optogenetics-coupled behavior task.

All experiments were conducted with 2-7 month-old subjects. Animals were kept in standard housing conditions (light/dark cycle of 12/12h with lights turned on at 08:00h; 22°C±2°C) with standard diet and water *ad libitum* (unless otherwise stated). Animals were housed up to a maximum of 6 mice per cage. All behavioral experiments were performed during the light period.

All protocols were approved by the Ethics Committee of the Life and Health Sciences Research Institute (ICVS) and by the national competent entity, the Direção-Geral de Alimentação e Veterinária (DGAV)(#8332, dated of 2021-05-08). All practices and techniques were performed following established ethical and legal standards, including the European Union Directive 2010/63/EU. Health monitoring was carried out according to FELASA guidelines and all experimenters and animal facilities were accredited by DGAV. All efforts were made to minimize the number of animals used, and their discomfort and suffering.

3.2. Drug treatments

4-hydroxytamoxifen (4-OHT, Sigma Aldrich) solution was prepared as stated by the manufacture. Briefly, 4-OHT was dissolved at a concentration of 50 mg/mL in 100 % ethanol by shaking at 52 °C for 15-20 min. Then a solution of 1:4 mixture of castor oil: sunflower seed oil (Sigma-Aldrich, Cat #s 259853 and S5007) was added and mixed by shaking at room temperature. The final concentration of the 4-OHT dissolved in the oil mixture was 5 mg/mL and solutions were always used on the day they were prepared. At the day of administration, the solution was kept in a water bath at 36°C, vortexed before administration. On TRAPing day, all mice were injected intraperitoneally (i.p) at a dose of 50 mg/Kg.

Cocaine hydrochloride (Sigma-Aldrich, Cat# C5776-1G) was dissolved in 0.9% saline solution for a final concentration of 2 mg/mL. Mice were administered i.p. at a dose of 20 mg/Kg.

3.3. Stereotaxic surgery: LDT viral injection and cannula implantation

TRAP2 mice (> 2 months old) used for anatomical analysis and optical manipulation of specific stimulus-responsive LDT ensembles went through stereotaxic surgery for virus injection and optic fiber cannula implantation in the LDT (Gene Therapy Center Vector Core (UNC) center; AAV5 vector titers were 2.1-6.6 x 10^{12} virus molecules/ml).

Animals were pre-treated with an analgesic (Buprenorphine, 0.05 mg/kg; Bupaq, Richter Pharma, Austria) and then anaesthetized with sevoflurane (induction: 8% (wt/vol)). Afterwards, they were positioned in the stereotaxic frame on top of a heating pad with the snout inside a nose cone for anesthesia maintenance (2-4% (wt/vol)). A lubricant eye gel was applied to prevent drying of the eyes and the head and fur were disinfected with 70% (vol/vol) ethanol. Next, an incision in the scalp over the skull midline was made and the skull was exposed. A solution of hydrogen peroxide was applied with cotton swabs to clean the area, facilitating the identification of the bregma and lambda. Under a stereoscope, the skull was leveled using the tip of the drill to place the bregma and lambda in the same dorsal-ventral coordinate, for lining the medial-lateral axis, the drill was moved 1.5 mm to the left and right from the midline. Following, a small craniotomy hole on the level of the LDT was made and cleaned with saline. Afterwards, AAV5–EF1a–DIO–hChR2–YFP virus was injected unilaterally in the LDT (coordinates from bregma, −5 mm AP, +0.5mm ML, and −3.0 mm DV (Paxinos and Franklin, 2001)) using a 30-gauge needle Hamilton syringe (Hamilton Company, Switzerland), at a rate of 100 nL/min for a total volume of 300 nL per animal. The syringe was left in place for 5 min before withdrawal to allow diffusion. Right after, an optic fiber cannula, with 2.5 mm stainless steel ferrule (200μm core fiber optic; Thorlabs, Germany) was implanted in the LDT using a cannula holder mounted on the stereotaxic frame, in the same coordinates except for DV (-2.9 mm), being fixed to the skull with dental cement (C&B kit, Sun Medical, Shiga, Japan).

At the end of the surgical procedures, after cement hardening, mice were sutured if necessary and removed from the stereotaxic frame. Postoperative care was carried out by administering analgesia (0.05 mg/kg buprenorphine; Bupaq, Richter Pharma, Austria) post-procedure, as well as during three successive days. A multivitamin supplement and saline were also administered post-procedure when necessary. Mice were left to recover for 1 week before initiating the 7-day habituation period.

3.4. Behavior

3.4.1. Apparatus

Three identical operant chambers (21.59cm length x 18.08cm width x 12.7cm height - working area; Med Associates, St. Albans, VT, USA), contained in light-and sound-attenuating boxes, and an open-

field (OF) arena (43.2 cm length x 43.2 cm width, with transparent acrylic walls and white floor, Med Associates, St. Albans, VT, USA) were used in the behavior assessment. The source of illumination was a 100mA, 2.8W house-light installed on the top-center of the wall opposite to the magazine wall. The house-light remained ON independently of the group. Aversive stimulation was generated by a Shocker module (Med Associates, St. Albans, VT, USA). A PC equipped with Med-PC software (Med Associates, St. Albans, VT, USA) was used to control the equipment and record the data.

3.4.2. LDT recruitment by positive and negative valence stimuli

Cocaine and sucrose were used as positive valence stimuli, and as negative valence stimulus, we used foot shocks. Cocaine stimulus consisted of a single i.p. injection of cocaine solution at a dose of 20 mg/Kg (Coca). In the sucrose group (Suc), 50 μL of 20% sucrose solution were delivered every 30 seconds (180 sucrose solution deliveries, 90 min session). In the shock group (Shock), 1.5 mA footshocks were delivered every 30 seconds (20 footshocks, 10 min session). These exposures were based on pilot experiments from our team and on (Gore *et al.*, 2015; Xiu *et al.*, 2014). Before the sacrifice for c-Fos detection or TRAPing day, all animals went through a 7-day period of habituation before the behavioral experimental day(s). During this period, animals spent the same amount of time in the apparatus as their respective stimulus session without receiving sucrose or shocks. Animals received a single i.p injection of saline if they were going to be exposed to cocaine and/or injected with tamoxifen. This process was repeated every day for 7 consecutive days to familiarize animals with the apparatus, handling and i.p injection to decrease novelty-induced c-Fos expression (based on Bobadilla *et al.*, 2020). In the 3.4.2.1. experiment, Coca and saline groups after i.p. injections were put in a OF arena for 45 minutes and their locomotion was measured (habituation to the arena was performed).

On the experimental days, controls for sucrose (NOsuc) did not receive any reward while in the operant box for 90 min; controls for the cocaine (Saline) were injected with saline i.p.; controls for shock (NOshock) were left to explore the same operant chambers for 10min. Animals assigned for sucrose session were food deprived two days prior to enhance motivational drive to consume the reward during the experimental days. The apparatus was cleaned with 10% ethanol between animals.

3.4.2.1. Endogenous c-Fos neural labelling experiment

Wild-type C57BL/6J mice, 2-4 months of age were randomly distributed into 6 groups according to the stimulus received: Coca (n= 6), Saline (n= 6), Shock (n= 6), NOshock (n= 6), Sucrose (n= 6) and NOsuc group (n= 6). On the experimental day, following the habituation period, the animals went through

the respective stimulus session and then isolated in individual cages (after 45 minutes OF session in the Saline and Coca groups), being sacrificed approximately 90 min after to detect endogenous c-Fos protein induced by the session. For the sucrose group, the peak of consumption was considered in the middle of the session therefore, the animals were sacrificed 45 min after exiting the apparatus.

3.4.2.2. TRAPing and neural labelling of two distinct stimuli experiment

Taking advantage of the TRAP2 mouse model, the recruited neuronal ensembles by a valence-specific stimulus can be identified/tagged with the red fluorescent protein, tdTomato ("TRAPed"; using TRAP2;Ai14 double transgenic animals). The TRAP2 model uses the *Fos* locus to drive the expression of a tamoxifen-inducible Cre-recombinase (*Fos*$^{2a\text{-}iCreER}$/TRAP2 allele) and a transgenic or virally-delivered recombinase-dependent effector. When cells are activated in the presence of 4-OHT, CreER enters the nucleus to catalyze the recombination, allowing the activity-dependent expression of the effector (DeNardo *et al.*, 2019). Combining with endogenous c-Fos detection, the overlap/segregation of neuronal ensembles recruited by different stimuli can be determined. Therefore, in this experiment, animals were exposed to 2 different stimuli.

TRAP2;Ai14 mice, 2-4 months of age were randomly assigned into 11 groups according to the two stimuli they were exposed to: Coca-Shock (n= 5), Saline-NOshock (n= 5), Sucrose-Shock (n= 5), NOsuc-NOshock (n= 5), Shock-Shock (n= 5), NOshock-NOshock (n= 5), Coca-Suc (n= 5), Coca-NOsuc (n=5), Coca-Coca (n= 6), Saline-Saline (n= 5) and a group exposed to shock but not injected with tamoxifen (n= 4; NOtamox). On the TRAPing day, following the habituation period, animals were exposed to one of the three different stimuli or control injection/session and immediately after, injected with 4-OHT. Animals were individually housed for about 6 hours before returning to the homecage. For manipulation of animals after tamoxifen injection, personal protection equipment (PPE) was employed. To minimize contact with animals after tamoxifen injection, during the two following days, animals were not manipulated. All equipment was washed with ethanol 70% and sodium hypochlorite 10%. Bedding was disposed properly according to the animal house protocol. Regarding the second exposure, animals went through a new 7-day habituation, after which, they were sacrificed for endogenous c-Fos detection following stimuli exposure or control injection/session.

3.4.3. Optogenetic manipulation of valence-responsive LDT ensembles

TRAP2 mice, 2-4 months of age, were used in this experiment. Animals were subjected to surgery for viral injection and optic fiber implantation in the LDT (as described in 3.3). Thus, in this experiment, the cre-dependent effector (ChR2-YFP) was virally delivered, allowing the expression of the opsin

specifically in stimuli-responsive LDT cells. Two weeks after surgery, to allow recovery and virus infection, animals were exposed to either cocaine or shock, receiving 4-OHT injection immediately after. Four weeks later, animals were tested in the behavioral tasks, in which TRAPed neurons were optically activated using optogenetics during a Real Time Place Preference (RTPP) test, the Conditioned Place Preference (CPP) paradigm, in order to assess the impact of activation of the LDT ensembles in behavior.

3.4.3.1. Real Time Place Preference

RTPP test apparatus consisted of a custom-made white acrylic arena (60 cm x 50 cm x 40 cm) comprised of two indistinguishable chambers connected by a central opening. The test was performed for 20 min in which the animal could freely explore the apparatus (Shen *et al.*, 2022; Zhang *et al.*, 2018). For each trial, the mouse was initially placed in the non-stimulation chamber (OFF chamber), and laser stimulation was constantly delivered (manual control) once the animal entered the stimulation chamber (ON chamber) and stopped when the animal exited. Before testing, animals were habituated two times to the apparatus for 20 min each and on the testing day, were let to acclimatize to the to the experimental room for at least 30 min. The stimulation chamber was randomly assigned to each animal and balanced for each group. Behavior was recorded via a video camera and time spent in each chamber and animal entries in the ON chamber were manually evaluated in a blind manner. Laser power output was tested at the tip of optic fiber and was checked every two to three animals. During behavior, the researcher was blind to the animal groups. Data is presented as percentage of time spent in each chamber and number of entries in the ON chamber.

3.4.3.2. Conditioned Place Preference

The CPP test apparatus (Med Associates Inc., St Albans, VT, USA) consisted of three compartments with different patterns, two main chambers with different patterns of walls and flooring (black walls with transparent acrylic floor and white walls with black acrylic floor; both 27.5 cm x 21 cm) and a center chamber (grey walls and gray plastic floor; 15.5 cm x 21 cm). Mouse location within the apparatus was monitored using an automated photo-beam system (Med Associates Inc., St. Albans, VT, USA) allowing the evaluation of time spent on each chamber. CPP protocol was executed based on previous reports (Coimbra *et al.*, 2021, 2019) with the exception that two conditioning days were performed (similar to (Fonseca *et al.*, 2015)) and a biased approach was used (similar to (Shinohara *et al.*, 2019)).

The protocol comprised three phases of behavioral stages across 4 days. During the 4 days, the animals were let to acclimatize to the experimental room for at least 30 min. On day 1, individual mice were placed in the center chamber and allowed to freely explore the entire apparatus for 20 min (pre-

test). On days 2 and 3, one of the side chambers was paired with photostimulation (ON chamber) and the other chamber was paired with no-stimulation (OFF chamber). For the Coca group, stimulation was paired with the side that the animals showed less preference, the opposite for the shock group, and for the control group, attribution was random. During this conditioning phase, mice were confined to one side chamber and given either optical stimulation or no stimulation, for 30 min and approximately 4 hours later, they were placed in the other side chamber and given the alternative treatment. The session order (stimulation or no-stimulation first) was counterbalanced across mice and on the second day of conditioning, the order of the treatments was reversed. Laser power output was tested at the tip of optic fiber and was checked every two to three animals.

On day 4, mice were again allowed to freely explore the entire apparatus for 20 min, in the absence of photostimulation (post-test). Subjects were placed in the neutral area, with the doors to the main chambers being opened at the start of the session. During behavior, the researcher was blind to the animal groups. Results are expressed as difference between time spent on each side of the apparatus in the test and the time spent on the same side in the pre-test.

3.4.3.3. Optical stimulation

Optogenetic stimulation was performed using blue light, 80 10 ms pulses delivered at a rate of 20Hz (Coimbra *et al.*, 2021, 2019), for all the period the animals were on the stimulation-paired side in the RTPP or during conditioning sessions, every 15 s, in the stimulation-associated chamber in the CPP. Laser power output was tested at the tip of optic fiber and was checked every two to three animals.

Blue light was produced by a 473 nm DPSS laser (CNI Laser, Changchun, China) and directed to the brain, at an intensity of 6-8 mW, via a fiber optic patch cord (0.22 NA, 200 μm diameter; Thorlabs, Newton, NJ, USA), which was connected to the implanted ferrule during behavior. Laser output was regulated by a Master-8 pulse generator (A.M.P.1, MN, USA).

3.5. Histology

3.5.1. Sacrifice and sectioning

For endogenous c-Fos induction analysis, approximately 90 min after stimulus exposure, mice were deeply anesthetized by a mixture of ketamine and medetomidine and transcardially perfused with 0.9% saline followed by 4% paraformaldehyde (PFA; pH 7.4 in 0.1M phosphate buffer). Brains were removed, post-fixed in PFA for 24 hours and then immersed in a 30% sucrose solution at 4°C until sectioning. Brains were sectioned coronally at a thickness of 40 μm, on a vibrating microtome (VT1000S, Leica,

Germany) and the slices stored in PBS 1x with 0.02 % azide at 4° C (or cryopreserved with cryoprotectant solution at -20°C for long-term storage). Slices from the areas of interest, Amy, LDT and NAc, were selected using the Mouse Brain Atlas (Paxinos and Franklin, 2001).

3.5.2. Immunofluorescence (IF)

Free-floating sections were washed three times for 10 min in PBS/Triton-X100 (0.3 %) (PBS-T) for membrane permeabilization and blocked, to avoid unspecific binding, for 30 min with 10% fetal bovine serum (FBS; Invitrogen, MA, USA) in PBS-T at room temperature (RT). When performing IF for two distinct molecular targets, antibody incubations were sequential meaning that, only one type of antibody was incubated at each time (target with the longer primary incubation period processed first) (**Table 2**). After primary antibody incubation, three 10 min PBS-T washes were performed to remove unbound antibody and, subsequently, the slices were incubated with the appropriate secondary fluorescent antibody. Between molecular targets, sections were washed three times with PBS-T for 10 min each. All antibodies were diluted in PBS-T containing 2% FBS. Before mounting the slices onto glass slides (SUPERFROST® PLUS, Thermo Scientific, USA), these were washed two times with PBS-T and one time with PBS 1x, incubated with 4',6-diamidino-2-phenylindole (DAPI; 1:1000; Invitrogen, MA, USA) for 10 min at RT and then mounted using Permafluor (Invitrogen, MA, USA). Slides were stored at 4°C and kept protected from light.

Table 2 - Antibody information for all immunofluorescence protocols used**.**

IF	Host	Against	Dilution	Conditions	Note
c-Fos	rabbit	anti-c-Fos	1:500	overnight, RT	AB_2314042*
c-Fos secondary	donkey	anti-rabbit	1:1000	2h, RT	Alexa Fluor® 647**
c-Fos secondary	goat	anti-rabbit	1:1000	2h, RT	Alexa Fluor® 488**
ChAT	sheep	anti-ChAT	1:500	48h, 4°C	Ab18736, Abcam***
ChAT secondary	donkey	anti-sheep	1:1000	2h, RT	Alexa Fluor® 647**
ChAT	goat	anti-ChAT	1:750	overnight, 4°C	AB144P*
ChAT secondary	donkey	anti-goat	1:1000	2h, RT	Alexa Fluor® 488**
GFP	goat	anti-GFP	1:750	overnight, 4°C	ab6673***
GFP secondary	donkey	anti-goat	1:500	2h, RT	Alexa Fluor® 488**
GFP secondary	donkey	anti-goat	1:500	2h, RT	Alexa Fluor® 568****

*Merck Millipore, Burlington, MA, USA **Invitrogen, Carlsbad, CA, USA *** Abcam, Cambridge, UK ****Eugene, OR, USA

3.5.3. Image acquisition and analysis

Images were collected either by confocal microscopy (Olympus FV3000, Olympus) under 20x magnification if colocalizations would be determined or regular upright fluorescence microscopy (Olympus Widefield Upright Microscope BX61) under 10-20x magnification.

About 4-10 slices for each animal were used for each analysis (every third slice, corresponding to a distance of 120 μm). Slices were classified in terms of stereotaxic coordinates relative to bregma and the areas of interested (*i.e.* amygdala - BLA, CeA; LDT and the main NAc subregions - core and shell) delineated using landmarks and neuro-anatomical nomenclature as described in Paxinos & Franklin (2001). The cytoarchitectonic boundaries of the LDT are difficult to determine because their neurons extend into the surrounding tegmentum (Luquin *et al.*, 2018; Wang and Morales, 2009). The delineation was made by outlining the area containing the core of ChAT-positive cells, thus excluding the ChAT-immunoreactive cells most peripherally located (Coimbra *et al.*, 2021, 2019; Dautan *et al.*, 2014; Pereira *et al.*, 2021). Using Fiji (Image J) software (Schindelin *et al.*, 2012) the regions of interest were measured in terms of area (mm^2) and positive cells within these regions were manually determined in a blind manner employing the Cell Counter plugin. Cell densities were presented as cells per mm^2 (cells/mm^2).

In animals injected with YFP construct, number of LDT starter/YFP+ cells were quantified. We sampled every third section from -4.84 to -5,40 from bregma according to Paxinos & Franklin (2001) and counted the cells manually and blindly using Image J. To determine the NAc innervation, we sampled every third section from 1.94 to 0.74 from bregma according to Paxinos & Franklin (2001) (7-10 slices per animal). Z-stack images (2 μm z-step) were acquired with the Olympus Widefield Upright Microscope BX61. Using Image J, the subdivisions of the NAc (core, medial shell and lateral shell) were delineated and the areas were determined. Then, using the pixel classification tool of the ilastik software (Berg *et al.*, 2019), axonal innervation was segmented, resulting in output binarized images (background and signal) that were subsequently analyzed for axon-labeled pixels (positive pixels) quantification using Image J Threshold function. To generate axon densities, presented as number of positive pixels/mm2, for each NAc subdivision, the number of axon-labeled pixels was divided by the area of each subregion. In order to control for viral infection variability between animals, the axon densities were divided by the LDT starter cell density. Therefore, the innervation is shown as positive pixels/YFP+ LDT cell. Furthermore, to take into account, infection spreading outside the LDT, the innervation was multiplied by the proportion of transfected cells within the LDT (for each animal, transfected cells inside and outside the LDT were quantified; the proportion was calculated by dividing total LDT transfected cells by total transfected cells).

Optic fiber placement was assessed in the animals subjected to optogenetic manipulation to confirm if light stimulation was accurately conducted in the LDT region. For this, slices where the presence of the optic fiber was detected were classified according to Paxinos & Franklin (2001) to estimate the stereotaxic coordinates.

3.6. Statistical analysis

Statistical analysis was performed in GraphPad Prism V9.3.1 (GraphPad Software, Inc., La Jolla, CA, USA). Normality was assessed in all data sets using the Kolmogorov-Smirnov test. Parametric tests were used whenever the normality assumption was met. Statistical analysis between two groups was made using unpaired Student's t test. Non-parametric analysis (Mann-Whitney test) was used when normality of data was not achieved. One-way analysis of variance (ANOVA) was used to compare three or more groups. Bonferroni's post hoc multiple comparison test was used for group difference determination. Two-way analysis of variance (Two-way ANOVA), followed by Bonferroni's post hoc analysis for multiple comparisons was used to compare groups with multiple measurements. Results are presented as scatterplots distribution and mean ± standard error of the mean (SEM). Statistical significance was accepted for $p < 0.05$.

4. Results

The LDT has shown to be involved in reward- and aversive-related behaviors however, it remains unclear which neuronal populations are involved in encoding positive and negative valence stimuli/events. Thus, in order to identify the LDT neuronal ensembles responsive (*i.e* encoding) to specific events, we used endogenous c-Fos labelling (the *c-fos* gene is an immediate early gene (IEG), meaning that its expression is rapidly induced by neuronal activity (Kawashima *et al.*, 2014; Morgan and Curran, 1991)). To study the overlap or segregation of LDT ensembles representing distinct stimuli, we took advantage of the transgenic mouse model TRAP2 (DeNardo *et al.*, 2019), which relies on the expression of Cre under *c-fos* promoter as it will be described below. Using this model, we are able to genetically access these ensembles to investigate their role in behavior and to find if the stimuli-responsive LDT ensembles project to the NAc.

4.1. Identification of Reward- or Aversion-responsive LDT neuronal ensembles

In order to assess if the LDT represents positive and negative stimuli, after a 7-day habituation period, wild-type (WT) C57BL/6J mice were exposed to negative or positive stimuli (**Figure 3a**). The negative stimulus consisted of electric footshocks (Shock group) (**Figure 3b**) whereas the rewarding stimuli consisted of a single intraperitoneal (i.p.) 20 mg/Kg cocaine injection (Coca group) (**Figure 3f**), or exposure to drops of 20% sucrose solution (Suc group) (**Figure 3k**). The control groups for each exposure paradigm were: exploration of the apparatus without receiving footshocks (NOshock group); i.p. injection of saline solution (Saline group); and exploration of the operant box with no sucrose rewards (NOsuc group) (**Figure 3b, f, k**). All mice were euthanized approximately 90 min after the beginning of stimulus exposure for assessment of endogenous c-Fos protein expression by immunofluorescence (**Figure 3a**). The boundaries of the LDT were delineated using the outline of the area immunohistochemically stained for the cholinergic marker ChAT and using the Paxinos mouse brain atlas.

We then calculated c-Fos cell density in the LDT (**Figure 3c, h, m**) and found that shock increased c-Fos+ cells in the LDT (**Figure 3d**; $t(10) = 12.05$, $p < 0.0001$). Additionally, there was a higher density of c-Fos expressing cells that were cholinergic in nature (**Figure 3e left and Annex 1**; $t(10) = 4.42$, $p = 0.0013$). Cholinergic cells comprised around 5 % of all shock-activated cells (**Figure 3e right**).

Exposure to single injection of cocaine is known to increase the locomotion of animals (Giros *et al.*, 1996), so we recorded the locomotor activity after saline or cocaine injection for 45 minutes in an open field. As expected, mice injected with cocaine showed a significant increase in locomotion, measured by total distance (**Figure 3g left**; $t(10) = 5.71$, $p = 0.0002$) and measured by distance traveled across the

session (**Figure 3g right**; Group effect: F (1, 10) = 32.55, $p = 0.0002$). In accordance, cocaine led to an increase in c-Fos+ cells in the LDT (**Figure 3i**; $t(10) = 11.45$, $p < 0.0001$) and an increase in ChAT+ cells (**Figure 3j left**; $t(10) = 4.38$, $p < 0.0014$). The cocaine-responsive ensemble was composed of 8 % cholinergic cells (**Figure 3j right**).

Regarding sucrose, a natural reward, we verified its consumption by counting the number of head entries into the receptacle of sucrose drops. No significant differences were observed on the number of head entries (**Figure 3l**; U (32, 46) = 11, $p = 0.3095$), suggesting that both groups visited the magazine in a similar way. Yet, exposure to sucrose induced an increase in c-Fos+ cells in the LDT (**Figure 3n**; $t(10) = 7.72$, $p < 0.0001$) with no significant recruitment of the cholinergic population (**Figure 3o left**; $t(10) = 2.083$, $p = 0.0639$). Around 9% of cells activated in the Suc group were cholinergic (**Figure 3o right**).

Together, these data demonstrate that the LDT ensembles are recruited for both negative and positive valence stimuli.

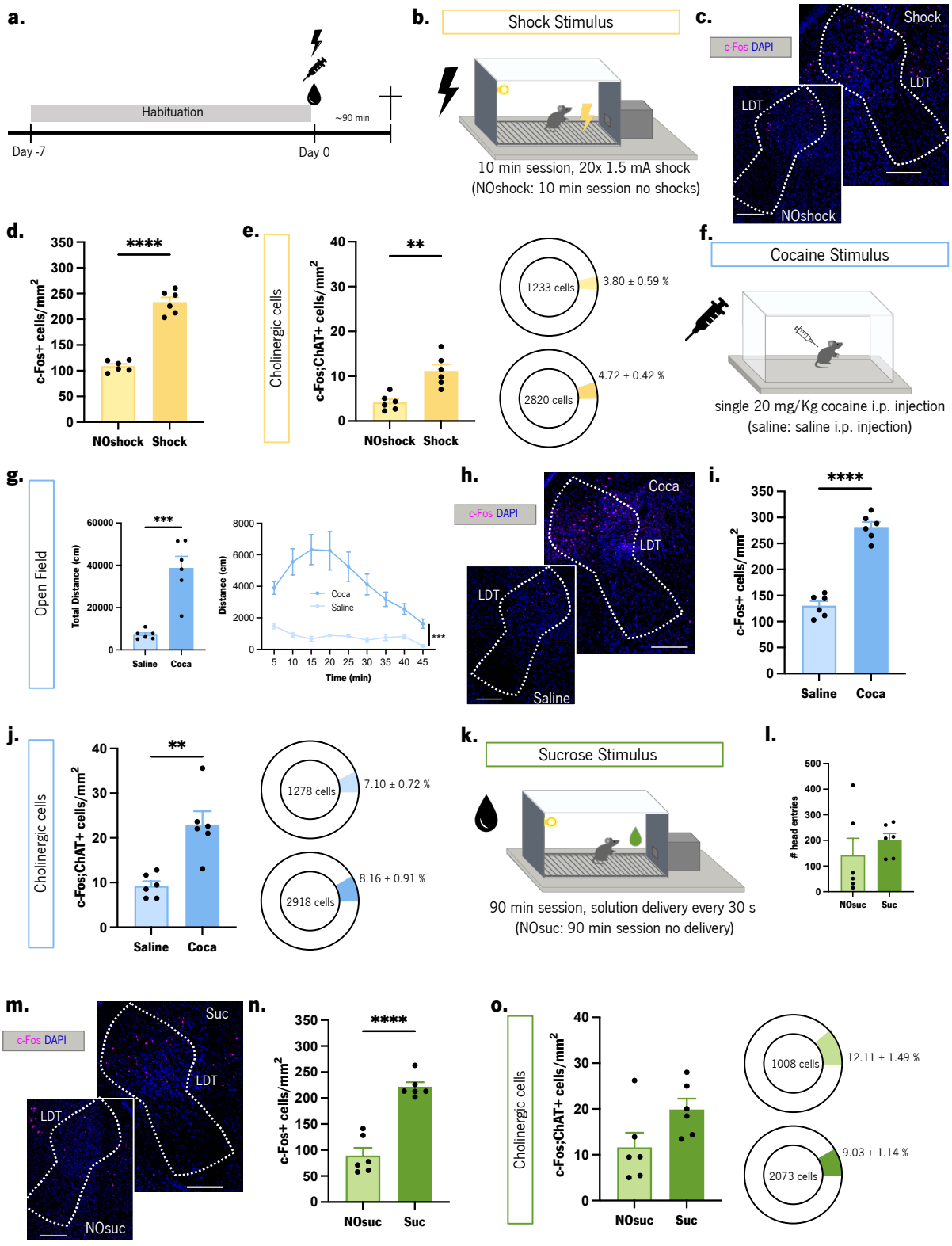


Figure 3- LDT cells are recruited in negative and positive valence events. **a.** Experimental timeline. Animals went through a 7-day habituation period. In the case of the Coca and Saline group, they were additionally habituated to an i.p. injection. On day 0, the animals were exposed to footshocks, cocaine or sucrose solution and sacrificed for endogenous c-Fos detection. **b**. Shock stimulus consisted of a 10 min session with 1.5 mA shock delivered every 30 seconds (control group: 10 min session with no shocks). **c**. Representative c-Fos+ immunofluorescence images showing endogenous c-Fos expression in

the LDT of NOshock and Shock animals. Scale bar 200 μm. **d**. Shock induced c-Fos+ cell density in the LDT (NOshock, n = 6, 109.0 ± 4.4 cells/mm^2; Shock, n = 6, 233.2 ± 9.3 cells/mm^2). **e**. Left: shock induced c-Fos;ChAT+ cell density in the LDT (NOshock, n = 6, 4.16 ± 0.72 cells/mm^2; Shock, n = 6, 11.19 ± 1.42 cells/mm^2). Right: pie chart quantification of extent of which c-Fos+ cells are ChAT+ (top: NOshock, n = 6, pooled data; bottom: Shock, n = 6, pooled data, *i.e.* sum of cells from all animals of the group). **f**. Cocaine stimulus consisted of a single cocaine injection at a dose of 20 mg/Kg (control group: saline injection). **g**. Cocaine enhanced locomotion in the open field. Left: total distance (cm) (saline, n = 6, 7176 ± 888 cm; coca, n = 6, 38775 ± 5467 cm). Right: distance (cm) traveled during the OF (saline, n = 6; coca, n = 6; two-way ANOVA: Time x Group $F(8, 80) = 11.67$ $p < 0.0001$, Time $F(8,80) = 14.94$ $p < 0.0001$; Group $F(1, 10) = 32.55$ $p = 0.0002$). **h**. Representative c-Fos+ immunofluorescence images showing endogenous c-Fos expression in the LDT of Saline and Coca animals. Scale bar 200 μm. **i**. Cocaine induced c-Fos+ cell density in the LDT (Saline, n = 6, 130.6 ± 8.6 cells/mm^2; Coca, n = 6, 281.6 ± 10.0 cells/mm^2). **j**. Left: cocaine induced c-Fos;ChAT+ cell density in the LDT (Saline, n = 6, 9.24 ± 1.07 cells/mm^2; Coca, n = 6, 23.00 ± 2.95 cells/mm^2). Right: pie chart quantification of extent of which c-Fos+ cells are ChAT+ (top: Saline, n = 6, pooled data; bottom: Cocaine, n = 6, pooled data). **k**. Sucrose stimulus consisted of a 90 min session with sucrose solution drop delivered every 30 seconds (control group: 90 min session with no solution). **l**. Number of head entries in the magazine performed during the sucrose session (NOsuc: n = 6, 142.0 ± 66.1 entries; Suc: n = 6, 201.5 ± 25.5 entries) **m**. Representative c-Fos+ immunofluorescence images showing endogenous c-Fos expression in the LDT of NOsuc and Suc animals. Scale bar 200 μm. **n**. Sucrose induced c-Fos+ cell density in the LDT (NOsuc, n = 6, 89.52 ± 14.69 cells/mm^2; Suc, n = 6, 221.7 ± 8.8 cells/mm^2). **o**. Left: sucrose induced c-Fos;ChAT+ cell density in the LDT (NOsuc, n = 6, 11.61 ± 3.21 cells/mm^2; Suc, n = 6, 19.90 ± 2.35 cells/mm^2). Right: pie chart quantification of extent of which c-Fos+ cells are ChAT+ (top: NOsuc, n = 6, pooled data; bottom; Suc, n = 6, pooled data). $^{**}p \leq 0.01$, $^{***}p \leq 0.001$, $^{****}p \leq 0.0001$. Data are represented as mean ± SEM.

4.2. Overlap/segregation of LDT ensembles representing distinct valence events

Another possible approach to dissect neuronal ensembles is using transgenic mouse lines to permanently label/tag neurons active during a specific event based on IEGs, like the TRAP2 mouse model (DeNardo and Luo, 2017; DeNardo *et al.*, 2019). The TRAP2 model (also known as Fos-TRAP) uses the *Fos* locus to drive the expression of a tamoxifen-inducible Cre-recombinase (*Fos*$^{2A\text{-}iCreERT2}$/TRAP2 allele). This can be combined with a transgenic (**Figure 4a**) or virally-delivered (**Figure 4b**) recombinase-dependent effector such as a fluorescent protein like tdTomato. Thus, only when cells are activated (c-Fos is active so Cre is expressed), and in the presence of tamoxifen, the CreERT2 is translocated to the nucleus and catalyzes recombination, allowing the permanent expression of the effector protein and, therefore, genetic access to transiently active cells upon exposure to a stimulus ('TRAPed' cells). In the TRAP2;Ai14 double transgenic mice, the TRAPed cells express the fluorescent protein tdTomato after neuronal activity (*fos* induction) but only when tamoxifen is administrated. This allows to assess the number of cells activated by two separate stimuli in the same animal. Thus, cells activated by a first stimulus in the presence of tamoxifen will be tdTomato-positive (tdTomato+) and cells activated by a second stimulus later will be

endogenous c-Fos+ (green), allowing the study of overlap or segregation between ensembles representing separate events (Allen *et al.*, 2017; Bobadilla *et al.*, 2020; DeNardo *et al.*, 2019).

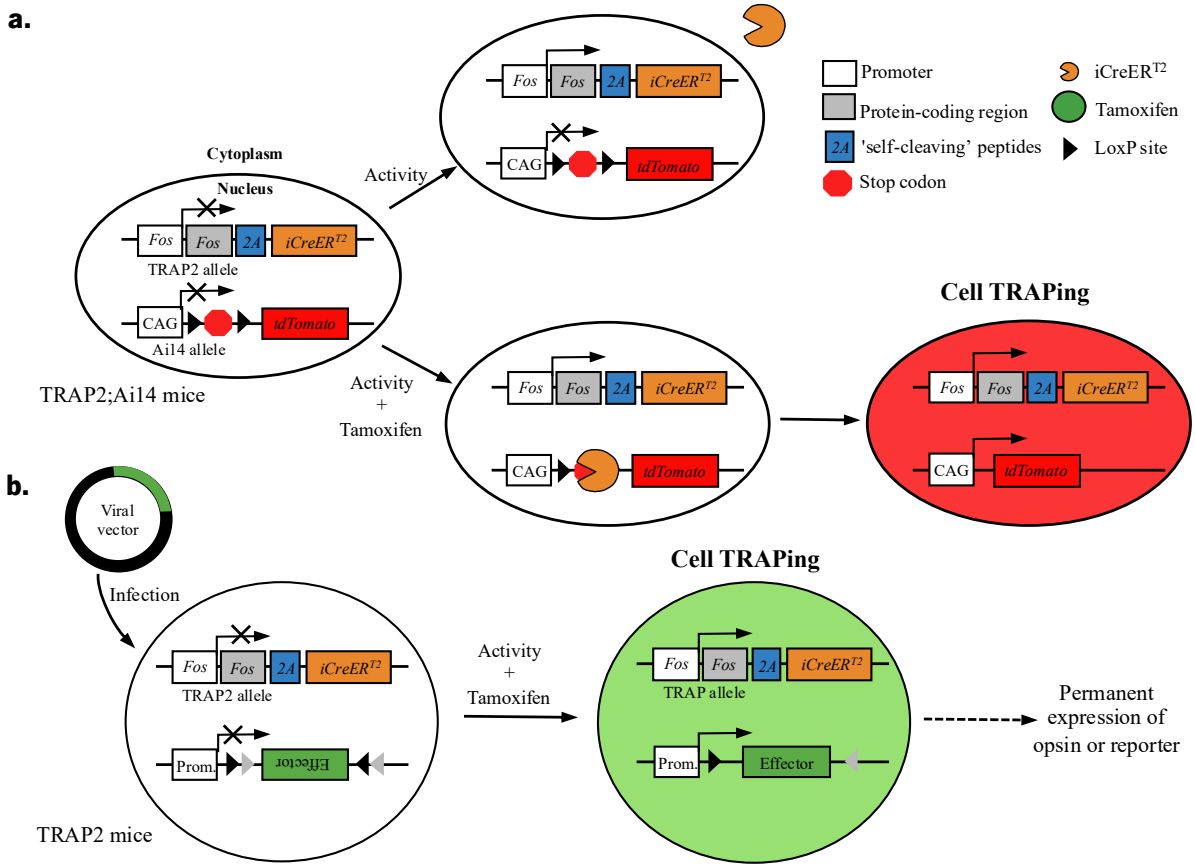


Figure 4- TRAP system. a. The immediate early gene *Fos* locus drives the expression of tamoxifen-inducible Cre recombinase (iCreERT2) that, after recombination, will allow the expression of the red fluorescent protein, tdTomato, of the Rosa 26 locus, in TRAP2;Ai14 double transgenic mice. **b**. Additionally, in TRAP2 mice, a viral vector encoding a Cre-dependent effector can be used. Based on (DeNardo and Luo, 2017; DeNardo *et al.*, 2019; Guenthner *et al.*, 2013).

In order to investigate whether the LDT ensembles recruited for positive or negative stimuli are overlapping or segregated, TRAP2;Ai14 double transgenic mice were exposed to different pairs of stimuli as depicted in **Figure 5b**. Cell density of single positive cells (tdTomato- or c-Fos-positive) and double positive cells were determined. Additionally, the percentage of tdTomato+ cells (cells responsive to the first stimulus) that also responded to the second stimulus (specificity: double+/tdTomato+) and the percentage of c-Fos+ cells (cells responsive to the second stimulus) that were active during the first stimulus (efficiency: double+/c-Fos+) were determined.

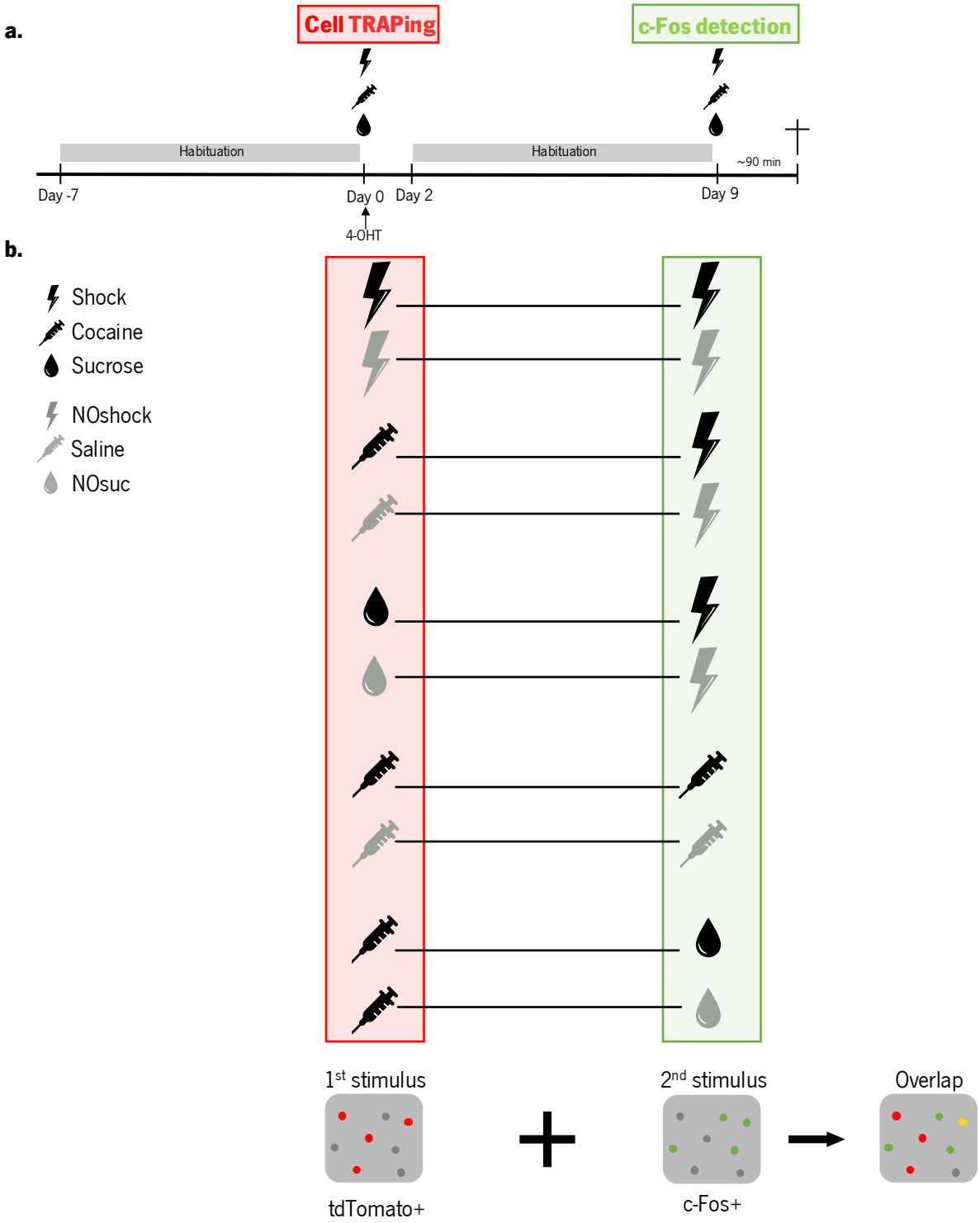


Figure 5- Experimental design of the TRAPing and overlap of LDT ensembles representing distinct valence events experiment. a. Experimental timeline. Animals went through a 7-day habituation period in which they were familiarized daily to the apparatus where they would receive the stimulus on the experimental day. In the case of the Coca and Saline group, they were habituated to i.p. injection before being isolated in individual boxes for 1 hour. On day 0, the animals were exposed to footshocks, cocaine or sucrose and, immediately after stimulus ending, they were injected with 4-OHT and kept individualized for 6 hours. Following a 2-day break, for safety precaution due to tamoxifen, animals underwent a new period of habituation and, on day 9, were exposed to a second stimulus. Approximately 90 minutes after stimulus ending, they were sacrificed for endogenous c-Fos detection: 90 minutes after shock stimulus session ending, 90 minutes after

cocaine/saline injection and 60 min after sucrose stimulus session ending. **b**. Experimental groups. 10 mice groups received different pairs of stimuli: Shock-Shock, NOshock-Noshock, Coca-Shock, Saline-NOshock, Suc-Shock, NOsuc-NOshock, Coca-Coca, Saline-Saline, Coca-Suc and Coca-NOsuc. Cells representing the first stimulus were captured with TRAPing and, therefore, are tdTomato+ and cells representing the second stimulus were captured with endogenous c-Fos detection following immunofluorescence (c-Fos+). These two independent ensembles can be overlapped in every single animal in order to determine the degree of segregation of the two representations/ensembles. To verify the TRAPing dependence of tamoxifen, an additional group was exposed to shock but did not receive 4-OHT after. Red depicts TRAPing, green depicts c-Fos and yellow is the overlap of the two.

4.2.1. Positive control for valence encoding: Amygdala

Firstly, to verify if the mouse model TRAP2 could be used to detect the recruitment of cells for the positive and negative stimuli that we used, we quantified tdTomato+ cells in the Amygdala, considering the well-known response of this region in response to valence-related stimuli (Gore *et al.*, 2015; Zhang and Li, 2018).

As seen by the tdTomato+ cell density, footshock significantly activated the Basolateral (BLA) subregion (NOshock *vs.* Shock $p = 0.02$) but not the Central nucleus (CeA) subregion (NOshock *vs.* Shock $p = 0.18$) (**Figure 6a-c**).

Cocaine showed a tendency to increase the locomotion of wild-type animals however, we did not perform the validity of cocaine in sufficient animals to apply statistics (**Figure 6d**). Furthermore, it increased tdTomato+ cells in both the BLA ($t(8) = 5.61$, $p = 0.0005$) and CeA ($t(8) = 3.27$, $p = 0.0114$) (**Figure 6e-g**).

Contrarily, although animals receiving sucrose performed significantly more magazine visits (**Figure 6h**; U (40, 186) = 2, $p = 0.0317$), the natural reward did not increase cell activation in neither subregion (BLA, $t(8) = 1.14$, $p = 0.2864$; CeA, $t(8) = 1.15$, $p = 0.2831$).

To address possible concerns regarding unspecific TRAPing, an additional group of animals was exposed to the shock stimulus without tamoxifen administration. Only a residual number of amygdala cells were TRAPed after shock exposure in the absence of 4-OHT (**Figure 6a-c**), confirming the tamoxifen-dependent nuclear translocation of Cre.

Together these data suggests that the model can successfully capture the recruitment of amygdalar ensembles for the shock and cocaine stimuli.

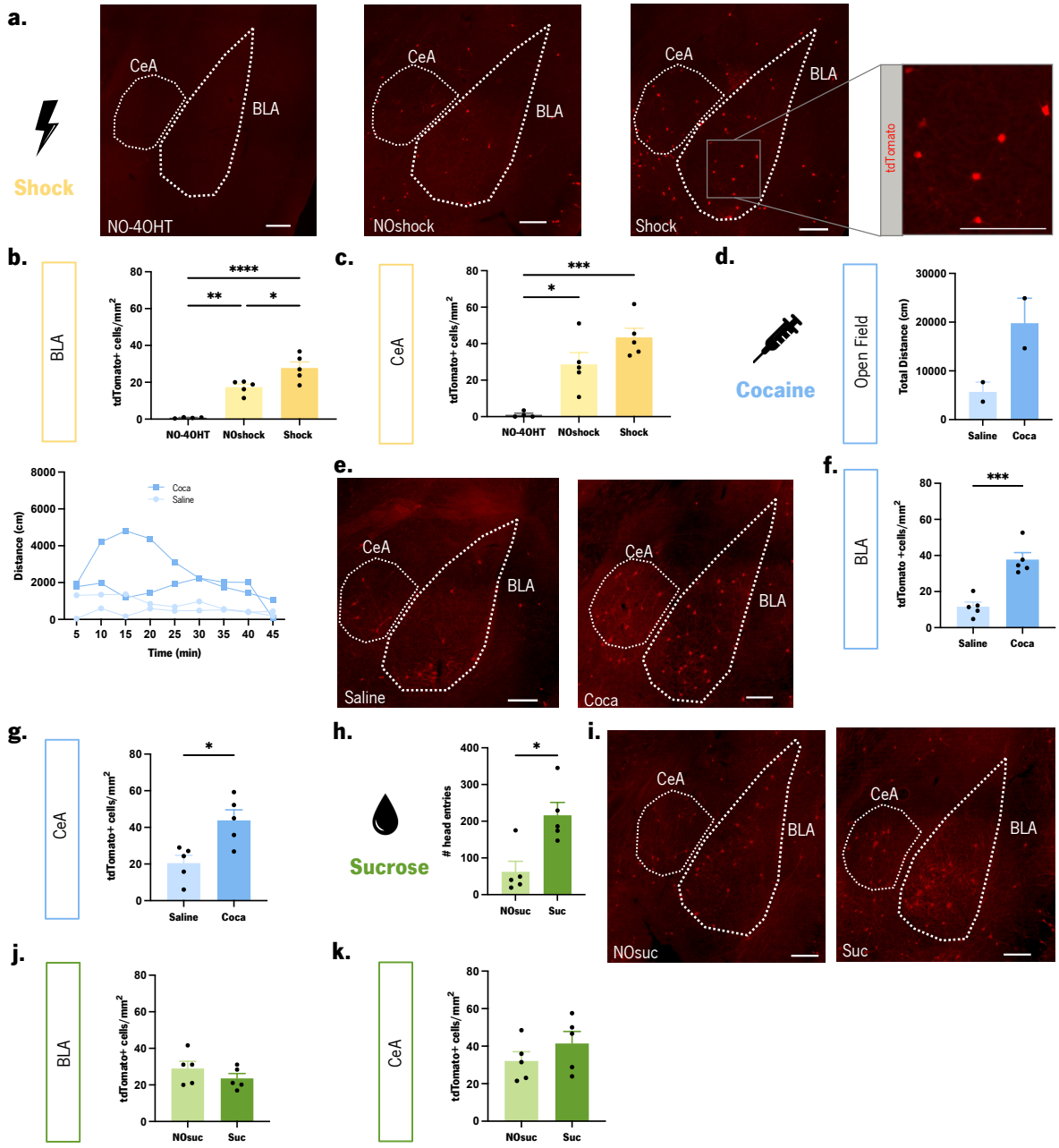


Figure 6- Amygdala recruitment for negative and positive stimuli is detected by TRAPing. **a**. Representative images showing tdTomato expression in the amygdala of tamoxifen-dependence recombination control group (NO-4OHT), NOshock and Shock animals. Scale bar 200 µm. **b**. Shock induced tdTomato+ cell density in the BLA (NO-4OHT, n = 4, 0.750 ± 0.143 cells/mm^2, NOshock, n = 5, 17.38 ± 3.25 cells/mm^2; Shock, n = 5, 27.76 ± 1.66 cells/mm^2; one-way ANOVA: F (2,11) = 33.64, $p < 0.0001$, NO-4OHT vs. NOshock $p = 0.0011$, NO-4OHT vs. Shock $p < 0.0001$). **c**. Shock induced tdTomato+ cell density in the CeA (NO-4OHT, n = 4, 1.07 ± 0.810 cells/mm^2, NOshock, n = 5, 28.61 ± 6.52 cells/mm^2; Shock, n = 5, 43.41 ± 5.02 cells/mm^2; one-way ANOVA: F (2,11) = 16.31, $p = 0.0005$, NO-4OHT vs. NOshock $p = 0.0107$, NO-4OHT vs. Shock p = 0.0004). **d**. Cocaine enhanced locomotion in the open field of wild-type animals. Up: total distance (cm) (Saline, n = 2, 5693 ± 2002 cm; Coca, n = 2, 19779 ± 5131 cm). Bottom: distance (cm) traveled during the OF (Saline, n = 2; Coca, n = 2; not enough animals to apply statistics). **e**. Representative images showing tdTomato expression in Saline and Coca animals. Scale bar 200 µm. **f**. Cocaine induced tdTomato+ cell density in the BLA (Saline, n = 5, 11.63 ± 2.53 cells/mm^2;

Coca, n = 5, 37.72 ± 3.90 cells/mm^2). **g**. Cocaine induced tdTomato+ cell density in the CeA (Saline, n = 5, 20.46 ± 4.25 cells/mm^2; Coca, n = 5, 43.82 ± 5.76 cells/mm^2). **h**. Number of head entries in the magazine performed during the sucrose session (NOsuc: n = 5, 62.20 ± 28.66 entries; Suc: n = 5, 216.2 ± 34.81 entries). **i**. Representative images showing tdTomato expression in NOsuc and Suc animals. Scale bar 200 μm. **j**. Sucrose induced tdTomato+ cell density in the BLA (NOsuc, n = 5, 28.98 ± 3.94 cells/mm^2; Suc, n = 5, 23.55 ± 2.65 cells/mm^2). **k**. Sucrose induced tdTomato+ cell density in the CeA (NOsuc, n = 5, 32.12 ± 4.89 cells/mm^2; Suc, n = 5, 41.41 ± 6.43 cells/mm^2). *$p \leq 0.05$, **$p \leq 0.01$, ***$p \leq 0.001$, ****$p \leq 0.0001$. Data are represented as mean ± SEM.

4.2.2. TRAPing of LDT ensembles responsive to negative- and positive-valence stimuli

TRAPing experiment with the order of the two stimuli is depicted in **Figure 5**.

Regarding the first stimulus, footshock significantly activated the LDT as seen by the tdTomato+ cell density (**Figure 7a and b**; NOshock vs. Shock $p = 0.003$). Cell density of tdTomato;ChAT+ cells was not statistically altered by the shock stimulus (**Figure 7c left**.; Cell density: $t(8) = 1.18$ $p = 0.271$). The shock-reactive ensemble was composed by 12 % of ChAT cells (**Figure 7c right**).

The cocaine stimulus increased TRAPing in the LDT (**Figure 7d and e**; $t(18) = 7.26$ $p < 0.0001$) and recruited cholinergic cells as seen by cell density (U (15, 195) = 0, $p = 0.0001$) (**Figure 7f left**). Around 23 % of the cells of the cocaine ensemble were cholinergic (**Figure 7f right**).

There was only a tendency for the sucrose stimulus to activate the LDT (**Figure 7h**; $t(8) = 2.14$ $p = 0.0644$). Additionally, no differences in the recruitment of cholinergic cells were detected (**Figure 7i left**; $t(8) = 0.016$ $p = 0.987$). 19 % of TRAPed cells upon sucrose exposure were ChAT+ (**Figure 7i right**).

These results indicate that the mouse model can be used to capture the footshock and cocaine-responsive LDT ensembles (LDT_{shock}– and $LDT_{cocaine}$-ensembles, respectively).

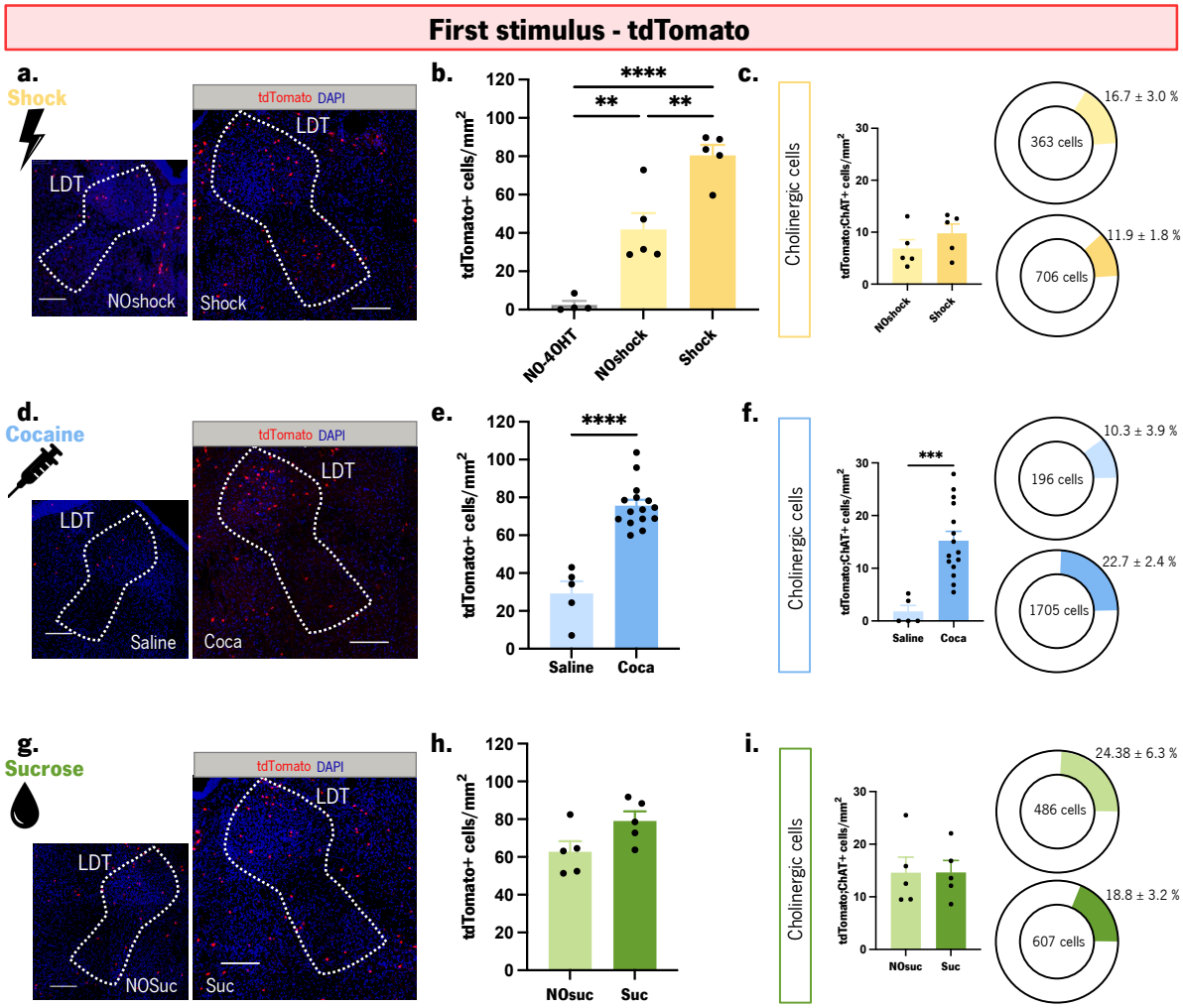


Figure 7- LDT recruitment for negative and positive events is detected by TRAPing. **a.** Representative images showing tdTomato expression in the LDT of NOshock and Shock animals (**Annex 2** for NO-4OHT representative image). Scale bar 200 µm. **b.** Shock induced tdTomato+ cell density (NO-4OHT, n = 4, 2.58 ± 2.02 cells/mm², NOshock, n = 5, 41.83 ± 9.48 cells/mm²; Shock, n = 5, 80.46 ± 5.49 cells/mm²; one-way ANOVA: F (2,11) = 35.63, $p < 0.0001$, NO-4OHT vs. NOshock $p = 0.0041$, NO-4OHT vs. Shock $p < 0.0001$). **c.** Left: shock induced tdTomato;ChAT+ cell density (NOshock, n = 5, 6.85 ± 1.71 cells/mm²; Shock, n = 5, 9.79 ± 1.80 cells/mm²). Right: pie chart quantification of extent of which tdTomato+ cells are ChAT+ (top: NOshock, n = 5, pooled data; bottom: Shock, n = 5, pooled data). **d.** Representative images showing tdTomato expression in Saline and Coca animals. Scale bar 200 µm. **e.** Cocaine induced tdTomato+ cell density (Saline, n = 5, 29.30 ± 6.33 cells/mm²; Coca, n = 15, 75.69 ± 3.05 cells/mm²). Coca values were pooled from Coca-Shock, Coca-NOsuc and Coca-Suc groups. **f.** Left: cocaine induced tdTomato;ChAT+ cell density (Saline, n = 5, 1.81 ± 1.13 cells/mm²; Coca, n = 15, 15.24 ± 1.78 cells/mm²). Right: pie chart quantification of extent of which tdTomato+ cells are ChAT+ (top: Saline, n = 5, pooled data; bottom: Coca, n = 15, pooled data). Coca values were pooled from Coca-Shock, Coca-NOsuc and Coca-Suc groups. **g.** Representative images showing tdTomato expression in NOsuc and Suc animals. Scale bar 200 µm. **h.** Sucrose induced tdTomato+ cell density (NOsuc, n = 5, 62.80 ± 5.59 cells/mm²; Suc, n = 5, 79.04 ± 5.11 cells/mm²). **i.** Left: sucrose induced tdTomato;ChAT+ cell density (NOsuc, n = 5, 14.58 ± 2.97 cells/mm²; Suc, n = 5, 14.64 ± 2.28 cells/mm²). Right: pie chart

quantification of extent of which tdTomato+ cells are ChAT+ (top: NOsuc, n = 5, pooled data; bottom: Suc, n = 5, pooled data). $^{**}p \leq 0.01$, $^{***}p \leq 0.001$, $^{****}p \leq 0.0001$. Data are represented as mean ± SEM.

Regarding the second stimulus, assessed by endogenous c-Fos detection (**Figure 8a**), shock increased the density of cells activated in the three groups exposed to this event (**Figure 8b, d and f;** $t(8) = 3.943$, $p = 0.0043$; $t(8) = 3.800$, $p = 0.0052$; $t(8) = 2.757$, $p = 0.0248$; respectively). Shock also increased the density of c-Fos;ChAT+ cells (**Figure 8 c and g**; $t(8) = 2.503$, $p = 0.0368$; U (17, 38) = 2, $p = 0.0317$; respectively), except in the group that was previously exposed to cocaine (Coca-Shock), that showed a similar density as its respective control (Saline-NOshock group) (**Figure 8e;** $t(8) = 0.1262$, $p = 0.9027$). As for percentage of c-Fos-expressing ChAT cells, the groups previously exposed to cocaine or sucrose had a similar proportion of cholinergic cells (**Figure 8e and g right**). The group first exposed to shock exhibited a lower percentage of shock-activated cells that were cholinergic in nature compared to the previously mentioned two groups (**Figure 8c right**).

In addition, cocaine increased the cell density of c-Fos+ cells (**Figure 8h**; $t(8) = 3.899$, $p = 0.0046$) and led to a slight, but not significant, increase in c-Fos;ChAT+ cell density (**Figure 8i left**, $t(8) = 1.874$, $p = 0.0978$). Cocaine exposure did not elicit a change in the percentage of recruited cholinergic cells (**Figure 8i right**).

Finally, sucrose, after a previous cocaine exposure, elicited a significant seeking behavior (**Figure 8j**; $t(8) = 3.471$, $p = 0.0084$), showed a tendency to recruit LDT cells (**Figure 8k**; $t(8) = 1.906$, $p = 0.0931$) and activated cholinergic cells, as seen by both cell density (**Figure 8l left**; $t(8) = 2.506$, $p = 0.0366$). Almost one third of TRAPed cells, in the Suc group, were immunoreactive for ChAT (**Figure 8l right**).

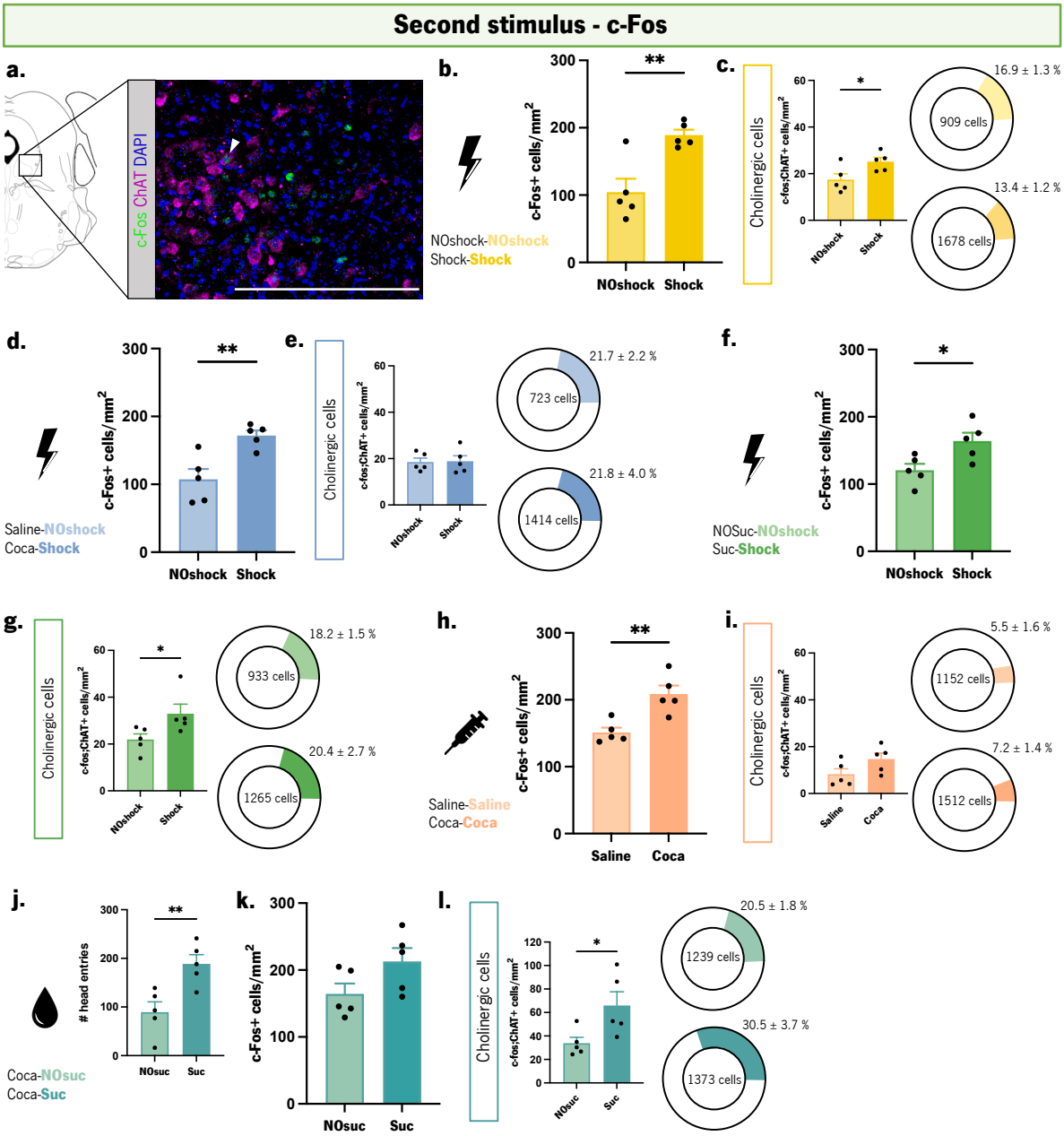


Figure 8- LDT recruitment for negative and positive events - endogenous c-Fos. **a**. Representative images showing c-Fos and ChAT immunofluorescence in the LDT. Scale bar 200 µm. **b**. Shock induced c-Fos+ cell density, NOshock-NOshock and Shock-Shock groups (NOshock, n = 5, 104.4 ± 19.9 cells/mm²; Shock, n = 5, 189.0 ± 8.0 cells/mm²). **c**. Left: shock induced c-Fos+;ChAT cell density, NOshock-NOshock and Shock-Shock groups (NOshock, n = 5, 17.41 ± 2.53 cells/mm²; Shock, n = 5, 25.15 ± 1.78 cells/mm²). Right: pie chart quantification of extent of which c-Fos+ cells are ChAT+, NOshock-NOshock and Shock-Shock groups (top: NOshock, n = 5, pooled data; bottom: Shock, n = 5, pooled data). **d.** Shock induced c-Fos+ cell density, Saline-NOshock and Coca-Shock groups (NOshock, n = 5, 107.3 ± 15.3 cells/mm²; Shock, n = 5, 172.0 ± 7.5 cells/mm²). **e**. Left: shock induced c-Fos;ChAT+ cell density, Saline-NOshock and Coca-Shock groups (NOshock, n = 5, 18.51 ± 1.74 cells/mm²; Shock, n = 5, 18.88 ± 2.37 cells/mm²). Right: pie chart quantification of extent of which c-Fos+ cells are ChAT+, Saline-NOshock and Coca-Shock groups (top: NOshock, n = 5, pooled data; bottom: Shock, n = 5, pooled data). **f**. Shock induced c-Fos+ cell density, NOsuc-NOshock and Suc-Shock groups (NOshock, n = 5, 120.5 ± 9.7 cells/mm²; Shock, n = 5, 164.0 ± 12.5 cells/mm²). **g**. Left: shock induced c-Fos;ChAT+ cell density, NOsuc-NOshock and Suc-Shock groups

(NOshock, n = 5, 21.91 ± 2.40 cells/mm²; Shock, n = 5, 32.91 ± 4.11 cells/mm²). Right: pie chart quantification of extent of which c-Fos+ cells are ChAT+, NOsuc-NOshock and Suc-Shock groups (top: NOshock, n = 5, pooled data; bottom: Shock, n = 5, pooled data). **h**. Cocaine induced c-Fos+ cell density, Saline-Saline and Coca-Coca groups (Saline, n = 5, 151.2 ± 7.1 cells/mm²; Coca, n = 5, 208.5 ± 12.9 cells/mm²). **i**. Left: cocaine induced c-Fos;ChAT+ cell density, Saline-Saline and Coca-Coca groups (Saline, n = 5, 8.22 ± 2.36 cells/mm²; Coca, n = 5, 14.73 ± 2.55 cells/mm²). Right: pie chart quantification of extent of which c-Fos+ cells are ChAT+, Saline-Saline and Coca-Coca groups (top: Saline, n = 5, pooled data; bottom: Coca, n = 5, pooled data). **j**. Number of head entries in the magazine performed during the sucrose session, Saline-NOsuc and Coca-Suc groups (NOsuc: n = 5, 89.4 ± 21.3 entries; Suc: n = 5, 188.6 ± 19.1 entries). **k**. Sucrose induced c-Fos+ cell density, Saline-NOsuc and Coca-Suc groups (NOsuc, n = 5, 164.3 ± 15.7 cells/mm²; Suc, n = 5, 212.8 ± 20.1 cells/mm²). **l**. Left: sucrose induced c-Fos;ChAT+ cell density, Saline-NOsuc and Coca-Suc groups (NOsuc, n = 5, 33.84 ± 5.05 cells/mm²; Suc, n = 5, 65.92 ± 11.76 cells/mm²). Right: pie chart quantification of extent of which c-Fos+ cells are ChAT+, Saline-NOsuc and Coca-Suc groups (top: NOsuc, n = 5, pooled data; bottom: Suc, n = 5, pooled data). *$p \leq 0.05$, **$p \leq 0.01$. Data are represented as mean ± SEM.

4.2.3. LDT ensembles representing distinct valence events

Next, to answer our main question of whether negative and positive stimuli (and different types of reward: natural vs. drug of abuse) activated different cells in the LDT, cell density of tdTomato;c-Fos positive cells (**Figure 9a**) and percentage of tdTomato+ cells reactivated by the second stimulus (specificity) were determined. Additionally, to verify if TRAPing was a faithful reporter of endogenous c-Fos activity, percentage of c-Fos+ cells that were active during the first stimulus (efficiency), in the groups exposed two times to the same stimulus, was determined.

Shock or cocaine stimuli followed by shock event, led to a significant increase in the density of tdTomato;c-Fos positive cells, compared to the density of overlap on the double negative controls (NOshock-Shock or Saline-NOshock) (**Figure 9b and c**; U (15, 40) = 0, $p = 0.0079$; U (17, 38) = 2, $p = 0.0317$; respectively), but not sucrose (**Figure 9d**; t (8) = 0.09448, $p = 0.9270$).

Cocaine stimulus followed by another cocaine event, increased the cell density of tdTomato;c-Fos+ cells, compared to its double negative control (Saline-Saline) (**Figure 9e**; t (8) = 3.185, $p = 0.0129$). Cocaine followed by sucrose or sucrose control session resulted in a tendency for higher tdTomato;c-Fos cell density in the group exposed to sucrose (**Figure 9f**; U (19, 36) = 4, $p = 0.0952$).

When we calculated the percentage of cells reactivated to the second stimulus (number of tdTomato;c-Fos+/number of tdTomato+), we observe that it was significantly higher in the groups exposed to the same stimuli (**Figure 9g**; Shock-Shock *vs.* Coca-Shock: $p < 0.0001$; Coca-Coca *vs.* Coca-Shock: $p < 0.0001$). For example, ~ 40% of cells activated in shock (first stimulus; TRAPed cells) are also activated during the second shock exposure (c-Fos+; **Figure 9g)**. Similarly, ~ 40% of cells that are

activated to cocaine are also activated during the second cocaine exposure (**Figure 9g)**. This percentage is lower when we combine stimuli of different natures (Shock-Shock *vs.* Suc-Shock: $p < 0.0001$; Coca-Coca *vs.* Coca-Suc: $p = 0.0016$).

Comparing labelled cells by TRAPing and by endogenous c-Fos staining (same stimulus, 9 days apart), the efficiency of TRAPing (percentage of c-Fos+ cells that are tdTomato+) was around 20 % (**Figure 9h**).

This data suggests that, in the LDT, the aversive stimulus shock and the rewarding stimulus cocaine recruit mainly different cell ensembles.

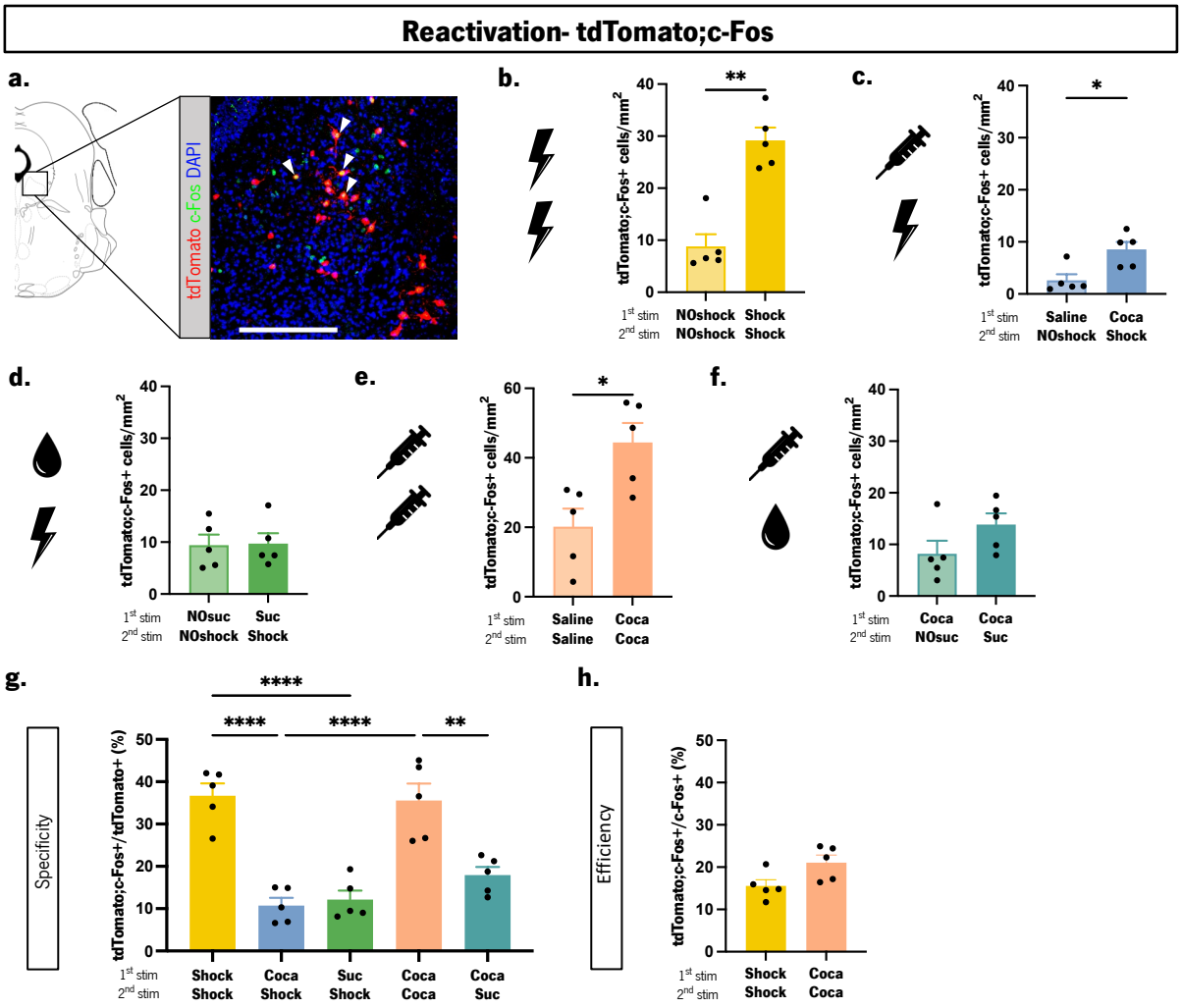


Figure 9- Shock and cocaine mainly recruit segregated ensembles in the LDT. a. Representative image showing tdTomato expression and c-Fos staining overlap in the LDT. Scale bar 200 µm. **b.** Cell density of cells expressing tdTomato and c-Fos in mice that underwent two shock stimuli, or two shock control sessions (NOshock-NOshock: 8.827 ± 2.337 cells/mm², Shock-Shock: 29.19 ± 2.446 cells/mm²). **c.** Cell density of cells expressing tdTomato and c-Fos in mice that underwent a cocaine injection and shock stimulus, or saline injection and shock control session (Saline-NOshock: 2.616 ± 1.151 cells/mm², Coca-Shock: 8.549 ± 1.438 cells/mm²). **d.** Cell density of cells expressing tdTomato and c-Fos in mice that

underwent a sucrose session and shock stimulus, or sucrose and shock control sessions (NOsuc-NOshock: 2.616 ± 2.012 cells/mm^2, Suc-Shock: 9.701 ± 2.016 cells/mm^2). **e.** Cell density of cells expressing tdTomato and c-Fos in mice that underwent two cocaine injections, or two saline injections (Saline-Saline: 20.16 ± 5.212 cells/mm^2, Coca-Coca: 44.44 ± 5.561 cells/mm^2). **f.** Cell density of cells expressing tdTomato and c-Fos in mice that underwent a cocaine injection and sucrose session, or cocaine injection and control sucrose session control sessions (Coca-NOsuc: 8.185 ± 2.531 cells/mm^2, Coca-Suc: 13.85 ± 2.155 cells/mm^2). **g.** Percentage of ensemble reactivation (tdTomato;c-Fos+) expressed in function of the number of cells expressing tdTomato (one-way ANOVA: F (4, 20) = 22.00, $p < 0.0001$; Shock-Shock: 36.69 ± 2.900 %, Coca-Shock: 10.74 ± 1.837 %, Suc-Shock: 12.15 ± 2.136 %, Coca-Coca: 35.56 ± 4.022 %, Coca-Suc: 17.92 ± 1.930 %). **h.** Efficiency of LDT shock and cocaine TRAPing (Shock-Shock: 15.55 ± 1.464 %, Coca-Coca: 21.06 ± 1.793 %). *$p \leq 0.05$, **$p \leq 0.01$, ****$p \leq 0.0001$. Data are represented as mean ± SEM.

4.3. Optogenetic modulation of LDT-responsive ensembles

To explore the role of shock- and cocaine-responsive LDT ensembles in behavior, TRAP2 mice were injected in the LDT with the construct AVV5-DIO-ChR2-eYFP and implanted with an optical fiber in the LDT for optogenetic modulation of these neuronal ensembles (**Figure 10a left**). One week later, animals underwent a 7-day habituation and at the end of that period, *i.e.* 2 weeks after surgery, animals were exposed to either shock or cocaine and, right after, injected with 4-OHT (**Figure 10a right**). In this way, we were able to express the opsin, selectively, in stimulus-responsive LDT cells. Four weeks later, to allow opsin expression, animals were tested in the behavioral tasks: real time place preference (**Figure 10b**) and conditioned place preference (**Figure 10f**) with optogenetic stimulation of responsive neurons.

Due to the low number of animals, we decided to join the saline and NOshock groups to form the CTR group. In theory, these animals are in *control conditions* and should present similar degree of TRAPed cells, as our anatomical data confirms (**Figure 11**).

Optogenetic activation of cocaine-responsive neurons did not induce preference in the RTPP paradigm, as seen by time on the ON chamber (**Figure 10c**; $t(6) = 0.05986$, $p = 0.9542$) and the difference in time spent in the ON chamber and the OFF chamber (**Figure 10d**; $t(6) = 0.05986$, $p = 0.9542$). In addition, there was not a statistically significant difference in number of entries in the ON chamber when activating the cocaine-responsive cells (**Figure 10e**; $t(6) = 1.032$, $p = 0.3419$). Due to the low sample size, we could not apply statistics with the shock group.

We could not statistically analyze the CPP data considering that only one group had three or more animals (**Figure 10g**), because several animals lost the implant before behavioral evaluation.

These experiments have to be repeated with an adequate number of animals.

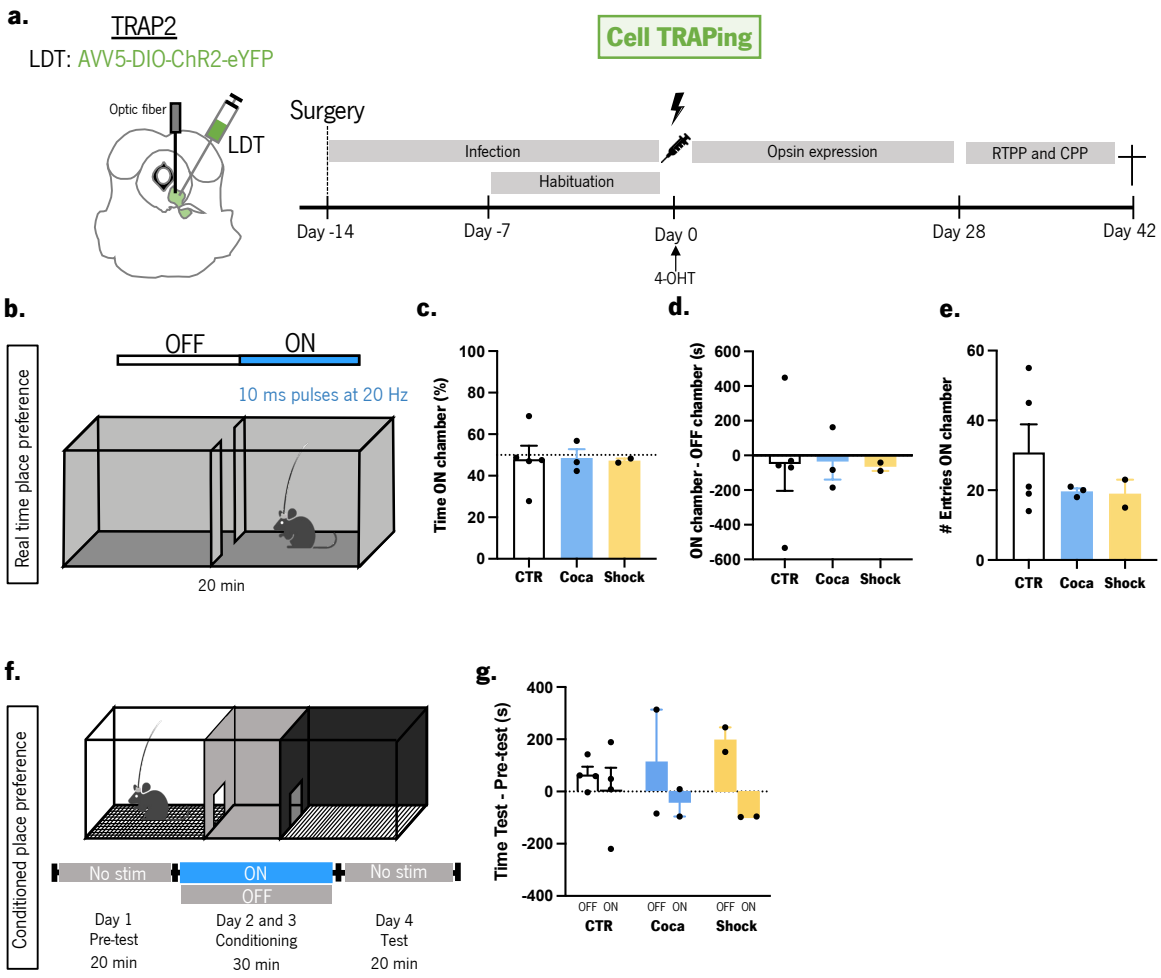


Figure 10- Optogenetic manipulation of LDT shock- and cocaine-responsive ensembles. **a**. Experimental design. Left: animals were injected with AVV5-DIO-ChR2-eYFP construct and implanted with an optic fiber in the LDT. Right: animals underwent a period of habituation one week after surgery, and posteriorly, exposed to either shock or cocaine. 4 weeks later, they were tested in the behavioral tasks RTPP and CPP. **b**. Schematic representation of the RTPP test with optogenetic stimulation protocol of 10 ms pulses at 20 Hz occurring in the stimulation (ON) side of the apparatus. **c**. Percentage of time spent on the ON side of the apparatus (CTR: n = 5, 47.95 ± 6.476 %; Coca: n = 3, 48.50 ± 4.304 %; Shock: n =2, 47.25 ± 1.00 %). **d**. Difference of time, in seconds, spent on the ON and OFF sides (CTR: n = 5, -49.20 ± 155.4 s; Coca: n = 3, -36.00 ± 103.3 %; Shock: n =2, -66.00 ± 24.00 s). **e**. Number of entries in the light-paired side during the 20 min test (CTR: n = 5, 30.80 ± 8.077 entries; Coca: n =2, 19.67 ± 0.88 entries; Shock: n = 3, 19.00 ± 4.00 entries). **f**. Schematic representation of the CPP test with optogenetic stimulation protocol of 80 10 ms pulses at 20Hz every 15s, occurring in the Stimulation (ON) chamber during the respective 30 min conditioning session (either session 1 or session 2 of the day 2 and 3). Pre- and pos-test sessions lasted 20 min. **g**. Difference between the time spent in each side of the apparatus in the post-test and the time spent in that same side in the pre-test (CTR: n = 5, 30.80 ± 8.077 entries; Coca: n =2, 19.67 ± 0.88 entries; Shock: n = 3, 19.00 ± 4.00 entries). Data are represented as mean ± SEM.

4.4. NAc innervation of LDT ensembles responsive to valence stimuli

The divergence of opposite valence-encoding ensembles has been studied in terms of genetics, functionality, and anatomy for other brain regions such as amygdala (Namburi *et al.*, 2016). Additionally, the LDT-NAc projections remain largely understudied. Therefore, in order to determine if the LDT ensembles reactive to shock or cocaine project differently to the NAc, TRAP2 mice were injected in the LDT with the construct AVV5-DIO-ChR2-eYFP (**Figure 11a left**). One week later, animals underwent a 7-day habituation and at the end of that period, *i.e.* 2 weeks after surgery, animals were exposed to either shock or cocaine and, right after, injected with 4-OHT (**Figure 11a right**). In this way, we were able to express the fluorescent reporter YFP selectively in stimulus-responsive LDT cells, and evaluate their terminals in the NAc. 6 weeks later, animals were sacrificed, the brains processed and LDT and NAc slices immunostained for YFP to check for LDT terminals.

In LDT, cell density of YFP+ cell bodies (**Figure 11b**) was determined. Shock significantly increased the number of YFP+ cells transfected cells and there was also a tendency for the Coca group to have a higher density of YFP+ cells (**Figure 11c**; $t(6) = 2.536$, $p = 0.0443$; $t(4) = 2.565$, $p = 0.0623$; respectively).

Next, in slices containing the NAc, innervation was quantified in the different NAc subregions (**Figure 11d**) and normalized to the LDT YFP+ cell density.

Regarding the negative-valence stimulus, shock-activated cells innervated significantly more the NAc than *control* cells (**Figure 11e**; $t(6) = 2.632$, $p = 0.0389$). The difference was significant only in more posterior coordinates, to where shock-responsive cells projected preferentially (**Figure 11f**; two-way ANOVA, Group effect: F (1, 6) = 10,95, $p = 0.0162$; Bregma effect: F (5, 27) = 3.507, $p = 0.0143$; multiple comparisons in **Table 3**). Interestingly, innervation was higher in the NAc shell subregion than the NAc core (**Figure 11g**; two-way ANOVA, Group effect: F (1, 6) = 6.349, $p = 0.0453$; Subregion effect: F (1, 6) = 62.56, $p = 0.0002$; multiple comparisons in **Table 3**). In the NAc core, there were no statistically significant differences in innervation along the anterior-posterior axis between the two groups although, a significant effect of Bregma was found (**Figure 11h**; two-way ANOVA, Group effect: F (1, 6) = 3.065, $p = 0.1306$; Bregma effect: F (5, 27) = 3.525, $p = 0.0140$; multiple comparisons in **Table 3**). In the NAc shell, the shock-responsive cells, comparing to control cells, had a higher innervation in more posterior coordinates. Furthermore, shock-responsive cells innervated more the posterior portion of the NAc shell (**Figure 11i**; Group effect: F (1, 33) = 16.21, $p = 0.0003$; Bregma: F (5, 33) = 2.982, $p = 0.0250$; multiple comparisons in **Table 3**). Within the NAc shell, there was a higher innervation by shock-responsive cells in the medial portion of this subregion, compared to control cells (**Figure 11j**; two-way

ANOVA, Group effect: F (1, 6) = 13.96, $p = 0.0097$; Medial—Lateral effect: F (1, 6) = 0.2644, $p = 0.2644$; multiple comparisons in **Table 3**).

Regarding the positive-stimulus (cocaine), there were no differences in total NAc innervation between the Coca and Saline groups (**Figure 11k**; $t(4) = 0.6300$, $p = 0.5629$). In addition, no statistical difference was found in innervation along the anterior-posterior axis between the two groups, although, in the Coca group, more fibers were present in the posterior coordinates (**Figure 11l**; two-way ANOVA, Group effect: F (1, 4) = 0.8750, $p = 0.4025$; Bregma effect: F (5, 16) = 10.86, $p = 0.0001$; multiple comparisons in **Table 3**). Finally, concerning the NAc subregions, no differences were found between the two groups or NAc subregions (**Figure 11m**; two-way ANOVA, Group effect: F (1, 4) = 0.3635, $p = 0.5791$; Subregion effect: F (1, 4) = 1.178, $p = 0.3388$).

Together this data indicates that shock-responsive LDT cells project to the NAc, preferentially to the posterior shell subregion. Cocaine-responsive cells do not appear to have preferential innervation of the NAc, although the number of animals was lower, and this group was very variable, so these results have to be interpreted with caution.

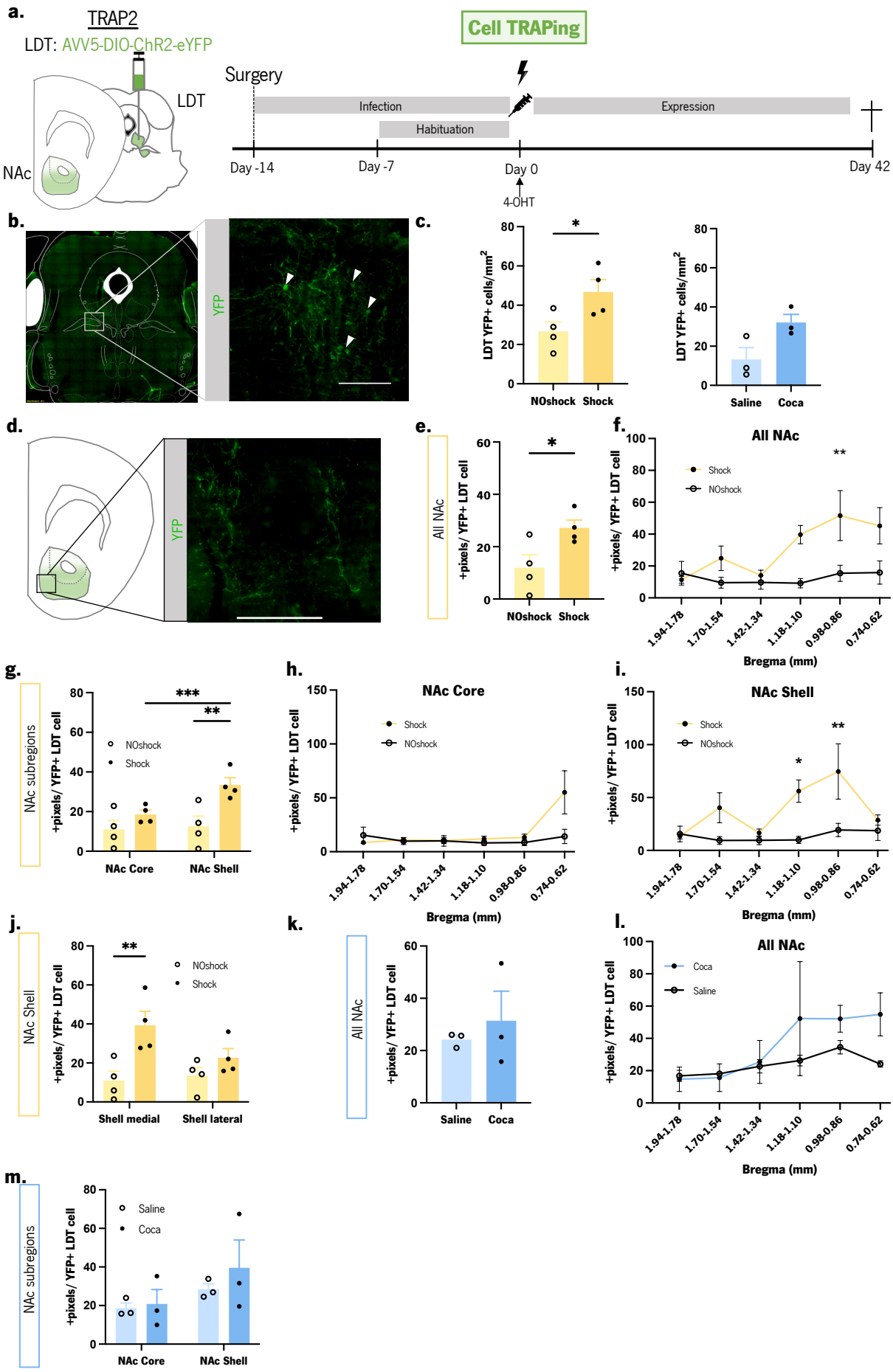

a.
TRAP2
LDT: AVV5-DIO-ChR2-eYFP
LDT
NAc
Cell TRAPing
Surgery
Infection
Habituation
Expression
Day -14
Day -7
Day 0
Day 42
4-OHT
b.
YFP
c.
LDT YFP+ cells/mm2
NOshock
Shock
Saline
Coca
d.
YFP
e.
All NAc
+pixels/ YFP+ LDT cell
NOshock
Shock
f.
All NAc
Shock
NOshock
+pixels/ YFP+ LDT cell
1.94-1.78
1.70-1.54
1.42-1.34
1.18-1.10
0.98-0.86
0.74-0.62
Bregma (mm)
g.
NAc subregions
+pixels/ YFP+ LDT cell
NOshock
Shock
NAc Core
NAc Shell
h.
NAc Core
Shock
NOshock
+pixels/ YFP+ LDT cell
Bregma (mm)
i.
NAc Shell
Shock
NOshock
+pixels/ YFP+ LDT cell
Bregma (mm)
j.
NAc Shell
+pixels/ YFP+ LDT cell
NOshock
Shock
Shell medial
Shell lateral
k.
All NAc
+pixels/ YFP+ LDT cell
Saline
Coca
l.
All NAc
Coca
Saline
+pixels/ YFP+ LDT cell
Bregma (mm)
m.
NAc subregions
+pixels/ YFP+ LDT cell
Saline
Coca
NAc Core
NAc Shell

Figure 11- Quantification of innervation of the NAc by LDT positive and negative-responsive cells. **a.** Experimental design. Left: animals were injected with AVV5-DIO-ChR2-eYFP construct in the LDT and in coronal slices of the NAc, YFP expression was analyzed. Right: animals underwent a period of habituation one week after surgery and, posteriorly, exposed to either shock or cocaine, being immediately after injected with 4-OHT. 6 weeks later, they were sacrificed. **b.** Representative image showing YFP expression in the LDT. Arrows indicate cell bodies. Scale bar 200 μm. **c.** Cell density of cells expressing YFP. Left: Shock stimulus (NOshock: n = 4, 26.69 ± 4.831 cells/mm^2; Shock: n = 4, 46.78 ± 6.281 cells/mm^2). Right: Cocaine stimulus (Saline: n = 3, 13.23 ± 6.058 cells/mm^2; Coca: n = 3, 32.08 ± 4.161 cells/mm^2). **d.** Representative image showing YFP-expressing fibers in the NAc. Scale bar 200 μm. **e.** All NAc quantification of normalized innervation (positive pixels per LDT transfected cell) by shock-responsive cells, or shock control session-activated cells (NOshock: n =4, 12.00 ± 4.915 +pixels/YFP LDT cell; Shock: n = 4, 27.16 ± 3.003 +pixels/YFP LDT cell; considered at least 7 slices per animal). **f.** All NAc normalized innervation by shock-responsive cells, or shock control session-activated cells along the anterior-posterior axis (coordinates in relation to the bregma; statistics in Table 3). **g.** NAc core and shell normalized innervation by shock-responsive cells, or shock control session-activated cells (NAc core: NOshock, n = 4, 11.03 ± 4.546 +pixels/YFP LDT cell; Shock: n = 4, 18.58 ± 2.213 +pixels/YFP LDT cell; NAc shell: NOshock, n = 4, 12.62 ± 33.45 +pixels/YFP LDT cell; Shock: n = 4, 55.20 ± 5.630 +pixels/YFP LDT cell; at least 7 slices per animal were considered). **h.** NAc core and **i.** NAc shell normalized innervation by shock-responsive cells, or shock control session-activated cells along the anterior-posterior axis (coordinates in relation to the bregma; statistics in Table 3). **j.** NAc medial shell and lateral shell normalized innervation by shock-responsive cells, or shock control session-activated cells (NAc medial shell: NOshock, n =4, 10.98 ± 4.877 +pixels/YFP LDT cell; Shock: n = 4, 39.27 ± 7.218 +pixels/YFP LDT cell; NAc lateral shell: NOshock, n =4, 13.60 ± 4.078 +pixels/YFP LDT cell; Shock: n = 4, 22.73 ± 4.634 +pixels/YFP LDT cell; statistics in Table 3). **k.** All NAc quantification of normalized innervation by cocaine-responsive cells, or saline injection-activated cells (Saline: n =3, 24.24 ± 1.616 +pixels/YFP LDT cell; Coca: n = 3, 31.43 ± 11.30 +pixels/YFP LDT cell; there were considered at least 7 slices per animal). **l.** All NAc normalized innervation by cocaine-responsive cells, or saline injection-activated cells along the anterior-posterior axis (coordinates in relation to the bregma; statistics in Table 3). **m.** NAc core and shell normalized innervation by cocaine-responsive cells, or saline injection-activated cells (NAc core: Saline, n =3, 18.62 ± 2.668 +pixels/YFP LDT cell; Coca: n = 3, 20.83 ± 7.499 +pixels/YFP LDT cell; NAc shell: Saline, n = 3, 28.42 ± 2.783 +pixels/YFP LDT cell; Coca: n = 3, 39.55 ± 14.41 +pixels/YFP LDT cell; at least 7 slices per animal were considered). *$p \leq 0.05$, **$p \leq 0.01$, ***$p \leq 0.001$. Data are represented as mean ± SEM.

Table 3 – Mixed effects models statistical report. $p \leq 0.05$, **$p \leq 0.01$, ***$p \leq 0.001$

Figure	Main Effects	Multiple comparisons
11f- All NAc	Group: F (1, 6) =	NOshock-Shock
	10.95, $p = 0.0162$	1.94-1.78, $p > 0.9999$
		1.70-1.54, $p = 0.8800$
		1.42-1.34, $p > 0.9999$
		1.18-1.10, $p = 0.0671$
		0.98-0.86, $p = 0.0078$ **

		0.74-0.62, $p = 0.0671$
	Bregma: F (5, 27) =	NOshock
	3.507, $p = 0.0143$	1.94-1.78 vs. 1.70-1.54, $p > 0.9999$
		1.94-1.78 vs. 1.42-1.34, $p > 0.9999$
		1.94-1.78 vs. 1.18-1.10, $p > 0.9999$
		1.94-1.78 vs. 0.98-0.86, $p > 0.9999$
		1.94-1.78 vs. 0.74-0.62, $p > 0.9999$
		1.70-1.54 vs. 1.42-1.34, $p > 0.9999$
		1.70-1.54 vs. 1.18-1.10, $p > 0.9999$
		1.70-1.54 vs. 0.98-0.86, $p > 0.9999$
		1.70-1.54 vs. 0.74-0.62, $p > 0.9999$
		1.42-1.34 vs. 1.18-1.10, $p > 0.9999$
		1.42-1.34 vs. 0.98-0.86, $p > 0.9999$
		1.42-1.34 vs. 0.74-0.62, $p > 0.9999$
		1.18-1.10 vs. 0.98-0.86, $p > 0.9999$
		1.18-1.10 vs. 0.74-0.62, $p > 0.9999$
		0.98-0.86 vs. 0.74-0.62, $p > 0.9999$
		Shock
		1.94-1.78 vs. 1.70-1.54, $p > 0.9999$
		1.94-1.78 vs. 1.42-1.34, $p > 0.9999$
		1.94-1.78 vs. 1.18-1.10, $p = 0.1878$
		1.94-1.78 vs. 0.98-0.86, $p = 0.0035$ **
		1.94-1.78 vs. 0.74-0.62, $p = 0.0203$ *
		1.70-1.54 vs. 1.42-1.34, $p > 0.9999$
		1.70-1.54 vs. 1.18-1.10, $p > 0.9999$
		1.70-1.54 vs. 0.98-0.86, $p = 0.1323$
		1.70-1.54 vs. 0.74-0.62, $p = 0.6092$
		1.42-1.34 vs. 1.18-1.10, $p = 0.3477$
		1.42-1.34 vs. 0.98-0.86, $p = 0.0075$ **
		1.42-1.34 vs. 0.74-0.62, $p = 0.0427$ *
		1.18-1.10 vs. 0.98-0.86, $p > 0.9999$
		1.18-1.10 vs. 0.74-0.62, $p > 0.9999$
		0.98-0.86 vs. 0.74-0.62, $p > 0.9999$
	Group x Bregma: F (5, 27) = 2.453, $p = 0.0589$	
11g- NAc subregions	Group: F (1, 6) = 6.349, $p = 0.0453$	NOshock-Shock
		NAc Core, $p = 0.4237$
		NAc Shell, $p = 0.0068$ **

	Subregion: F (1, 6) = 62.56, $p = 0.0002$	NAc Core-NAc Shell NOshock, $p = 0.6422$ Shock, $p = 0.0001$ ***
	Group x Subregion: F (1, 6) = 40.71, $p = 0.0007$	
11h- NAc core	Group: F (1, 6) = 3.065, $p = 0.1306$	
	Bregma: F (5, 27) = 3.525, $p = 0.0140$	NOshock 1.94-1.78 vs. 1.70-1.54, $p > 0.9999$ 1.94-1.78 vs. 1.42-1.34, $p > 0.9999$ 1.94-1.78 vs. 1.18-1.10, $p > 0.9999$ 1.94-1.78 vs. 0.98-0.86, $p > 0.9999$ 1.94-1.78 vs. 0.74-0.62, $p > 0.9999$ 1.70-1.54 vs. 1.42-1.34, $p > 0.9999$ 1.70-1.54 vs. 1.18-1.10, $p > 0.9999$ 1.70-1.54 vs. 0.98-0.86, $p > 0.9999$ 1.70-1.54 vs. 0.74-0.62, $p > 0.9999$ 1.42-1.34 vs. 1.18-1.10, $p > 0.9999$ 1.42-1.34 vs. 0.98-0.86, $p > 0.9999$ 1.42-1.34 vs. 0.74-0.62, $p > 0.9999$ 1.18-1.10 vs. 0.98-0.86, $p > 0.9999$ 1.18-1.10 vs. 0.74-0.62, $p > 0.9999$ 0.98-0.86 vs. 0.74-0.62, $p > 0.9999$ Shock 1.94-1.78 vs. 1.70-1.54, $p > 0.9999$ 1.94-1.78 vs. 1.42-1.34, $p > 0.9999$ 1.94-1.78 vs. 1.18-1.10, $p > 0.9999$ 1.94-1.78 vs. 0.98-0.86, $p > 0.9999$ 1.94-1.78 vs. 0.74-0.62, $p = 0.0008$ *** 1.70-1.54 vs. 1.42-1.34, $p > 0.9999$ 1.70-1.54 vs. 1.18-1.10, $p > 0.9999$ 1.70-1.54 vs. 0.98-0.86, $p > 0.9999$ 1.70-1.54 vs. 0.74-0.62, $p = 0.0016$** 1.42-1.34 vs. 1.18-1.10, $p > 0.9999$ 1.42-1.34 vs. 0.98-0.86, $p > 0.9999$ 1.42-1.34 vs. 0.74-0.62, $p = 0.0014$ ** 1.18-1.10 vs. 0.98-0.86, $p > 0.9999$ 1.18-1.10 vs. 0.74-0.62, $p = 0.0050$ ** 0.98-0.86 vs. 0.74-0.62, $p = 0.031$ **

	Group x Bregma: F (5, 27) = 2.610, $p = 0.0475$	
11i- NAc shell	Group: F (1, 33) = 16.21, $p = 0.0003$	NOshock-Shock
		1.94-1.78, $p > 0.9999$
		1.70-1.54, $p = 0.2329$
		1.42-1.34, $p > 0.9999$
		1.18-1.10, $p = 0.0328$ *
		0.98-0.86, $p = 0.0031$ **
		0.74-0.62, $p > 0.9999$
	Bregma: F (5, 33) = 2.982, $p = 0.0250$	NOshock
		1.94-1.78 vs. 1.70-1.54, $p > 0.9999$
		1.94-1.78 vs. 1.42-1.34, $p > 0.9999$
		1.94-1.78 vs. 1.18-1.10, $p > 0.9999$
		1.94-1.78 vs. 0.98-0.86, $p > 0.9999$
		1.94-1.78 vs. 0.74-0.62, $p > 0.9999$
		1.70-1.54 vs. 1.42-1.34, $p > 0.9999$
		1.70-1.54 vs. 1.18-1.10, $p > 0.9999$
		1.70-1.54 vs. 0.98-0.86, $p > 0.9999$
		1.70-1.54 vs. 0.74-0.62, $p > 0.9999$
		1.42-1.34 vs. 1.18-1.10, $p > 0.9999$
		1.42-1.34 vs. 0.98-0.86, $p > 0.9999$
		1.42-1.34 vs. 0.74-0.62, $p > 0.9999$
		1.18-1.10 vs. 0.98-0.86, $p > 0.9999$
		1.18-1.10 vs. 0.74-0.62, $p > 0.9999$
		0.98-0.86 vs. 0.74-0.62, $p > 0.9999$
		Shock
		1.94-1.78 vs. 1.70-1.54, $p > 0.9999$
		1.94-1.78 vs. 1.42-1.34, $p > 0.9999$
		1.94-1.78 vs. 1.18-1.10, $p = 0.1452$
		1.94-1.78 vs. 0.98-0.86, $p = 0.0024$ **
		1.94-1.78 vs. 0.74-0.62, $p > 0.9999$
		1.70-1.54 vs. 1.42-1.34, $p > 0.9999$
		1.70-1.54 vs. 1.18-1.10, $p > 0.9999$
		1.70-1.54 vs. 0.98-0.86, $p = 0.3374$

		1.70-1.54 vs. 0.74-0.62, $p > 0.9999$
		1.42-1.34 vs. 1.18-1.10, $p = 0.2378$
		1.42-1.34 vs. 0.98-0.86, $p = 0.0045$ **
		1.42-1.34 vs. 0.74-0.62, $p > 0.9999$
		1.18-1.10 vs. 0.98-0.86, $p > 0.9999$
		1.18-1.10 vs. 0.74-0.62, $p > 0.9999$
		0.98-0.86 vs. 0.74-0.62, $p = 0.0456$ *
	Group x Bregma: F (5, 33) = 2.405, $p = 0.0577$	
11j- NAc medial and lateral shell	Group: F (1, 6) = 13.96, $p = 0.0097$	NOshock-Shock Shell medial, $p = 0.0056$ ** Shell lateral, $p = 0.5000$
	Medial-Lateral: F (1, 6) = 0.2644	
	Group x Medial-Lateral: F (1, 6) = 2.876, $p = 0.1408$	
11l- All NAc	Group: F (1, 4) = 0.8750, $p = 0.4025$	
	Bregma: F (5, 16) = 10.86, $p = 0.0001$	Saline 1.94-1.78 vs. 1.70-1.54, $p > 0.9999$
		1.94-1.78 vs. 1.42-1.34, $p > 0.9999$
		1.94-1.78 vs. 1.18-1.10, $p > 0.9999$
		1.94-1.78 vs. 0.98-0.86, $p = 0.4056$
		1.94-1.78 vs. 0.74-0.62, $p > 0.9999$
		1.70-1.54 vs. 1.42-1.34, $p > 0.9999$
		1.70-1.54 vs. 1.18-1.10, $p > 0.9999$
		1.70-1.54 vs. 0.98-0.86, $p = 0.5752$
		1.70-1.54 vs. 0.74-0.62, $p > 0.9999$
		1.42-1.34 vs. 1.18-1.10, $p > 0.9999$
		1.42-1.34 vs. 0.98-0.86, $p > 0.9999$
		1.42-1.34 vs. 0.74-0.62, $p > 0.9999$
		1.18-1.10 vs. 0.98-0.86, $p > 0.9999$
		1.18-1.10 vs. 0.74-0.62, $p > 0.9999$
		0.98-0.86 vs. 0.74-0.62, $p > 0.9999$
		Coca
		1.94-1.78 vs. 1.70-1.54, $p > 0.9999$
		1.94-1.78 vs. 1.42-1.34, $p > 0.9999$
		1.94-1.78 vs. 1.18-1.10, $p = 0.0118$ *

1.94-1.78 vs. 0.98-0.86, p = 0,0015 **

1.94-1.78 vs. 0.74-0.62, p = 0.0007 ***

1.70-1.54 vs. 1.42-1.34, p > 0.9999

1.70-1.54 vs. 1.18-1.10, p = 0.0152 *

1.70-1.54 vs. 0.98-0.86, p = 0.0020 **

1.70-1.54 vs. 0.74-0.62, p = 0.0009 ***

1.42-1.34 vs. 1.18-1.10, p = 0.0775

1.42-1.34 vs. 0.98-0.86, p = 0.0146 *

1.42-1.34 vs. 0.74-0.62, p = 0.0074 **

1.18-1.10 vs. 0.98-0.86, p > 0.9999

1.18-1.10 vs. 0.74-0.62, p > 0.9999

0.98-0.86 vs. 0.74-0.62, p > 0.9999

Group x Bregma: F (5, 16) = 3.310, p = 0.0305

5. Discussion, conclusion and future perspectives

5.1. Discussion

Understanding the cellular mechanisms underlying reward and aversion can help elucidate the pathophysiology of disorders characterized by affective impairments such as MDD and SUD (Bressan and Crippa, 2005; Heshmati and Russo, 2015; Russo and Nestler, 2013; Scheres *et al.*, 2007; Sternat and Katzman, 2016). In this sense, studying how negative and positive valence is encoded/processed in a cellular or populational manner is essential. As mentioned, both valence poles appear to be represented concurrently in some brain regions. However, if these brain regions contain a largely distinct or overlapping populations of neurons encoding the opposite valences is still a current matter of study. In addition, efforts are being made to understand if these co-existing populations are distinguishable in terms of genetic characteristics (*i.e.* gene expression), anatomy (*i.e.* inputs/outputs or spatial organization) or functionality/activity in response to stimuli (Namburi *et al.*, 2016). Some populations with the above distinct characteristics have been described in the NAc, Amygdala and VTA (Lammel *et al.*, 2012; Namburi *et al.*, 2016; Roitman *et al.*, 2005; Zhang *et al.*, 2021; Zhang and Li, 2018). However, the knowledge on how this occurs in the LDT populations is scarce.

5.1.1. Recruitment of LDT ensembles upon exposure to negative *vs.* positive valence stimuli

To study valence encoding, researchers have been using different strategies for characterizing neuronal activity patterns in response to positive or negative valence stimuli, cues predicting those stimuli and changes in stimuli-associations contingency. Strategies including electrophysiology, immediate early genes-based labelling and, more recently, calcium and neurotransmitter imaging.

Evaluation of the expression of IEGs, like *c-Fos*, has gained popularity and is now broadly used as a proxy of cell activation (Kawashima *et al.*, 2014). When a neuron is depolarized, the transient rise of intracellular Ca^{2+} and downstream second messenger pathways transiently activate the expression of immediate early genes within minutes (Sheng and Greenberg, 1990). Thus, IEGs have been exploited to map neuronal activation patterns associated with specific animal behaviors or stimuli at a cellular resolution (Kawashima *et al.*, 2014). *Fos* can be induced by stimuli of different modalities, such as dehydration (Allen *et al.*, 2017; da Silveira *et al.*, 2007; Sagar *et al.*, 1988), visual and tactile stimulation (Filipkowski *et al.*, 2000; Montero and Jian, 1995), odors (Bepari *et al.*, 2012), acute stressors (Cullinan *et al.*, 1995; Girotti *et al.*, 2006), sweet or bitter tastants (King *et al.*, 2014; Streefland *et al.*, 1996; Tan *et al.*, 2020; Travers, 2002) and drugs of abuse (Whitaker and Hope, 2018), amongst others (Kovács,

2008). It is induced by different patterns of neural activity (DeNardo and Luo, 2017) and acts, ultimately, as a transcription factor to regulate expression of many genes (Halazonetis *et al.*, 1988). Labelling endogenous c-Fos is typically used to assess neuronal activation on short-term analysis, as mRNA levels peak around 30-60 min, with protein levels peaking around 1-2 hours (depending on specific brain region and type of stimulus) (Cullinan *et al.*, 1995; Kazi *et al.*, 2004; Morgan *et al.*, 1987; Sonnenberg *et al.*, 1989). The biggest advantage of this approach, compared to others like electrophysiology or calcium imaging that are typically restricted to one brain region, is that it efficiently labels recently activated neurons, with cellular resolution, across the entire brain (Körber and Sommer, 2022).

To identify neuronal populations encoding negative- and positive-valence stimuli, we exposed mice to footshocks or to rewarding stimuli, cocaine or sucrose, and then labelled endogenous c-Fos to investigate neuronal activation in the LDT. Electrical footshocks were delivered at an intensity (1.5 mA), duration (1 second) and frequency (every 30 seconds, total 20 shocks) known to induce neuronal activation in the BLA, as well as producing negative-valence responses (Gore *et al.*, 2015). Cocaine was injected at a dose of 20 mg/Kg based on (Xiu *et al.*, 2014) and pilot experiments from our team. This dose was previously shown to enhance motor activity and induce CPP, thus having a robust rewarding/appetitive value or property (Itzhak and Martin, 2002; Tilley *et al.*, 2007; Zhang *et al.*, 2002). The protocol for the sucrose session was based on preliminary data obtained in a pilot study performed by our team.

The LDT neurons have shown to respond to negative and positive valence stimuli. Specifically, in the LDT, c-Fos expression is elevated after several aversion-inducing stimuli, like inescapable or conditioned/escapable footshock (Liu *et al.*, 2009, 2003), predator odorant (Yang *et al.*, 2016), air puffs (Brudzynski *et al.*, 2011), 30 minutes acute restraint (Tang *et al.*, 2021) and social defeat stress (Fernandez *et al.*, 2018). In addition, although a low number of cells were recorded, LDT neurons have demonstrated to respond to an air puff to the face (Koyama *et al.*, 1994). In agreement, in the current work, we showed that unconditioned footshock (*i.e.* first exposure) increased c-Fos+ cells in the LDT, indicating that the LDT responds to this stimulus.

Regarding positive stimuli, Fos-expressing LDT cells have shown to be increased upon single nicotine injection (Baur *et al.*, 2018; José Lança *et al.*, 2000). Furthermore, intravenous self- or passive-administration of cocaine (not acute) increased c-Fos-expressing cells in the LDT, including VTA-projecting cells (Geisler *et al.*, 2008; Zahm *et al.*, 2010). *Ex vivo* experiments further confirm that nicotine and cocaine lead to LDT activation (Ishibashi *et al.*, 2009; Lambert *et al.*, 2017). In agreement, we saw

significant cell activation, in terms of c-Fos cell density, after a non-contingent single cocaine (20 mg/Kg) i.p. injection.

Regarding natural rewards, to our knowledge, the only study involving the LDT is a study showing that some LDT cells increase firing rate when consuming chocolate milk rewards in a spatial discrimination task (Redila *et al.*, 2015). Accordingly, we show that another sweet tastant, sucrose solution, increased c-Fos expression in the LDT. It is important to note that we cannot guarantee that the animals did consume sucrose as we only measured head entries in the magazine during the session. A more direct and reliable behavioral measure would be quantifying licking events with a lickometer. Although not having sucrose solution available, two animals of the NOsuc group performed a similar number of magazine visits during the session as the Suc group animals. Though we cleaned the receptable with 10 % ethanol between animals, residues of the sucrose solution could have remained, leading to control animals to visit the magazine.

Overall, these results are in line with previous studies measuring LDT activation upon aversive or rewarding stimuli. Additionally, we found that shock- and cocaine-ensembles in the LDT, recruited cholinergic cells (to note that in the sucrose, only a tendency was observed).

The c-Fos-labelling approach has some limitations that should be kept in mind: (1) failure to detect c-Fos immunoreactivity in a neuron does not necessarily mean that it has not responded. (1.1) it is well established that activity-dependent genes (*i.e.* IEGs) are differentially regulated in different cell types in distinct brain areas (*i.e.* different expression levels and induction thresholds in different brain regions or cell types) (Kawashima *et al.*, 2014; Körber and Sommer, 2022). This highlights the importance of choosing the right type of the activity-dependent gene to correctly target the neural activity to be studied. (1.2) cells's inhibitory responses are not detected (Cohen *et al.*, 2012; Roitman *et al.*, 2005); (2) basal conditions of the neuronal ensembles prior to acutely induction of activation cannot be assessed (particularly relevant when training/learning may alter the observed activation); (3) IEGs transcripts or proteins are present in neurons for a limited time after expression induction therefore, for IEG detection, animals must be sacrificed after the stimulus, preventing further studies; (4) the signal-to-noise ratio heavily depend on the labeling protocol and the quality of the antibodies or hybridization probes, which can cause high variability/low reliability of the results.

To address these limitations, analysis of multiple IEGs and complementary electrophysiological or calcium imaging approaches can be used. Concerning the points (3) and (4), the use of fluorescent reporters under the promotor of *c-Fos* (or other IEGs) would allow the labelling with a higher signal-to-noise ratio and allow access to activated cells for a period much longer than the IEG timescale. Currently

there are several transgenic mice models using this strategy like the TRAP model that we used in this work (reviewed in (DeNardo and Luo, 2017)).

5.1.2. Overlap of LDT ensembles responsive to negative and positive valence stimuli

Knowing that the LDT contains ensembles responsive to negative and positive valence stimuli, next we aimed to investigate if these ensembles were superimposed or segregated. In order to do so, we employed the TRAP2 mouse model, that allowed us to overlay ensembles that were active during two temporally separate events. This model has been used to label cell ensembles active during a variety of stimulus or events like, water deprivation (Allen *et al.*, 2017), natural or drug reward-cues (Bobadilla *et al.*, 2020), fear conditioning or retrieval (DeNardo *et al.*, 2019; Dixsaut and Gräff, 2022; Ivashkina *et al.*, 2021; Li *et al.*, 2021; Roy *et al.*, 2022; Shpokayte *et al.*, 2022), social defeat stress (Koutlas *et al.*, 2022; Niu *et al.*, 2022), female interaction reward (Shpokayte *et al.*, 2022), acute cocaine administration (Wall *et al.*, 2019; Ye *et al.*, 2016), social interaction (Xing *et al.*, 2021), quinine (Tanaka *et al.*, 2021b) and feeding after fasting (Imoto *et al.*, 2021).

Firstly, to verify if the model (*i.e.* TRAPing) would detect the stimuli we had used before, we focused on an extensively studied area, the amygdala. Amygdala neurons have shown to encode a variety of appetitive and aversive stimuli. BLA neurons respond to sucrose (Muramoto *et al.*, 1993), nicotine (Gore *et al.*, 2015) and footshocks (Gore *et al.*, 2015; Kim *et al.*, 2017; Muramoto *et al.*, 1993). The CeA has populations responding to footshock and sucrose (Steinberg *et al.*, 2020). In agreement, the shock stimulus induced cell activation (tdTomato expression) in the BLA however, did not induce significant activation of the CeA. In addition, cocaine injection induced cell activation in both the BLA and CeA. Unexpectedly, sucrose exposure did not induce an increase in cell activation in neither subregions, though animals with sucrose solution available visited more the magazine than controls.

Regarding the LDT, and in accordance with the aforementioned results, cell activation was detected after shock and cocaine stimulus, but not sucrose. These discrepancies with the sucrose stimulus could be due to the sensitivity of the model, *i.e.*, sucrose may activate fewer cells than the other two stimuli and we cannot observe these subtle differences. A more probable hypothesis lies with an experimental aspect that was performed in the first experiment (c-Fos labelling) but not in the TRAPing experiment. The food dispenser was not ON during the habituation sessions in the TRAPing experiment. The elevation and retraction of the feeder made a considerable amount of noise that could have led to an abnormal cell activation on the experimental days due to this novel sound even in control animals, and this could "mask" the increase in cell activation by sucrose. In fact, LDT cells have shown to respond to auditory stimulus

(Koyama *et al.*, 1994). It is plausible that familiarizing the animals to the feeder's noise during the habituation period could have reduce 'unspecific' neuronal activation due to novelty (rather than to sucrose) in the experiment with wild-type animals. Neverthless, there was a slight tendency for the sucrose group to have a higher tdTomato+ and c-Fos+ cell density. Considering the technical limitation described, we opted not to draw any conclusions from the overlap of ensembles involving the sucrose session.

Positive and negative valence stimuli appear to be encoded in the same brain areas. In several brain regions, stimuli of opposite valence have shown to activate separate but intermingled neuronal substrates. Ye *et al.* 2016, found that in the PFC, cocaine and footshocks are represented by different cell populations with distinct characteristics (Ye *et al.*, 2016). Furthermore, it was found that the ventral hippocampus processes appetitive and aversive experiences in defined populations of cells that are partially distinct at the molecular, cellular, and projection-specific levels (Shpokayte *et al.*, 2022). In the dorsomedial shell of the NAc, opposing valence stimuli (morphine-footshock or morphine–restraint) activated ensembles that showed limited overlap, whereas two distinct positive or negative stimuli (morphine-cocaine or morphine-chocolate and shock-restraint), activated highly overlapping ensembles. (Nawarawong and Olsen, 2020; Xiu *et al.*, 2014). Even different types of rewards appear to be represented in a segregated manner in some brain regions. For instance, in the ventromedial PFC, cocaine and palatable food pellets activate functionally different ensembles (Kane *et al.*, 2020). In the NAc core, ensembles responsive to cocaine or sucrose-cues (reward seeking-ensembles) were found to be largely distinct (Bobadilla *et al.*, 2020). While a study reported that largely overlapping ensembles (around 50 %) in the infralimbic PFC responded to both ethanol and saccharin (a sweet tastant) (Pfarr *et al.*, 2018). Thus, each reward seems to recruit specific subset of neurons, while another subset of neurons may be recruited by rewards in general, probably controlling certain aspects of reward-related encoding that are common (Körber and Sommer, 2022).

Our approach, allowed within subjects comparisons between shock- and cocaine-responsive LDT ensembles. We found that, even though shock and cocaine induced comparable cell activation levels in separate populations (in terms of tdTomato+ and c-Fos+ cell density), percentage of overlap of cocaine and shock ensembles was significantly smaller when compared with the overlap of shock-shock or cocaine-cocaine sessions (around 3 times less overlap). Nevertheless, a group exposed firstly to shock and then to cocaine would be needed to further support this conclusion.

Regarding the overlap between LDT cocaine- and shock-ensembles, a 'common ensemble', probably does not represent valence, as it responded similarly to stimuli of opposite valence (Namburi *et al.*, 2016). Namburi and colleagues propose that a neuron encodes valence 'if its output is either

oppositely or selectively modulated by the positive/negative properties of a stimulus'. Meaning that a neuron coding valence must either: (1) increase its firing rate to a stimulus of one valence and decrease its firing rate to a stimulus of the opposite valence or (2) modulate its firing rate to a stimulus of one valence, but not a stimulus of the opposite valence (Namburi *et al.*, 2016). Electrophysiological or imaging studies would allow us to test this hypothesis in the LDT.

It is important to note that cell populations tagged with immunofluorescence (c-Fos+) were larger than those measured by recombination (tdTomato+) (leading to low efficiency), which is similar to what has been reported in the literature (Bobadilla *et al.*, 2020; Guenthner *et al.*, 2013; Koutlas *et al.*, 2022). It seems unlikely that an expansion of the ensembles occurred between the two stimuli sessions, since c-Fos expression decreases with repeated exposure to the same context/experience (Girotti *et al.*, 2006; Martinez *et al.*, 1998; Struthers *et al.*, 2005). Likely, the c-Fos dependent Cre-recombination is less efficient than direct c-Fos protein detection, since tdTomato labelling requires expression of Cre linked to the ER, ER-4-OHT binding, Cre translocation to the nucleus and subsequent recombination of floxed STOP codon to disinhibit tdTomato expression (DeNardo *et al.*, 2019; Guenthner *et al.*, 2013). Additionally, as TRAPing is binary (either tdTomato+ or not) and c-Fos immunolabelling is a gradient, cells with low c-Fos expression may be considered as positive but may not be sufficient to complete the process for the tdTomato expression.

Additionally, we and others have observed tamoxifen-independent labelling (DeNardo *et al.*, 2019; Guenthner *et al.*, 2013; Koutlas *et al.*, 2022), although in the regions we analyzed, the amygdala and LDT, it was reduced compared to controls.

5.1.3. Optogenetic stimulation of LDT shock- or cocaine-responsive ensembles

As stated before, valence has a behavioral aspect, the consequent reactions induced on the individual, such that, rewarding stimuli support approach-motivated behaviors whereas aversive ones support avoidance-motivated behaviors (Guitart-Masip *et al.*, 2014; Tye, 2018). Approach and avoidance of stimuli/manipulations are commonly assessed using place preference paradigms like the RTPP or CPP. Both allow to infer the rewarding or aversive properties of a stimulus based on the establishment of place preference or avoidance, respectively (or in the case that the stimulus is neutral, neither occur).

Taking advantage of the TRAP2 model, we were able to confine opsin expression to cells that were active during shock or cocaine exposure (activity-dependent) in the LDT (spatial control). Subsequently, this enabled optically controlling this cell during RTPP and CPP. Similar approaches, have been used to: (1) stimulate specifically BLA shock- or nicotine-responsive neurons, inducing place avoidance or

preference, respectively (Gore *et al.*, 2015; Redondo *et al.*, 2014); (2) optogenetically activate dentate gyrus (DG) cells responsive to either shock or interaction with female mouse, inducing place avoidance or preference, respectively (Redondo *et al.*, 2014); (3) manipulate water-deprivation-responsive hypothalamic median preoptic nucleus (MnPO) neurons, inducing place avoidance (Allen *et al.*, 2017); (4) optogenetically excite mPFC shock- or cocaine-activated ensembles, inducing place avoidance or preference, respectively (Ye *et al.*, 2016); (5) chemogenetically inhibit cocaine-activated orbital frontal cortex (OFC) or dorsal striatum neurons, inhibiting cocaine locomotor sensitization (Wall *et al.*, 2019); (5) activate social-stress-responsive neurons of the hypothalamic subnucleus, evoking fear-like behaviors (Sakurai *et al.*, 2016); (6) optogenetically excite prelimbic cortex BLA-projecting neurons responsive to footshock, disrupting social interactions (Huang *et al.*, 2020).

Unfortunately, due to experimental/technical problems - implant loss and injection/fiber misplacement, which reduced our sample size, we were not able to draw any conclusions. Nonetheless, a recent report by Roy *et al.*, 2022, activating selectively LDT cells recruited during context fear conditioning (CFC), induced freezing responses (Roy *et al.*, 2022). They tagged cells employing a double virus approach, which included an activity-dependent vector c-Fos-tetracycline transactivator (tTA) and a ChR2-tagging vector tetracycline response element (TRE)-ChR2-eYFP. This approach, called TetTag, uses the *Fos* promoter to drive the expression of a doxycycline (Dox)-repressible tTA in the absence of Dox (Reijmers *et al.*, 2007). Thus, this system is off in the presence of Dox (normally administered through the diet or drinking water) and once doxycycline is removed (in this particular study, 24 hours before CFC (Roy *et al.*, 2022)) and a *Fos* inducing stimulus occurs, the tTA is expressed, ultimately driving the expression of the TRE-driven effector, in this case, the ChR2. Although they did not further investigate the CFC-responsive ensembles influence on place preference paradigms, we hypothesize that its activation would lead to place avoidance based on previous literature (**Table 1**) that show a role of the LDT in aversion-related behaviors.

In relation to the TRAP2 system, in which the tagging time window is controlled by 4-OHT presence, and thus, its metabolism, rendering it a few hours long (around 12 hours (DeNardo *et al.*, 2019)), the TetTag system has a timewindow of days (Reijmers *et al.*, 2007). This loss of temporal resolution potentially leads to labeling of more neurons, in comparison to TRAP2 approach, than those activated in the behavior in interest, that may reduce the capability of the method to find statistically significant variations or, in fact, the opposite. Therefore, highlighting the importance of controls that have the same treatment except the relevant stimulus/event, like we did in the present work. It is important to note, that

also the TRAP2 model suffers from the same problem, however it has a significantly lower timewindow than TetTag (DeNardo and Luo, 2017).

Recent approaches including activity-dependent tools that are switched on by coincidence of calcium concentration elevation and light stimulation seem to have a great potential to capture neural activity with a better temporal precision than TRAP2 and TegTag (Choi *et al.*, 2020; Lee *et al.*, 2017; Wang *et al.*, 2017).

Lastly, an important limitation of our approach is the lack of an YFP-expressing control group, which is essential when utilizing optogenetics to control for artifacts.

5.1.4. NAc innervation by LDT shock- or cocaine-responsive ensembles

In this work, after verifying the existence of positive- and negative-valence ensembles with activity-dependent labelling in the LDT, we examined to where in the NAc these neurons projected to.

We found that LDT cells projecting to the NAc were recruited during the shock-stimulus. In the NAc, it was found that the higher innervation by these cells was present in medial shell subregion. In agreement with this finding, the medial shell neurons were found to respond to footshocks (Xiu *et al.*, 2014). Within the medial shell, the shock-responsive LDT cells preferentially innervated the posterior/caudal portion of this subregion. Curiously, an 'affective keyboard' has been described in the NAc shell, with a rostrocaudal pattern from positive- to negative-valence responses, with the more rostral area being associated with appetitive behaviors and the more caudal NAc shell being associated with fear-related behaviors (Berridge and Kringelbach, 2015; Faure *et al.*, 2010). It is tempting to try to associate this keyboard with our findings however, further studies are needed to explore the role of these LDT_{shock}-NAc projections in behavior.

Regarding the cocaine-responsive LDT ensemble, we found that there was no preferential innervation of any NAc region (compared with controls). This was unexpected since the LDT-NAc projections have shown a prominent role in reward-related behaviors (Coimbra *et al.*, 2019). However, this might mean that shock and cocaine recruit different LDT projecting neuronal populations and that cocaine might recruit LDT projections to other outputs like the VTA. In agreement, cocaine administration has shown to induce c-Fos expression in VTA-projecting LDT cells (Geisler *et al.*, 2008; Zahm *et al.*, 2010). Further work is needed to investigate in other brain regions (like the VTA) the pattern of innervation of the stimuli-responsive LDT cells. However, since the sample size was smaller, we have to repeat this experiment with additional animals.

Finally, it is important to note that our approach has a relevant limitation. As innervation does not directly mean that there are synaptic contacts, we cannot guarantee that the projections we found do in fact synapse with NAc cells. To circumvent this, we could optogenetically activate the terminals in the NAc, and simultaneously perform electrophysiological recordings to evaluate evoked responses. Nonetheless, varicosities-like structures were observed in the NAc stained slices. In addition, some YFP-expressing cell bodies were detected outside the LDT. To try to take into account this variability, we normalized the NAc innervation, for each animal, by multiplying it by the proportion of YFP+ cells within the LDT (for each slice that we quantified LDT YFP+ cells, positive cells outside the LDT were also determined; the proportion for each animal was calculated by dividing total LDT YFP+ cells by total positive cells, including inside and outside the LDT).

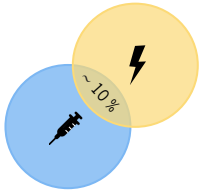
5.2. Conclusion

Studies have provided evidence involving the LDT in responding to stimuli of positive- and negative-valence and reward- and aversion-related behaviors. However, ensembles that process each valence stimulus to drive behavior still requires further exploration.

Table 4, summarizes the main findings of this thesis. We have shown that electric footshock, cocaine and sucrose recruit LDT cells, as evaluated by endogenous c-Fos and TRAPing (tendency in sucrose TRAPing). Overlapping the ensembles in a same-animal manner, we found that shock and cocaine activate mainly segregated populations. Moreover, the experimental conditions need further optimization for the sucrose stimulus.

We also analyzed NAc innervation by shock- and cocaine-responsive LDT ensembles and found that the shock-ensemble projected preferentially to the posterior medial NAc Shell, while the cocaine-ensemble did not show a preferential innervation of the NAc.

Table 4- Summary of the main results obtained by evaluating neuronal activation after exposure to negative- and positive-valence stimuli via c-Fos labelling or TRAPing, overlap of shock- and cocaine-ensembles and NAc innervation by these two ensembles.

Stimulus	c-Fos+ cell density	TRAPing (tdTomato+ cell density)	Overlap	NAc projections
Footshock	↑	↑		↑
Cocaine	↑	↑		–
Sucrose	↑	≈↑		

↑ higher values/innervation; ≈↑ tendency for higher values; – no preferential innervation

5.3. Future perspectives

Additional studies are still necessary to identify and characterize neuronal populations encoding negative- and positive-valence stimuli in the LDT and study their influence in valence-specific behaviors (*i.e.* their functional role):

1) **Study thoroughly the phenotypic/genetic nature of the LDT-responsive ensembles.** We could use fluorescent in-situ hybridization (FISH), like other have used in the LDT (Hernandez *et al.*, 2021), to characterize the shock-, cocaine- and sucrose-responsive ensembles in terms of proportion of the three main LDT populations (cholinergic, GABAergic and glutamatergic). We could also use single-cell RNA sequencing tools applied to activated neuronal populations (*i.e.* focusing on IEG expression) (Wu *et al.*, 2017) to identify neuronal clusters responsive to each stimuli.

2) **Investigate the LDT-responsive ensembles innervation of other brain regions.** It would be interesting to investigate the innervation of other brain regions by responsive-LDT cells, specifically the VTA as it is a major target of the LDT and VTA-projecting LDT neurons have shown to be activated by cocaine (Geisler *et al.*, 2008).

3) **Selectively modulate specific projections of the LDT-responsive ensembles.** As shock-responsive LDT cells showed a very specific projection pattern in the NAc, it would be interesting to modulate the LDT-NAc shock-responsive projections and observe the impact in behavior.

4) **Confirm that other opposite-valence stimuli recruit segregated ensembles in the LDT.** Does the segregated pattern of activation in the LDT reflect representation of affective values or other features (like, specific sensory properties) associated with cocaine or footshock? To better distinguish this, we would need to further test the dual labelling with additional appetitive and aversive stimulus that are experienced through different sensory modalities.

5) **Record the LDT's activity in freely moving animals while being exposed to different valence stimuli**. A technique like fiber photometry would allow to record bulk fluorescence of calcium signals in the LDT, though lacking cellular resolution. This limitation could be overcome with the use miniaturized microscopy (miniscopes), like other have used in the DRN, a nearby structure (Paquelet *et al.*, 2022).

6) **Investigate the afferents that contact with LDT-responsive ensembles.** The synaptic connectivity of the LDT activated neuronal ensembles is unknown, as is the behavioral relevance of such connectivity. By combining the TRAP2 model with a monosynaptic rabies virus tracing approach, the afferents to specific stimulus responsive LDT cells can be identified and even modulated optogenetically, like other have done to dorsal striatum cocaine-responsive ensembles (Wall *et al.*, 2019).

6. References

Adolphs, Ralph, and David J. Anderson. 2018. *The Neuroscience of Emotion: A New Synthesis*. Princeton University Press.

Alderson, Helen L., Mary P. Latimer, and Philip Winn. 2005. "Involvement of the Laterodorsal Tegmental Nucleus in the Locomotor Response to Repeated Nicotine Administration." *Neuroscience Letters* 380(3):335–39. doi: 10.1016/j.neulet.2005.01.067.

Al-Hasani, Ream, Raajaram Gowrishankar, Gavin P. Schmitz, Christian E. Pedersen, David J. Marcus, Sofia E. Shirley, Taylor E. Hobbs, Abigail J. Elerding, Sophie J. Renaud, Miao Jing, Yulong Li, Veronica A. Alvarez, Julia C. Lemos, and Michael R. Bruchas. 2021. "Ventral Tegmental Area GABAergic Inhibition of Cholinergic Interneurons in the Ventral Nucleus Accumbens Shell Promotes Reward Reinforcement." *Nature Neuroscience* 24(10):1414–28. doi: 10.1038/s41593-021-00898-2.

Al-Hasani, Ream, Jordan G. McCall, Gunchul Shin, Adrian M. Gomez, Gavin P. Schmitz, Julio M. Bernardi, Chang-O. Pyo, Sung Il Park, Catherine M. Marcinkiewcz, Nicole A. Crowley, Michael J. Krashes, Bradford B. Lowell, Thomas L. Kash, John A. Rogers, and Michael R. Bruchas. 2015. "Distinct Subpopulations of Nucleus Accumbens Dynorphin Neurons Drive Aversion and Reward." *Neuron* 87(5):1063–77. doi: 10.1016/j.neuron.2015.08.019.

Allen, Timothy G. J., Fe C. Abogadie, and David A. Brown. 2006. "Simultaneous Release of Glutamate and Acetylcholine from Single Magnocellular 'Cholinergic' Basal Forebrain Neurons." *The Journal of Neuroscience* 26(5):1588–95. doi: 10.1523/JNEUROSCI.3979-05.2006.

Allen, William E., Laura A. DeNardo, Michael Z. Chen, Cindy D. Liu, Kyle M. Loh, Lief E. Fenno, Charu Ramakrishnan, Karl Deisseroth, and Liqun Luo. 2017. "Thirst-Associated Preoptic Neurons Encode an Aversive Motivational Drive." *Science (New York, N.Y.)* 357(6356):1149–55. doi: 10.1126/science.aan6747.

Anderson, David J., and Ralph Adolphs. 2014. "A Framework for Studying Emotions across Species." *Cell* 157(1):187–200. doi: 10.1016/j.cell.2014.03.003.

Armstrong, D. M., C. B. Saper, A. I. Levey, B. H. Wainer, and R. D. Terry. 1983. "Distribution of Cholinergic Neurons in Rat Brain: Demonstrated by the Immunocytochemical Localization of

Choline Acetyltransferase." *The Journal of Comparative Neurology* 216(1):53–68. doi: 10.1002/cne.902160106.

Badrinarayan, Aneesha, Seth A. Wescott, Caitlin M. Vander Weele, Benjamin T. Saunders, Brenann E. Couturier, Stephen Maren, and Brandon J. Aragona. 2012. "Aversive Stimuli Differentially Modulate Real-Time Dopamine Transmission Dynamics within the Nucleus Accumbens Core and Shell." *The Journal of Neuroscience: The Official Journal of the Society for Neuroscience* 32(45):15779–90. doi: 10.1523/JNEUROSCI.3557-12.2012.

Baghdoyan, Helen A., Margarita L. Rodrigo-Angulo, Robert W. McCarley, and J. Allan Hobson. 1987. "A Neuroanatomical Gradient in the Pontine Tegmentum for the Cholinoceptive Induction of Desynchronized Sleep Signs." *Brain Research* 414(2):245–61. doi: 10.1016/0006-8993(87)90005-9.

Bardo, M. T., and R. A. Bevins. 2000. "Conditioned Place Preference: What Does It Add to Our Preclinical Understanding of Drug Reward?" *Psychopharmacology* 153(1):31–43. doi: 10.1007/s002130000569.

Baur, Katja, Arian Hach, Rick E. Bernardi, Rainer Spanagel, Hilmar Bading, and C. Peter Bengtson. 2018. "C-Fos Marking of Identified Midbrain Neurons Coactive after Nicotine Administration in-Vivo." *The Journal of Comparative Neurology* 526(13):2019–31. doi: 10.1002/cne.24471.

Bepari, Asim K., Keisuke Watanabe, Masahiro Yamaguchi, Nobuaki Tamamaki, and Takebayashi Hirohide. 2012. "Visualization of Odor-Induced Neuronal Activity by Immediate Early Gene Expression." *BMC Neuroscience* 13:140. doi: 10.1186/1471-2202-13-140.

Berg, Stuart, Dominik Kutra, Thorben Kroeger, Christoph N. Straehle, Bernhard X. Kausler, Carsten Haubold, Martin Schiegg, Janez Ales, Thorsten Beier, Markus Rudy, Kemal Eren, Jaime I. Cervantes, Buote Xu, Fynn Beuttenmueller, Adrian Wolny, Chong Zhang, Ullrich Koethe, Fred A. Hamprecht, and Anna Kreshuk. 2019. "Ilastik: Interactive Machine Learning for (Bio)Image Analysis." *Nature Methods* 16(12):1226–32. doi: 10.1038/s41592-019-0582-9.

Berridge, Kent C. 2018. "Evolving Concepts of Emotion and Motivation." *Frontiers in Psychology* 9:1647. doi: 10.3389/fpsyg.2018.01647.

Berridge, Kent C. 2019. "Affective Valence in the Brain: Modules or Modes?" *Nature Reviews*

Neuroscience 20(4):225–34. doi: 10.1038/s41583-019-0122-8.

Berridge, Kent C., and Morten L. Kringelbach. 2008. "Affective Neuroscience of Pleasure: Reward in Humans and Animals." *Psychopharmacology* 199(3):457–80. doi: 10.1007/s00213-008-1099-6.

Berridge, Kent C., and Morten L. Kringelbach. 2015. "Pleasure Systems in the Brain." *Neuron* 86(3):646–64. doi: 10.1016/j.neuron.2015.02.018.

Bimpisidis, Zisis, Niclas König, and Åsa Wallén-Mackenzie. 2020. "Two Different Real-Time Place Preference Paradigms Using Optogenetics within the Ventral Tegmental Area of the Mouse." *JoVE (Journal of Visualized Experiments)* (156):e60867. doi: 10.3791/60867.

Blaha, C. D., L. F. Allen, S. Das, W. L. Inglis, M. P. Latimer, S. R. Vincent, and P. Winn. 1996. "Modulation of Dopamine Efflux in the Nucleus Accumbens after Cholinergic Stimulation of the Ventral Tegmental Area in Intact, Pedunculopontine Tegmental Nucleus-Lesioned, and Laterodorsal Tegmental Nucleus-Lesioned Rats." *The Journal of Neuroscience: The Official Journal of the Society for Neuroscience* 16(2):714–22.

Bobadilla, Ana-Clara, Eric Dereschewitz, Lucio Vaccaro, Jasper A. Heinsbroek, Michael D. Scofield, and Peter W. Kalivas. 2020. "Cocaine and Sucrose Rewards Recruit Different Seeking Ensembles in the Nucleus Accumbens Core." *Molecular Psychiatry* 25(12):3150–63. doi: 10.1038/s41380-020-00888-z.

Bolam, J. P., C. M. Francis, and Z. Henderson. 1991. "Cholinergic Input to Dopaminergic Neurons in the Substantia Nigra: A Double Immunocytochemical Study." *Neuroscience* 41(2–3):483–94. doi: 10.1016/0306-4522(91)90343-m.

Boucetta, Soufiane, Youssouf Cissé, Lynda Mainville, Marisela Morales, and Barbara E. Jones. 2014. "Discharge Profiles across the Sleep–Waking Cycle of Identified Cholinergic, GABAergic, and Glutamatergic Neurons in the Pontomesencephalic Tegmentum of the Rat." *Journal of Neuroscience* 34(13):4708–27. doi: 10.1523/JNEUROSCI.2617-13.2014.

Bouret, Sebastien, and Barry J. Richmond. 2015. "Sensitivity of Locus Ceruleus Neurons to Reward Value for Goal-Directed Actions." *The Journal of Neuroscience: The Official Journal of the Society for Neuroscience* 35(9):4005–14. doi: 10.1523/JNEUROSCI.4553-14.2015.

Bressan, R. A., and J. A. Crippa. 2005. "The Role of Dopamine in Reward and Pleasure Behaviour–Review of Data from Preclinical Research." *Acta Psychiatrica Scandinavica. Supplementum* (427):14–21. doi: 10.1111/j.1600-0447.2005.00540.x.

Brischoux, Frédéric, Subhojit Chakraborty, Daniel I. Brierley, and Mark A. Ungless. 2009. "Phasic Excitation of Dopamine Neurons in Ventral VTA by Noxious Stimuli." *Proceedings of the National Academy of Sciences* 106(12):4894–99. doi: 10.1073/pnas.0811507106.

Broussot, Loïc, Thomas Contesse, Renan Costa-Campos, Christelle Glangetas, Léa Royon, Hugo Fofo, Thomas Lorivel, François Georges, Sebastian P. Fernandez, and Jacques Barik. 2022. "A Non-Canonical GABAergic Pathway to the VTA Promotes Unconditioned Freezing." *Molecular Psychiatry* 1–13. doi: 10.1038/s41380-022-01765-7.

Brudzynski, Stefan M. 2007. "Ultrasonic Calls of Rats as Indicator Variables of Negative or Positive States: Acetylcholine–Dopamine Interaction and Acoustic Coding." *Behavioural Brain Research* 182(2):261–73. doi: 10.1016/j.bbr.2007.03.004.

Brudzynski, Stefan M. 2021. "Biological Functions of Rat Ultrasonic Vocalizations, Arousal Mechanisms, and Call Initiation." *Brain Sciences* 11(5):605. doi: 10.3390/brainsci11050605.

Brudzynski, Stefan M., Amaka Iku, and Alison Harness (neé Savoy). 2011. "Activity of Cholinergic Neurons in the Laterodorsal Tegmental Nucleus during Emission of 22kHz Vocalization in Rats." *Behavioural Brain Research* 225(1):276–83. doi: 10.1016/j.bbr.2011.07.040.

Bueno, Debora, Leandro B. Lima, Rudieri Souza, Luciano Gonçalves, Fernanda Leite, Stefani Souza, Isadora C. Furigo, Jose Donato, and Martin Metzger. 2019. "Connections of the Laterodorsal Tegmental Nucleus with the Habenular-Interpeduncular-Raphe System." *The Journal of Comparative Neurology* 527(18):3046–72. doi: 10.1002/cne.24729.

Bux, Faiza, Adhil Bhagwandin, Kjell Fuxe, and Paul R. Manger. 2010. "Organization of Cholinergic, Putative Catecholaminergic and Serotonergic Nuclei in the Diencephalon, Mibrain and Pons of Sub-Adult Male Giraffes." *Journal of Chemical Neuroanatomy* 39(3):189–203. doi: 10.1016/j.jchemneu.2009.09.006.

Calvey, Tanya, Nina Patzke, Consolate Kaswera-Kyamakya, Emmanuel Gilissen, Mads F. Bertelsen, John D. Pettigrew, and Paul R. Manger. 2015. "Organization of Cholinergic, Catecholaminergic,

Serotonergic and Orexinergic Nuclei in Three Strepsirrhine Primates: Galago Demidoff, Perodicticus Potto and Lemur Catta." *Journal of Chemical Neuroanatomy* 70:42–57. doi: 10.1016/j.jchemneu.2015.10.002.

Cameron, Courtney M., and Regina M. Carelli. 2012. "Cocaine Abstinence Alters Nucleus Accumbens Firing Dynamics during Goal-Directed Behaviors for Cocaine and Sucrose." *European Journal of Neuroscience* 35(6):940–51. doi: 10.1111/j.1460-9568.2012.08024.x.

Carelli, R. M., S. G. Ijames, and A. J. Crumling. 2000. "Evidence That Separate Neural Circuits in the Nucleus Accumbens Encode Cocaine versus 'Natural' (Water and Food) Reward." *The Journal of Neuroscience: The Official Journal of the Society for Neuroscience* 20(11):4255–66.

Carlezon, William A., and Elena H. Chartoff. 2007. "Intracranial Self-Stimulation (ICSS) in Rodents to Study the Neurobiology of Motivation." *Nature Protocols* 2(11):2987–95. doi: 10.1038/nprot.2007.441.

Carretié, L., E. Ruiz-Padial, S. López-Martín, and J. Albert. 2011. "Decomposing Unpleasantness: Differential Exogenous Attention to Disgusting and Fearful Stimuli." *Biological Psychology* 86(3):247–53. doi: 10.1016/j.biopsycho.2010.12.005.

Castro, Daniel C., Corinna S. Oswell, Eric T. Zhang, Christian E. Pedersen, Sean C. Piantadosi, Mark A. Rossi, Avery C. Hunker, Anthony Guglin, Jose A. Morón, Larry S. Zweifel, Garret D. Stuber, and Michael R. Bruchas. 2021. "An Endogenous Opioid Circuit Determines State-Dependent Reward Consumption." *Nature* 598(7882):646–51. doi: 10.1038/s41586-021-04013-0.

Chapman, Hanah A., Kristen Johannes, Jordan L. Poppenk, Morris Moscovitch, and Adam K. Anderson. 2013. "Evidence for the Differential Salience of Disgust and Fear in Episodic Memory." *Journal of Experimental Psychology. General* 142(4):1100–1112. doi: 10.1037/a0030503.

Choi, Jung-Eun, Jiwon Kim, and Jinhyun Kim. 2020. "Capturing Activated Neurons and Synapses." *Neuroscience Research* 152:25–34. doi: 10.1016/j.neures.2019.12.020.

Cisler, Josh M., Bunmi O. Olatunji, and Jeffrey M. Lohr. 2009. "Disgust, Fear, and the Anxiety Disorders: A Critical Review." *Clinical Psychology Review* 29(1):34–46. doi: 10.1016/j.cpr.2008.09.007.

Cissé, Youssouf, Hanieh Toossi, Masaru Ishibashi, Lynda Mainville, Christopher S. Leonard, Antoine

Adamantidis, and Barbara E. Jones. 2018. "Discharge and Role of Acetylcholine Pontomesencephalic Neurons in Cortical Activity and Sleep-Wake States Examined by Optogenetics and Juxtacellular Recording in Mice." *ENeuro* 5(4):ENEURO.0270-18.2018. doi: 10.1523/ENEURO.0270-18.2018.

Clarke, P. B. S., D. W. Hommer, A. Pert, and L. R. Skirboll. 1987. "Innervation of Substantia Nigra Neurons by Cholinergic Afferents from Pedunculopontine Nucleus in the Rat: Neuroanatomical and Electrophysiological Evidence." *Neuroscience* 23(3):1011–19. doi: 10.1016/0306-4522(87)90176-X.

Clements, J. R., and S. Grant. 1990. "Glutamate-like Immunoreactivity in Neurons of the Laterodorsal Tegmental and Pedunculopontine Nuclei in the Rat." *Neuroscience Letters* 120(1):70–73. doi: 10.1016/0304-3940(90)90170-E.

Clements, J. R., D. D. Toth, D. A. Highfield, and S. J. Grant. 1991. "Glutamate-Like Immunoreactivity Is Present within Cholinergic Neurons of the Laterodorsal Tegmental and Pedunculopontine Nuclei." Pp. 127–42 in *The Basal Forebrain*, *Advances in Experimental Medicine and Biology*. Springer, Boston, MA.

Cohen, Jeremiah Y., Mackenzie W. Amoroso, and Naoshige Uchida. 2015. "Serotonergic Neurons Signal Reward and Punishment on Multiple Timescales." *ELife* 4. doi: 10.7554/eLife.06346.

Cohen, Jeremiah Y., Sebastian Haesler, Linh Vong, Bradford B. Lowell, and Naoshige Uchida. 2012. "Neuron-Type Specific Signals for Reward and Punishment in the Ventral Tegmental Area." *Nature* 482(7383):85–88. doi: 10.1038/nature10754.

Coimbra, Bárbara, Ana Verónica Domingues, Carina Soares-Cunha, Raquel Correia, Luísa Pinto, Nuno Sousa, and Ana João Rodrigues. 2021. "Laterodorsal Tegmentum-Ventral Tegmental Area Projections Encode Positive Reinforcement Signals." *Journal of Neuroscience Research* 99(11):3084–3100. doi: 10.1002/jnr.24931.

Coimbra, Bárbara, Carina Soares-Cunha, Nivaldo A. P. Vasconcelos, Ana Verónica Domingues, Sónia Borges, Nuno Sousa, and Ana João Rodrigues. 2019. "Role of Laterodorsal Tegmentum Projections to Nucleus Accumbens in Reward-Related Behaviors." *Nature Communications* 10(1):4138. doi: 10.1038/s41467-019-11557-3.

Coizet, V., E. J. Dommett, P. Redgrave, and P. G. Overton. 2006. "Nociceptive Responses of Midbrain Dopaminergic Neurones Are Modulated by the Superior Colliculus in the Rat." *Neuroscience* 139(4):1479–93. doi: 10.1016/j.neuroscience.2006.01.030.

Coley, Austin A., Nancy Padilla-Coreano, Reesha Patel, and Kay M. Tye. 2021. "Valence Processing in the PFC: Reconciling Circuit-Level and Systems-Level Views." Pp. 171–212 in *International Review of Neurobiology*. Vol. 158. Elsevier.

Cooper, Sarah, A. J. Robison, and Michelle S. Mazei-Robison. 2017. "Reward Circuitry in Addiction." *Neurotherapeutics: The Journal of the American Society for Experimental NeuroTherapeutics* 14(3):687–97. doi: 10.1007/s13311-017-0525-z.

Cornwall, J., J. D. Cooper, and O. T. Phillipson. 1990. "Afferent and Efferent Connections of the Laterodorsal Tegmental Nucleus in the Rat." *Brain Research Bulletin* 25(2):271–84. doi: 10.1016/0361-9230(90)90072-8.

Critchley, Hugo D., Jessica Eccles, and Sarah N. Garfinkel. 2013. "Chapter 6 - Interaction between Cognition, Emotion, and the Autonomic Nervous System." Pp. 59–77 in *Handbook of Clinical Neurology*. Vol. 117, *Autonomic Nervous System*, edited by R. M. Buijs and D. F. Swaab. Elsevier.

Cullinan, W. E., J. P. Herman, D. F. Battaglia, H. Akil, and S. J. Watson. 1995. "Pattern and Time Course of Immediate Early Gene Expression in Rat Brain Following Acute Stress." *Neuroscience* 64(2):477–505. doi: 10.1016/0306-4522(94)00355-9.

Cummings, Kirstie A., Sabina Bayshtok, Tri N. Dong, Paul J. Kenny, and Roger L. Clem. 2022. "Control of Fear by Discrete Prefrontal GABAergic Populations Encoding Valence-Specific Information." *Neuron*. doi: 10.1016/j.neuron.2022.07.004.

Da, Evans, Stempel Av, Vale R, and Branco T. 2019. "Cognitive Control of Escape Behaviour." *Trends in Cognitive Sciences* 23(4). doi: 10.1016/j.tics.2019.01.012.

Damsma, Geert, James G. Pfaus, Danielle Wenkstern, Anthony G. Phillips, and Hans C. Fibiger. 1992. "Sexual Behavior Increases Dopamine Transmission in the Nucleus Accumbens and Striatum of Male Rats: Comparison with Novelty and Locomotion." *Behavioral Neuroscience* 106(1):181–91. doi: 10.1037/0735-7044.106.1.181.

Dautan, Daniel, Husniye Hacioğlu Bay, J. Paul Bolam, Todor V. Gerdjikov, and Juan Mena-Segovia. 2016. "Extrinsic Sources of Cholinergic Innervation of the Striatal Complex: A Whole-Brain Mapping Analysis." *Frontiers in Neuroanatomy* 10:1. doi: 10.3389/fnana.2016.00001.

Dautan, Daniel, Icnelia Huerta-Ocampo, Nadine K. Gut, Miguel Valencia, Krishnakanth Kondabolu, Yuwoong Kim, Todor V. Gerdjikov, and Juan Mena-Segovia. 2020. "Cholinergic Midbrain Afferents Modulate Striatal Circuits and Shape Encoding of Action Strategies." *Nature Communications* 11(1):1739. doi: 10.1038/s41467-020-15514-3.

Dautan, Daniel, Icnelia Huerta-Ocampo, Ilana B. Witten, Karl Deisseroth, J. Paul Bolam, Todor Gerdjikov, and Juan Mena-Segovia. 2014. "A Major External Source of Cholinergic Innervation of the Striatum and Nucleus Accumbens Originates in the Brainstem." *The Journal of Neuroscience* 34(13):4509–18. doi: 10.1523/JNEUROSCI.5071-13.2014.

Dautan, Daniel, Albert S. Souza, Icnelia Huerta-Ocampo, Miguel Valencia, Maxime Assous, Ilana B. Witten, Karl Deisseroth, James M. Tepper, J. Paul Bolam, Todor V. Gerdjikov, and Juan Mena-Segovia. 2016. "Segregated Cholinergic Transmission Modulates Dopamine Neurons Integrated in Distinct Functional Circuits." *Nature Neuroscience* 19(8):1025–33. doi: 10.1038/nn.4335.

Davis, Michael, David L. Walker, Leigh Miles, and Christian Grillon. 2010. "Phasic vs Sustained Fear in Rats and Humans: Role of the Extended Amygdala in Fear vs Anxiety." *Neuropsychopharmacology: Official Publication of the American College of Neuropsychopharmacology* 35(1):105–35. doi: 10.1038/npp.2009.109.

De Franceschi, Gioia, Tipok Vivattanasarn, Aman B. Saleem, and Samuel G. Solomon. 2016. "Vision Guides Selection of Freeze or Flight Defense Strategies in Mice." *Current Biology: CB* 26(16):2150–54. doi: 10.1016/j.cub.2016.06.006.

Del Arco, Alberto, Junchol Park, and Bita Moghaddam. 2020. "Unanticipated Stressful and Rewarding Experiences Engage the Same Prefrontal Cortex and Ventral Tegmental Area Neuronal Populations." *ENeuro* 7(3):ENEURO.0029-20.2020. doi: 10.1523/ENEURO.0029-20.2020.

DeNardo, Laura A., Cindy D. Liu, William E. Allen, Eliza L. Adams, Drew Friedmann, Lisa Fu, Casey J. Guenthner, Marc Tessier-Lavigne, and Liqun Luo. 2019. "Temporal Evolution of Cortical Ensembles Promoting Remote Memory Retrieval." *Nature Neuroscience* 22(3):460–69. doi:

10.1038/s41593-018-0318-7.

DeNardo, Laura, and Liqun Luo. 2017. "Genetic Strategies to Access Activated Neurons." *Current Opinion in Neurobiology* 45:121–29. doi: 10.1016/j.conb.2017.05.014.

Di Chiara, G., and A. Imperato. 1988. "Drugs Abused by Humans Preferentially Increase Synaptic Dopamine Concentrations in the Mesolimbic System of Freely Moving Rats." *Proceedings of the National Academy of Sciences of the United States of America* 85(14):5274–78.

Dixsaut, Lucie, and Johannes Gräff. 2022. "Brain-Wide Screen of Prelimbic Cortex Inputs Reveals a Functional Shift during Early Fear Memory Consolidation." *ELife* 11:e78542. doi: 10.7554/eLife.78542.

Dobbs, L. K., and G. P. Mark. 2008. "Comparison of Systemic and Local Methamphetamine Treatment on Acetylcholine and Dopamine Levels in the Ventral Tegmental Area in the Mouse." *Neuroscience* 156(3):700–711. doi: 10.1016/j.neuroscience.2008.07.052.

Dobbs, Lauren K., and Christopher L. Cunningham. 2014. "The Role of the Laterodorsal Tegmental Nucleus in Methamphetamine Conditioned Place Preference and Locomotor Activity." *Behavioural Brain Research* 265:198–202. doi: 10.1016/j.bbr.2014.02.021.

Dobbs, Lauren K., and Gregory P. Mark. 2012. "Acetylcholine from the Mesopontine Tegmental Nuclei Differentially Affects Methamphetamine Induced Locomotor Activity and Neurotransmitter Levels in the Mesolimbic Pathway." *Behavioural Brain Research* 226(1):224–34. doi: 10.1016/j.bbr.2011.09.022.

Druhan, J. P., H. C. Fibiger, and A. G. Phillips. 1990. "Amphetamine-like Stimulus Properties Produced by Electrical Stimulation of Reward Sites in the Ventral Tegmental Area." *Behavioural Brain Research* 38(2):175–84. doi: 10.1016/0166-4328(90)90015-7.

Fadok, Jonathan P., Milica Markovic, Philip Tovote, and Andreas Lüthi. 2018. "New Perspectives on Central Amygdala Function." *Current Opinion in Neurobiology* 49:141–47. doi: 10.1016/j.conb.2018.02.009.

Fanselow, Michael S. 2018. "The Role of Learning in Threat Imminence and Defensive Behaviors." *Current Opinion in Behavioral Sciences* 24:44–49. doi: 10.1016/j.cobeha.2018.03.003.

Faure, Alexis, Jocelyn M. Richard, and Kent C. Berridge. 2010. "Desire and Dread from the Nucleus Accumbens: Cortical Glutamate and Subcortical GABA Differentially Generate Motivation and Hedonic Impact in the Rat." *PLOS ONE* 5(6):e11223. doi: 10.1371/journal.pone.0011223.

Fernandez, Sebastian P., Loïc Broussot, Fabio Marti, Thomas Contesse, Xavier Mouska, Mariano Soiza-Reilly, Hélène Marie, Philippe Faure, and Jacques Barik. 2018. "Mesopontine Cholinergic Inputs to Midbrain Dopamine Neurons Drive Stress-Induced Depressive-like Behaviors." *Nature Communications* 9(1):4449. doi: 10.1038/s41467-018-06809-7.

Filipkowski, Robert K., Marek Rydz, Bozena Berdel, Janusz Morys, and Leszek Kaczmarek. 2000. "Tactile Experience Induces C-Fos Expression in Rat Barrel Cortex." *Learning & Memory* 7(2):116–22.

Floresco, Stan B., Anthony R. West, Brian Ash, Holly Moore, and Anthony A. Grace. 2003. "Afferent Modulation of Dopamine Neuron Firing Differentially Regulates Tonic and Phasic Dopamine Transmission." *Nature Neuroscience* 6(9):968–73. doi: 10.1038/nn1103.

Fonseca, Madalena S., Masayoshi Murakami, and Zachary F. Mainen. 2015. "Activation of Dorsal Raphe Serotonergic Neurons Promotes Waiting but Is Not Reinforcing." *Current Biology* 25(3):306–15. doi: 10.1016/j.cub.2014.12.002.

Ford, Blair, Colin J. Holmes, Lynda Mainville, and Barbara E. Jones. 1995. "GABAergic Neurons in the Rat Pontomesencephalic Tegmentum: Codistribution with Cholinergic and Other Tegmental Neurons Projecting to the Posterior Lateral Hypothalamus." *Journal of Comparative Neurology* 363(2):177–96. doi: 10.1002/cne.903630203.

Forster, G. L., and C. D. Blaha. 2000. "Laterodorsal Tegmental Stimulation Elicits Dopamine Efflux in the Rat Nucleus Accumbens by Activation of Acetylcholine and Glutamate Receptors in the Ventral Tegmental Area." *The European Journal of Neuroscience* 12(10):3596–3604. doi: 10.1046/j.1460-9568.2000.00250.x.

Forster, G. L., A. J. Falcon, A. D. Miller, G. A. Heruc, and C. D. Blaha. 2002. "Effects of Laterodorsal Tegmentum Excitotoxic Lesions on Behavioral and Dopamine Responses Evoked by Morphine and D-Amphetamine." *Neuroscience* 114(4):817–23. doi: 10.1016/S0306-4522(02)00365-2.

Geisler, Stefanie, Michela Marinelli, Beth DeGarmo, Mary L. Becker, Alexander J. Freiman, Mitch Beales, Gloria E. Meredith, and Daniel S. Zahm. 2008. "Prominent Activation of Brainstem and Pallidal

Afferents of the Ventral Tegmental Area by Cocaine." *Neuropsychopharmacology* 33(11):2688–2700. doi: 10.1038/sj.npp.1301650.

Giros, B., M. Jaber, S. R. Jones, R. M. Wightman, and M. G. Caron. 1996. "Hyperlocomotion and Indifference to Cocaine and Amphetamine in Mice Lacking the Dopamine Transporter." *Nature* 379(6566):606–12. doi: 10.1038/379606a0.

Girotti, M., T. W. W. Pace, R. I. Gaylord, B. A. Rubin, J. P. Herman, and R. L. Spencer. 2006. "Habituation to Repeated Restraint Stress Is Associated with Lack of Stress-Induced c-Fos Expression in Primary Sensory Processing Areas of the Rat Brain." *Neuroscience* 138(4):1067–81. doi: 10.1016/j.neuroscience.2005.12.002.

Gore, Felicity, Edmund C. Schwartz, Baylor C. Brangers, Stanley Aladi, Joseph M. Stujenske, Ekaterina Likhtik, Marco J. Russo, Joshua A. Gordon, C. Daniel Salzman, and Richard Axel. 2015. "Neural Representations of Unconditioned Stimuli in Basolateral Amygdala Mediate Innate and Learned Responses." *Cell* 162(1):134–45. doi: 10.1016/j.cell.2015.06.027.

Gould, E., N. J. Woolf, and L. L. Butcher. 1989. "Cholinergic Projections to the Substantia Nigra from the Pedunculopontine and Laterodorsal Tegmental Nuclei." *Neuroscience* 28(3):611–23. doi: 10.1016/0306-4522(89)90008-0.

Grewe, Benjamin F., Jan Gründemann, Lacey J. Kitch, Jerome A. Lecoq, Jones G. Parker, Jesse D. Marshall, Margaret C. Larkin, Pablo E. Jercog, Francois Grenier, Jin Zhong Li, Andreas Lüthi, and Mark J. Schnitzer. 2017. "Neural Ensemble Dynamics Underlying a Long-Term Associative Memory." *Nature* 543(7647):670–75. doi: 10.1038/nature21682.

Grupe, Dan W., and Jack B. Nitschke. 2013. "Uncertainty and Anticipation in Anxiety: An Integrated Neurobiological and Psychological Perspective." *Nature Reviews Neuroscience* 14(7):488–501. doi: 10.1038/nrn3524.

Guenthner, Casey J., Kazunari Miyamichi, Helen H. Yang, H. Craig Heller, and Liqun Luo. 2013. "Permanent Genetic Access to Transiently Active Neurons via TRAP: Targeted Recombination in Active Populations." *Neuron* 78(5):773–84. doi: 10.1016/j.neuron.2013.03.025.

Guitart-Masip, Marc, Emrah Duzel, Ray Dolan, and Peter Dayan. 2014. "Action versus Valence in Decision Making." *Trends in Cognitive Sciences* 18(4):194–202. doi: 10.1016/j.tics.2014.01.003.

Hadad, Natalie A., and Lori A. Knackstedt. 2014. "Addicted to Palatable Foods: Comparing the Neurobiology of Bulimia Nervosa to That of Drug Addiction." *Psychopharmacology* 231(9):1897–1912. doi: 10.1007/s00213-014-3461-1.

Halazonetis, Thanos D., Katia Georgopoulos, Michael E. Greenberg, and Philip Leder. 1988. "C-Jun Dimerizes with Itself and with c-Fos, Forming Complexes of Different DNA Binding Affinities." *Cell* 55(5):917–24. doi: 10.1016/0092-8674(88)90147-X.

Hansen, S., Å. H. Bergvall, and S. Nyiredi. 1993. "Interaction with Pups Enhances Dopamine Release in the Ventral Striatum of Maternal Rats: A Microdialysis Study." *Pharmacology Biochemistry and Behavior* 45(3):673–76. doi: 10.1016/0091-3057(93)90523-V.

Herbst, Matthew R., Robert C. Twining, and Marieke R. Gilmartin. 2022. "Ventral Hippocampal Shock Encoding Modulates the Expression of Trace Cued Fear." *Neurobiology of Learning and Memory* 190:107610. doi: 10.1016/j.nlm.2022.107610.

Hernandez, Nicole S., Vanessa R. Weir, Kael Ragnini, Riley Merkel, Yafang Zhang, Kyla Mace, Matthew T. Rich, R. Christopher Pierce, and Heath D. Schmidt. 2021. *Molecular Psychiatry* 26(8):4394–4408. doi: 10.1038/s41380-020-00957-3.

Heshmati, Mitra, and Scott J. Russo. 2015. "Anhedonia and the Brain Reward Circuitry in Depression." *Current Behavioral Neuroscience Reports* 2(3):146–53. doi: 10.1007/s40473-015-0044-3.

Hofmeister, Jeremy, and Virginie Sterpenich. 2015. "A Role for the Locus Ceruleus in Reward Processing: Encoding Behavioral Energy Required for Goal-Directed Actions." *Journal of Neuroscience* 35(29):10387–89. doi: 10.1523/JNEUROSCI.1734-15.2015.

Holmstrand, Ericka C., Josephine Asafu-Adjei, Allan R. Sampson, Randy D. Blakely, and Susan R. Sesack. 2010. "Ultrastructural Localization of High-Affinity Choline Transporter in the Rat Anteroventral Thalamus and Ventral Tegmental Area: Differences in Axon Morphology and Transporter Distribution." *Journal of Comparative Neurology* 518(11):1908–24. doi: 10.1002/cne.22310.

Holmstrand, Ericka C., and Susan R. Sesack. 2011. "Projections from the Rat Pedunculopontine and Laterodorsal Tegmental Nuclei to the Anterior Thalamus and Ventral Tegmental Area Arise from Largely Separate Populations of Neurons." *Brain Structure & Function* 216(4):331–45. doi: 10.1007/s00429-011-0320-2.

Hoover, Walter B., and Robert P. Vertes. 2011. "Projections of the Medial Orbital and Ventral Orbital Cortex in the Rat." *The Journal of Comparative Neurology* 519(18):3766–3801. doi: 10.1002/cne.22733.

Huang, Wen-Chin, Aya Zucca, Jenna Levy, and Damon T. Page. 2020. "Social Behavior Is Modulated by Valence-Encoding MPFC-Amygdala Sub-Circuitry." *Cell Reports* 32(2):107899. doi: 10.1016/j.celrep.2020.107899.

Huerta-Ocampo, Icnelia, Daniel Dautan, Nadine K. Gut, Bakhtawer Khan, and Juan Mena-Segovia. 2021. "Whole-Brain Mapping of Monosynaptic Inputs to Midbrain Cholinergic Neurons." *Scientific Reports* 11(1):9055. doi: 10.1038/s41598-021-88374-6.

Huerta-Ocampo, Icnelia, Husniye Hacioglu-Bay, Daniel Dautan, and Juan Mena-Segovia. 2020. "Distribution of Midbrain Cholinergic Axons in the Thalamus." *ENeuro* 7(1):ENEURO.0454-19.2019. doi: 10.1523/ENEURO.0454-19.2019.

Imoto, Daigo, Izumi Yamamoto, Hirokazu Matsunaga, Toya Yonekura, Ming-Liang Lee, Kan X. Kato, Takeshi Yamasaki, Shucheng Xu, Taiga Ishimoto, Satoshi Yamagata, Ken-ichi Otsuguro, Motohiro Horiuchi, Norifumi Iijima, Kazuhiro Kimura, and Chitoku Toda. 2021. "Refeeding Activates Neurons in the Dorsomedial Hypothalamus to Inhibit Food Intake and Promote Positive Valence." *Molecular Metabolism* 54:101366. doi: 10.1016/j.molmet.2021.101366.

Ishibashi, Masaru, Christopher S. Leonard, and Kristi A. Kohlmeier. 2009. "Nicotinic Activation of Laterodorsal Tegmental Neurons: Implications for Addiction to Nicotine." *Neuropsychopharmacology* 34(12):2529–47. doi: 10.1038/npp.2009.82.

Itzhak, Yossef, and Julio L. Martin. 2002. "Cocaine-Induced Conditioned Place Preference in Mice: Induction, Extinction and Reinstatement by Related Psychostimulants." *Neuropsychopharmacology* 26:130–34. doi: 10.1016/S0893-133X(01)00303-7.

Ivashkina, Olga I., Anna M. Gruzdeva, Marina A. Roshchina, Ksenia A. Toropova, and Konstantin V. Anokhin. 2021. "Imaging of C-Fos Activity in Neurons of the Mouse Parietal Association Cortex during Acquisition and Retrieval of Associative Fear Memory." *International Journal of Molecular Sciences* 22(15):8244. doi: 10.3390/ijms22158244.

Jarzebowski, Przemyslaw, Y. Audrey Hay, Benjamin F. Grewe, and Ole Paulsen. 2022. "Different

Encoding of Reward Location in Dorsal and Intermediate Hippocampus." *Current Biology: CB* 32(4):834-841.e5. doi: 10.1016/j.cub.2021.12.024.

Jean-Richard-Dit-Bressel, Philip, Simon Killcross, and Gavan P. McNally. 2018. "Behavioral and Neurobiological Mechanisms of Punishment: Implications for Psychiatric Disorders." *Neuropsychopharmacology* 43(8):1639–50. doi: 10.1038/s41386-018-0047-3.

Jerlhag, Elisabet, Emil Egecioglu, Sara Landgren, Nicolas Salomé, Markus Heilig, Diederik Moechars, Rakesh Datta, Daniel Perrissoud, Suzanne L. Dickson, and Jörgen A. Engel. 2009. "Requirement of Central Ghrelin Signaling for Alcohol Reward." *Proceedings of the National Academy of Sciences* 106(27):11318–23. doi: 10.1073/pnas.0812809106.

Jerlhag, Elisabet, Anna Carin Janson, Susanna Waters, and Jörgen A. Engel. 2012. "Concomitant Release of Ventral Tegmental Acetylcholine and Accumbal Dopamine by Ghrelin in Rats" edited by M. Minami. *PLoS ONE* 7(11):e49557. doi: 10.1371/journal.pone.0049557.

Jia, Hong-Ge, Jack Yamuy, Sharon Sampogna, Francisco R. Morales, and Michael H. Chase. 2003. "Colocalization of Gamma-Aminobutyric Acid and Acetylcholine in Neurons in the Laterodorsal and Pedunculopontine Tegmental Nuclei in the Cat: A Light and Electron Microscopic Study." *Brain Research* 992(2):205–19.

Jimenez, Jessica C., Jack E. Berry, Sean C. Lim, Samantha K. Ong, Mazen A. Kheirbek, and Rene Hen. 2020. "Contextual Fear Memory Retrieval by Correlated Ensembles of Ventral CA1 Neurons." *Nature Communications* 11(1):3492. doi: 10.1038/s41467-020-17270-w.

Jones, B. E., and A. Beaudet. 1987. "Distribution of Acetylcholine and Catecholamine Neurons in the Cat Brainstem: A Choline Acetyltransferase and Tyrosine Hydroxylase Immunohistochemical Study." *The Journal of Comparative Neurology* 261(1):15–32. doi: 10.1002/cne.902610103.

José Lança, A., T. R. Sanelli, and W. A. Corrigall. 2000. "Nicotine-Induced Fos Expression in the Pedunculopontine Mesencephalic Tegmentum in the Rat." *Neuropharmacology* 39(13):2808–17. doi: 10.1016/s0028-3908(00)00129-5.

Joshua, Mati, Avital Adler, Yifat Prut, Eilon Vaadia, Jeffery R. Wickens, and Hagai Bergman. 2009. "Synchronization of Midbrain Dopaminergic Neurons Is Enhanced by Rewarding Events." *Neuron* 62(5):695–704. doi: 10.1016/j.neuron.2009.04.026.

K Namboodiri, Vijay Mohan, Taylor Hobbs, Ivan Trujillo-Pisanty, Rhiana C. Simon, Madelyn M. Gray, and Garret D. Stuber. 2021. "Relative Salience Signaling within a Thalamo-Orbitofrontal Circuit Governs Learning Rate." *Current Biology: CB* 31(23):5176-5191.e5. doi: 10.1016/j.cub.2021.09.037.

Kalafateli, Aimilia Lydia, Cajsa Aranäs, and Elisabet Jerlhag. 2021. "Activation of the Amylin Pathway Modulates Cocaine-Induced Activation of the Mesolimbic Dopamine System in Male Mice." *Hormones and Behavior* 127:104885. doi: 10.1016/j.yhbeh.2020.104885.

Kalafateli, Aimilia Lydia, Tugce Munise Satir, Daniel Vallöf, Henrik Zetterberg, and Elisabet Jerlhag. 2021. "An Amylin and Calcitonin Receptor Agonist Modulates Alcohol Behaviors by Acting on Reward-Related Areas in the Brain." *Progress in Neurobiology* 200:101969. doi: 10.1016/j.pneurobio.2020.101969.

Kamii, Hironori, Naofumi Taoka, Masabumi Minami, and Katsuyuki Kaneda. 2017. "Nitric Oxide in the Medial Prefrontal Cortex Contributes to the Acquisition of Cocaine Place Preference and Synaptic Plasticity in the Laterodorsal Tegmental Nucleus." *Neuroscience Letters* 660:39–44. doi: 10.1016/j.neulet.2017.09.015.

Kane, Louisa, Marco Venniro, Richard Quintana-Feliciano, Rajtarun Madangopal, F. Javier Rubio, Jennifer M. Bossert, Daniele Caprioli, Yavin Shaham, Bruce T. Hope, and Brandon L. Warren. 2020. "Fos-Expressing Neuronal Ensemble in Rat Ventromedial Prefrontal Cortex Encodes Cocaine Seeking but Not Food Seeking in Rats." *Addiction Biology* e12943. doi: 10.1111/adb.12943.

Kawashima, Takashi, Hiroyuki Okuno, and Haruhiko Bito. 2014. "A New Era for Functional Labeling of Neurons: Activity-Dependent Promoters Have Come of Age." *Frontiers in Neural Circuits* 8.

Kazi, Jamil Ahsan, Shiro Mori, Satoshi Kuchiiwa, and Shiro Nakagawa. 2004. "Prolonged Expression of C-Fos Protein in the Lateral Habenular Nucleus of the Japanese Monkey (Macaca Fuscata) after Eye Enucleation." *Neuro-Signals* 13(3):130–33. doi: 10.1159/000076566.

Kim, Joshua, Xiangyu Zhang, Shruti Muralidhar, Sarah A. LeBlanc, and Susumu Tonegawa. 2017. "Basolateral to Central Amygdala Neural Circuits for Appetitive Behaviors." *Neuron* 93(6):1464-1479.e5. doi: 10.1016/j.neuron.2017.02.034.

Kim, Woong Bin, and Jun-Hyeong Cho. 2020. "Encoding of Contextual Fear Memory in Hippocampal-

Amygdala Circuit." *Nature Communications* 11(1):1382. doi: 10.1038/s41467-020-15121-2.

King, Camille Tessitore, Mircea Garcea, and Alan C. Spector. 2014. "Restoration of Quinine-Stimulated Fos-Immunoreactive Neurons in the Central Nucleus of the Amygdala and Gustatory Cortex Following Reinnervation or Cross-Reinnervation of the Lingual Taste Nerves in Rats." *The Journal of Comparative Neurology* 522(11):2498–2517. doi: 10.1002/cne.23546.

Kiyatkin, Eugene A., and Alain Gratton. 1994. "Electrochemical Monitoring of Extracellular Dopamine in Nucleus Accumbens of Rats Lever-Pressing for Food." *Brain Research* 652(2):225–34. doi: 10.1016/0006-8993(94)90231-3.

Kljakic, Ornela, Helena Janickova, Vania F. Prado, and Marco A. M. Prado. 2017. "Cholinergic/Glutamatergic Co-Transmission in Striatal Cholinergic Interneurons: New Mechanisms Regulating Striatal Computation." *Journal of Neurochemistry* 142(S2):90–102. doi: 10.1111/jnc.14003.

Kobayashi, Yasushi, Yuka Inoue, and Tadashi Isa. 2003. "Cognitive Function of the Brainstem Cholinergic System." *International Congress Series* 1250:397–406. doi: 10.1016/S0531-5131(03)00967-1.

Kohlmeier, Kristi A. 2013. "Off the Beaten Path: Drug Addiction and the Pontine Laterodorsal Tegmentum." *ISRN Neuroscience* 2013:604847. doi: 10.1155/2013/604847.

Kohlmeier, Kristi A., and Filip S. Polli. 2020. "Plasticity in the Brainstem: Prenatal and Postnatal Experience Can Alter Laterodorsal Tegmental (LDT) Structure and Function." *Frontiers in Synaptic Neuroscience* 12:3. doi: 10.3389/fnsyn.2020.00003.

Koob, George F. 2009. "Neurobiological Substrates for the Dark Side of Compulsivity in Addiction." *Neuropharmacology* 56 Suppl 1:18–31. doi: 10.1016/j.neuropharm.2008.07.043.

Körber, Christoph, and Wolfgang H. Sommer. 2022. "From Ensembles to Meta-Ensembles: Specific Reward Encoding by Correlated Network Activity." *Frontiers in Behavioral Neuroscience* 16.

Koutlas, Ioannis, Louisa E. Linders, Stef E. van der Starre, Inge G. Wolterink-Donselaar, Roger A. H. Adan, and Frank J. Meye. 2022. "Characterizing and TRAPing a Social Stress-Activated Neuronal Ensemble in the Ventral Tegmental Area." *Frontiers in Behavioral Neuroscience* 16:936087. doi:

10.3389/fnbeh.2022.936087.

Kovács, K. J. 2008. "Measurement of Immediate-Early Gene Activation- c-Fos and Beyond." *Journal of Neuroendocrinology* 20(6):665–72. doi: 10.1111/j.1365-2826.2008.01734.x.

Koyama, Y., E. Jodo, and Y. Kayama. 1994. "Sensory Responsiveness of 'Broad-Spike' Neurons in the Laterodorsal Tegmental Nucleus, Locus Coeruleus and Dorsal Raphe of Awake Rats: Implications for Cholinergic and Monoaminergic Neuron-Specific Responses." *Neuroscience* 63(4):1021–31. doi: 10.1016/0306-4522(94)90569-X.

Kringelbach, Morten L. 2005. "The Human Orbitofrontal Cortex: Linking Reward to Hedonic Experience." *Nature Reviews Neuroscience* 6(9):691–702. doi: 10.1038/nrn1747.

Lambert, Mads Ødum, Theis Højland Ipsen, and Kristi Anne Kohlmeier. 2017. "Acute Cocaine Exposure Elicits Rises in Calcium in Arousal-Related Laterodorsal Tegmental Neurons." *Pharmacology Research & Perspectives* 5(1):e00282. doi: 10.1002/prp2.282.

Lammel, Stephan, Byung Kook Lim, Chen Ran, Kee Wui Huang, Michael J. Betley, Kay M. Tye, Karl Deisseroth, and Robert C. Malenka. 2012. "Input-Specific Control of Reward and Aversion in the Ventral Tegmental Area." *Nature* 491(7423):212–17. doi: 10.1038/nature11527.

Lang, Peter J. 1995. "The Emotion Probe: Studies of Motivation and Attention." *American Psychologist* 50(5):372–85. doi: 10.1037/0003-066X.50.5.372.

Laviolette, S. R., R. P. Priebe, and J. S. Yeomans. 2000. "Role of the Laterodorsal Tegmental Nucleus in Scopolamine- and Amphetamine-Induced Locomotion and Stereotypy." *Pharmacology, Biochemistry, and Behavior* 65(1):163–74. doi: 10.1016/s0091-3057(99)00195-1.

Lavoie, B., and A. Parent. 1994a. "Pedunculopontine Nucleus in the Squirrel Monkey: Cholinergic and Glutamatergic Projections to the Substantia Nigra." *The Journal of Comparative Neurology* 344(2):232–41. doi: 10.1002/cne.903440205.

Lavoie, B., and A. Parent. 1994b. "Pedunculopontine Nucleus in the Squirrel Monkey: Distribution of Cholinergic and Monoaminergic Neurons in the Mesopontine Tegmentum with Evidence for the Presence of Glutamate in Cholinergic Neurons." *The Journal of Comparative Neurology* 344(2):190–209. doi: 10.1002/cne.903440203.

Lecca, Salvatore, Vijay M. K. Namboodiri, Leonardo Restivo, Nicolas Gervasi, Giuliano Pillolla, Garret D. Stuber, and Manuel Mameli. 2020. "Heterogeneous Habenular Neuronal Ensembles during Selection of Defensive Behaviors." *Cell Reports* 31(10):107752. doi: 10.1016/j.celrep.2020.107752.

LeDoux, Joseph. 2012. "Rethinking the Emotional Brain." *Neuron* 73(4):653–76. doi: 10.1016/j.neuron.2012.02.004.

LeDoux, Joseph, and Nathaniel D. Daw. 2018. "Surviving Threats: Neural Circuit and Computational Implications of a New Taxonomy of Defensive Behaviour." *Nature Reviews Neuroscience* 19(5):269–82. doi: 10.1038/nrn.2018.22.

LeDoux, Joseph E. 2014. "Coming to Terms with Fear." *Proceedings of the National Academy of Sciences of the United States of America* 111(8):2871–78. doi: 10.1073/pnas.1400335111.

Lee, Dongmin, Jung Ho Hyun, Kanghoon Jung, Patrick Hannan, and Hyung-Bae Kwon. 2017. "A Calcium- and Light-Gated Switch to Induce Gene Expression in Activated Neurons." *Nature Biotechnology* 35(9):858–63. doi: 10.1038/nbt.3902.

Lee, In-Seon, Elizabeth A. Necka, and Lauren Y. Atlas. 2020. "Distinguishing Pain from Nociception, Salience, and Arousal: How Autonomic Nervous System Activity Can Improve Neuroimaging Tests of Specificity." *NeuroImage* 204:116254. doi: 10.1016/j.neuroimage.2019.116254.

Lester, Deranda B., Anthony D. Miller, and Charles D. Blaha. 2010. "Muscarinic Receptor Blockade in the Ventral Tegmental Area Attenuates Cocaine Enhancement of Laterodorsal Tegmentum Stimulation-Evoked Accumbens Dopamine Efflux in the Mouse." *Synapse (New York, N.Y.)* 64(3):216–23. doi: 10.1002/syn.20717.

Lester, Deranda B., Anthony D. Miller, Tiffany D. Pate, and Charles D. Blaha. 2008. "Midbrain Acetylcholine and Glutamate Receptors Modulate Accumbal Dopamine Release." *Neuroreport* 19(9):991–95. doi: 10.1097/WNR.0b013e3283036e5e.

Li, Wei-Guang, Yan-Jiao Wu, Xue Gu, Hui-Ran Fan, Qi Wang, Jia-Jie Zhu, Xin Yi, Qin Wang, Qin Jiang, Ying Li, Ti-Fei Yuan, Han Xu, Jiangteng Lu, Nan-Jie Xu, Michael Xi Zhu, and Tian-Le Xu. 2021. "Input Associativity Underlies Fear Memory Renewal." *National Science Review* 8(9):nwab004. doi: 10.1093/nsr/nwab004.

Liu, Christine, Amanda J. Tose, Jeroen P. H. Verharen, Yichen Zhu, Lilly W. Tang, Johannes W. de Jong, Jessica X. Du, Kevin T. Beier, and Stephan Lammel. 2022. "An Inhibitory Brainstem Input to Dopamine Neurons Encodes Nicotine Aversion." *Neuron*. doi: 10.1016/j.neuron.2022.07.003.

Liu, X., X. Tang, and LD Sanford. 2009. "Stressor Controllability and Fos Expression in Stress Regulatory Regions in Mice." *Physiology & Behavior* 97(3–4):321–26. doi: 10.1016/j.physbeh.2009.02.038.

Liu, Xianling, Xiangdong Tang, and Larry D. Sanford. 2003. "Fear-Conditioned Suppression of REM Sleep: Relationship to Fos Expression Patterns in Limbic and Brainstem Regions in BALB/CJ Mice." *Brain Research* 991(1–2):1–17. doi: 10.1016/j.brainres.2003.07.003.

Lodge, D. J., and A. A. Grace. 2006. "The Laterodorsal Tegmentum Is Essential for Burst Firing of Ventral Tegmental Area Dopamine Neurons." *Proceedings of the National Academy of Sciences of the United States of America* 103(13):5167–72. doi: 10.1073/pnas.0510715103.

Luquin, Esther, Ibone Huerta, María S. Aymerich, and Elisa Mengual. 2018. "Stereological Estimates of Glutamatergic, GABAergic, and Cholinergic Neurons in the Pedunculopontine and Laterodorsal Tegmental Nuclei in the Rat." *Frontiers in Neuroanatomy* 12.

Luquin, Esther, Beatriz Paternain, Inés Zugasti, Carmen Santomá, and Elisa Mengual. 2022. "Stereological Estimations and Neurochemical Characterization of Neurons Expressing GABAA and GABAB Receptors in the Rat Pedunculopontine and Laterodorsal Tegmental Nuclei." *Brain Structure & Function* 227(1):89–110. doi: 10.1007/s00429-021-02375-9.

Mahady, Laura, Sylvia E. Perez, Dwaine F. Emerich, Lars U. Wahlberg, and Elliott J. Mufson. 2017. "Cholinergic Profiles in the Goettingen Miniature Pig (Sus Scrofa Domesticus) Brain." *The Journal of Comparative Neurology* 525(3):553–73. doi: 10.1002/cne.24087.

Maley, B. E., M. L. Frick, A. I. Levey, B. H. Wainer, and R. P. Elde. 1988. "Immunohistochemistry of Choline Acetyltransferase in the Guinea Pig Brain." *Neuroscience Letters* 84(2):137–42. doi: 10.1016/0304-3940(88)90397-7.

Marcos, Pilar, and Rafael Coveñas. 2021. "Immunohistochemical Study of the Brainstem Cholinergic System in the Alpaca (Lama Pacos) and Colocalization with CGRP." *European Journal of Histochemistry : EJH* 65(Suppl 1):3266. doi: 10.4081/ejh.2021.3266.

Martinez, M., P. J. Phillips, and J. Herbert. 1998. "Adaptation in Patterns of C-Fos Expression in the Brain Associated with Exposure to Either Single or Repeated Social Stress in Male Rats." *The European Journal of Neuroscience* 10(1):20–33. doi: 10.1046/j.1460-9568.1998.00011.x.

Matsumoto, Masayuki, and Okihide Hikosaka. 2009. "Two Types of Dopamine Neuron Distinctly Convey Positive and Negative Motivational Signals." *Nature* 459(7248):837–41. doi: 10.1038/nature08028.

McCall, Jordan G., Ream Al-Hasani, Edward R. Siuda, Daniel Y. Hong, Aaron J. Norris, Christopher P. Ford, and Michael R. Bruchas. 2015. "CRH Engagement of the Locus Coeruleus Noradrenergic System Mediates Stress-Induced Anxiety." *Neuron* 87(3):605–20. doi: 10.1016/j.neuron.2015.07.002.

McLaughlin, Ian, John A. Dani, and Mariella De Biasi. 2017. "The Medial Habenula and Interpeduncular Nucleus Circuitry Is Critical in Addiction, Anxiety, and Mood Regulation." *Journal of Neurochemistry* 142(Suppl 2):130–43. doi: 10.1111/jnc.14008.

Mesulam, M. M., C. Geula, M. A. Bothwell, and L. B. Hersh. 1989. "Human Reticular Formation: Cholinergic Neurons of the Pedunculopontine and Laterodorsal Tegmental Nuclei and Some Cytochemical Comparisons to Forebrain Cholinergic Neurons." *The Journal of Comparative Neurology* 283(4):611–33. doi: 10.1002/cne.902830414.

Mesulam, M. M., E. J. Mufson, B. H. Wainer, and A. I. Levey. 1983. "Central Cholinergic Pathways in the Rat: An Overview Based on an Alternative Nomenclature (Ch1–Ch6)." *Neuroscience* 10(4):1185–1201. doi: 10.1016/0306-4522(83)90108-2.

Montague, P. Read, Steven E. Hyman, and Jonathan D. Cohen. 2004. "Computational Roles for Dopamine in Behavioural Control." *Nature* 431(7010):760–67. doi: 10.1038/nature03015.

Montero, V. M., and S. Jian. 1995. "Induction of C-Fos Protein by Patterned Visual Stimulation in Central Visual Pathways of the Rat." *Brain Research* 690(2):189–99. doi: 10.1016/0006-8993(95)00620-6.

Morales, Ileana, and Kent C. Berridge. 2020. "'Liking' and 'Wanting' in Eating and Food Reward: Brain Mechanisms and Clinical Implications." *Physiology & Behavior* 227:113152. doi: 10.1016/j.physbeh.2020.113152.

Morgan, J. I., D. R. Cohen, J. L. Hempstead, and T. Curran. 1987. "Mapping Patterns of C-Fos Expression in the Central Nervous System after Seizure." *Science (New York, N.Y.)* 237(4811):192–97. doi: 10.1126/science.3037702.

Morgan, J. I., and T. Curran. 1991. "Stimulus-Transcription Coupling in the Nervous System: Involvement of the Inducible Proto-Oncogenes Fos and Jun." *Annual Review of Neuroscience* 14:421–51. doi: 10.1146/annurev.ne.14.030191.002225.

Mori, Kensaku, and Hitoshi Sakano. 2022. "Neural Circuitry for Stress Information of Environmental and Internal Odor Worlds." *Frontiers in Behavioral Neuroscience* 16:943647. doi: 10.3389/fnbeh.2022.943647.

Muramoto, K., T. Ono, H. Nishijo, and M. Fukuda. 1993. "Rat Amygdaloid Neuron Responses during Auditory Discrimination." *Neuroscience* 52(3):621–36. doi: 10.1016/0306-4522(93)90411-8.

Nall, Rusty W., Jasper A. Heinsbroek, Todd B. Nentwig, Peter W. Kalivas, and Ana-Clara Bobadilla. 2021. "Circuit Selectivity in Drug versus Natural Reward Seeking Behaviors." *Journal of Neurochemistry* 157(5):1450–72. doi: 10.1111/jnc.15297.

Namburi, Praneeth, Ream Al-Hasani, Gwendolyn G. Calhoon, Michael R. Bruchas, and Kay M. Tye. 2016. "Architectural Representation of Valence in the Limbic System." *Neuropsychopharmacology* 41(7):1697–1715. doi: 10.1038/npp.2015.358.

Nawarawong, Natalie N., and Christopher M. Olsen. 2020. "Within-Animal Comparisons of Novelty and Cocaine Neuronal Ensemble Overlap in the Nucleus Accumbens and Prefrontal Cortex." *Behavioural Brain Research* 379:112275. doi: 10.1016/j.bbr.2019.112275.

Negus, S. Stevens, and Laurence L. Miller. 2014. "Intracranial Self-Stimulation to Evaluate Abuse Potential of Drugs." *Pharmacological Reviews* 66(3):869–917. doi: 10.1124/pr.112.007419.

Nelson, C. L., J. B. Wetter, M. Milovanovic, and M. E. Wolf. 2007. "The Laterodorsal Tegmentum Contributes to Behavioral Sensitization to Amphetamine." *Neuroscience* 146(1):41–49. doi: 10.1016/j.neuroscience.2007.01.027.

Niedringhaus, Mark, and Elizabeth A. West. 2022. "Prelimbic Cortex Neural Encoding Dynamically Tracks Expected Outcome Value." *Physiology & Behavior* 113938. doi:

10.1016/j.physbeh.2022.113938.

Nieh, Edward H., Caitlin M. Vander Weele, Gillian A. Matthews, Kara N. Presbrey, Romy Wichmann, Christopher A. Leppla, Ehsan M. Izadmehr, and Kay M. Tye. 2016. "Inhibitory Input from the Lateral Hypothalamus to the Ventral Tegmental Area Disinhibits Dopamine Neurons and Promotes Behavioral Activation." *Neuron* 90(6):1286–98. doi: 10.1016/j.neuron.2016.04.035.

Niu, Misaki, Atsushi Kasai, Masato Tanuma, Kaoru Seiriki, Hisato Igarashi, Takahiro Kuwaki, Kazuki Nagayasu, Keita Miyaji, Hiroki Ueno, Wataru Tanabe, Kei Seo, Rei Yokoyama, Jin Ohkubo, Yukio Ago, Misuzu Hayashida, Ken-Ichi Inoue, Masahiko Takada, Shun Yamaguchi, Takanobu Nakazawa, Shuji Kaneko, Hiroyuki Okuno, Akihiro Yamanaka, and Hitoshi Hashimoto. 2022. "Claustrum Mediates Bidirectional and Reversible Control of Stress-Induced Anxiety Responses." *Science Advances* 8(11):eabi6375. doi: 10.1126/sciadv.abi6375.

Oakman, Sa, Pl Faris, Pe Kerr, C. Cozzari, and Bk Hartman. 1995. "Distribution of Pontomesencephalic Cholinergic Neurons Projecting to Substantia Nigra Differs Significantly from Those Projecting to Ventral Tegmental Area." *The Journal of Neuroscience* 15(9):5859–69. doi: 10.1523/JNEUROSCI.15-09-05859.1995.

Oaten, Megan, Richard J. Stevenson, and Trevor I. Case. 2009. "Disgust as a Disease-Avoidance Mechanism." *Psychological Bulletin* 135(2):303–21. doi: 10.1037/a0014823.

Olney, Jeffrey J., Shelley M. Warlow, Erin E. Naffziger, and Kent C. Berridge. 2018. "Current Perspectives on Incentive Salience and Applications to Clinical Disorders." *Current Opinion in Behavioral Sciences* 22:59–69. doi: 10.1016/j.cobeha.2018.01.007.

Omelchenko, Natalia, and Susan R. Sesack. 2005. "Laterodorsal Tegmental Projections to Identified Cell Populations in the Rat Ventral Tegmental Area." *The Journal of Comparative Neurology* 483(2):217–35. doi: 10.1002/cne.20417.

Paquelet, Grace E., Kassandra Carrion, Clay O. Lacefield, Pengcheng Zhou, René Hen, and Bradley R. Miller. 2022. "Single-Cell Activity and Network Properties of Dorsal Raphe Nucleus Serotonin Neurons during Emotionally Salient Behaviors." *Neuron* 110(16):2664-2679.e8. doi: 10.1016/j.neuron.2022.05.015.

Parent, Martin, and Laurent Descarries. 2008. "Acetylcholine Innervation of the Adult Rat Thalamus:

Distribution and Ultrastructural Features in Dorsolateral Geniculate, Parafascicular, and Reticular Thalamic Nuclei." *Journal of Comparative Neurology* 511(5):678–91. doi: 10.1002/cne.21868.

Pascoli, Vincent, Jean Terrier, Agnès Hiver, and Christian Lüscher. 2015. "Sufficiency of Mesolimbic Dopamine Neuron Stimulation for the Progression to Addiction." *Neuron* 88(5):1054–66. doi: 10.1016/j.neuron.2015.10.017.

Paton, Joseph J., Marina A. Belova, Sara E. Morrison, and C. Daniel Salzman. 2006. "The Primate Amygdala Represents the Positive and Negative Value of Visual Stimuli during Learning." *Nature* 439(7078):865–70. doi: 10.1038/nature04490.

Pavlov (1927), P. Ivan. 2010. "Conditioned Reflexes: An Investigation of the Physiological Activity of the Cerebral Cortex." *Annals of Neurosciences* 17(3):136–41. doi: 10.5214/ans.0972-7531.1017309.

Paxinos, George, and Keith B. J. Franklin. 2001. *The Mouse Brain in Stereotaxic Coordinates, Second Edition*. 2◦ edição. San Diego: Academic Press.

Peciña, Susana, Kyle S. Smith, and Kent C. Berridge. 2006. "Hedonic Hot Spots in the Brain." *The Neuroscientist: A Review Journal Bringing Neurobiology, Neurology and Psychiatry* 12(6):500–511. doi: 10.1177/1073858406293154.

Pereira, Pedro A., Joana Coelho, Ana Silva, and M. Dulce Madeira. 2021. "Effects of Aging on the Cholinergic Innervation of the Rat Ventral Tegmental Area: A Stereological Study." *Experimental Gerontology* 148:111298. doi: 10.1016/j.exger.2021.111298.

Pereira, Pedro A., Eugénio Gonçalves, Ana Silva, Tiago Millner, and M. Dulce Madeira. 2020. "Effects of Chronic Alcohol Consumption and Withdrawal on the Cholinergic Neurons of the Pedunculopontine and Laterodorsal Tegmental Nuclei of the Rat: An Unbiased Stereological Study." *NeuroToxicology* 76:58–66. doi: 10.1016/j.neuro.2019.10.005.

Pfarr, Simone, Laura Schaaf, Janine K. Reinert, Elisabeth Paul, Frank Herrmannsdörfer, Martin Roßmanith, Thomas Kuner, Anita C. Hansson, Rainer Spanagel, Christoph Körber, and Wolfgang H. Sommer. 2018. "Choice for Drug or Natural Reward Engages Largely Overlapping Neuronal Ensembles in the Infralimbic Prefrontal Cortex." *The Journal of Neuroscience* 38(14):3507–19. doi: 10.1523/JNEUROSCI.0026-18.2018.

Pierce, R. Christopher, and Vidhya Kumaresan. 2006. "The Mesolimbic Dopamine System: The Final Common Pathway for the Reinforcing Effect of Drugs of Abuse?" *Neuroscience and Biobehavioral Reviews* 30(2):215–38. doi: 10.1016/j.neubiorev.2005.04.016.

Prieto-Garcia, Luna, Emil Egecioglu, Erik Studer, Lars Westberg, and Elisabet Jerlhag. 2015. *Psychoneuroendocrinology* 62:392–402. doi: 10.1016/j.psyneuen.2015.09.009.

Puranik, Amit, Nicole Buie, Dena Arizanovska, Paul Vezina, and Stephan Steidl. 2022. "Glutamate Inputs from the Laterodorsal Tegmental Nucleus to the Ventral Tegmental Area Are Essential for the Induction of Cocaine Sensitization in Male Mice." *Psychopharmacology*. doi: 10.1007/s00213-022-06209-2.

Rawls, Eric, and Connie Lamm. 2021. "The Aversion Positivity: Mediofrontal Cortical Potentials Reflect Parametric Aversive Prediction Errors and Drive Behavioral Modification Following Negative Reinforcement." *Cortex; a Journal Devoted to the Study of the Nervous System and Behavior* 140:26–39. doi: 10.1016/j.cortex.2021.03.012.

Redila, Van, Chantelle Kinzel, Yong Sang Jo, Corey B. Puryear, and Sheri J. Y. Mizumori. 2015. "A Role for the Lateral Dorsal Tegmentum in Memory and Decision Neural Circuitry." *Neurobiology of Learning and Memory* 117:93–108. doi: 10.1016/j.nlm.2014.05.009.

Redondo, Roger L., Joshua Kim, Autumn L. Arons, Steve Ramirez, Xu Liu, and Susumu Tonegawa. 2014. "Bidirectional Switch of the Valence Associated with a Hippocampal Contextual Memory Engram." *Nature* 513(7518):426–30. doi: 10.1038/nature13725.

Reijmers, Leon G., Brian L. Perkins, Naoki Matsuo, and Mark Mayford. 2007. "Localization of a Stable Neural Correlate of Associative Memory." *Science (New York, N.Y.)* 317(5842):1230–33. doi: 10.1126/science.1143839.

Reiner, David J., Rosa M. Leon, Lauren E. McGrath, Kieran Koch-Laskowski, Joel D. Hahn, Scott E. Kanoski, Elizabeth G. Mietlicki-Baase, and Matthew R. Hayes. 2018. "Glucagon-Like Peptide-1 Receptor Signaling in the Lateral Dorsal Tegmental Nucleus Regulates Energy Balance." *Neuropsychopharmacology* 43(3):627–37. doi: 10.1038/npp.2017.225.

Reiner, David J., Elizabeth G. Mietlicki-Baase, Diana R. Olivos, Lauren E. McGrath, Derek J. Zimmer, Kieran Koch-Laskowski, Joanna Krawczyk, Christopher A. Turner, Emily E. Noble, Joel D. Hahn,

Heath D. Schmidt, Scott E. Kanoski, and Matthew R. Hayes. 2017. "Amylin Acts in the Lateral Dorsal Tegmental Nucleus to Regulate Energy Balance Through Gamma-Aminobutyric Acid Signaling." *Biological Psychiatry* 82(11):828–38. doi: 10.1016/j.biopsych.2016.12.028.

Ren, Jing, Chang Qin, Fei Hu, Jie Tan, Li Qiu, Shengli Zhao, Guoping Feng, and Minmin Luo. 2011. "Habenula 'Cholinergic' Neurons Co-Release Glutamate and Acetylcholine and Activate Postsynaptic Neurons via Distinct Transmission Modes." *Neuron* 69(3):445–52. doi: 10.1016/j.neuron.2010.12.038.

Roberts, David C. S., Drake Morgan, and Yu Liu. 2007. "How to Make a Rat Addicted to Cocaine." *Progress in Neuro-Psychopharmacology & Biological Psychiatry* 31(8):1614–24. doi: 10.1016/j.pnpbp.2007.08.028.

Robledo, P., R. Maldonado-Lopez, and G. F. Koob. 1992. "Role of Dopamine Receptors in the Nucleus Accumbens in the Rewarding Properties of Cocaine." *Annals of the New York Academy of Sciences* 654:509–12. doi: 10.1111/j.1749-6632.1992.tb26015.x.

Roitman, Mitchell F., Robert A. Wheeler, and Regina M. Carelli. 2005. "Nucleus Accumbens Neurons Are Innately Tuned for Rewarding and Aversive Taste Stimuli, Encode Their Predictors, and Are Linked to Motor Output." *Neuron* 45(4):587–97. doi: 10.1016/j.neuron.2004.12.055.

Roy, Dheeraj S., Young-Gyun Park, Minyoung E. Kim, Ying Zhang, Sachie K. Ogawa, Nicholas DiNapoli, Xinyi Gu, Jae H. Cho, Heejin Choi, Lee Kamentsky, Jared Martin, Olivia Mosto, Tomomi Aida, Kwanghun Chung, and Susumu Tonegawa. 2022. "Brain-Wide Mapping Reveals That Engrams for a Single Memory Are Distributed across Multiple Brain Regions." *Nature Communications* 13:1799. doi: 10.1038/s41467-022-29384-4.

Russell, James A. 1980. "A Circumplex Model of Affect." *Journal of Personality and Social Psychology* 39(6):1161–78. doi: 10.1037/h0077714.

Russo, Scott J., and Eric J. Nestler. 2013. "The Brain Reward Circuitry in Mood Disorders." *Nature Reviews Neuroscience* 14(9):609–25. doi: 10.1038/nrn3381.

Sagar, S. M., F. R. Sharp, and T. Curran. 1988. "Expression of C-Fos Protein in Brain: Metabolic Mapping at the Cellular Level." *Science (New York, N.Y.)* 240(4857):1328–31. doi: 10.1126/science.3131879.

Sakurai, Katsuyasu, Shengli Zhao, Jun Takatoh, Erica Rodriguez, Jinghao Lu, Andrew D. Leavitt, Min Fu, Bao-Xia Han, and Fan Wang. 2016. "Capturing and Manipulating Activated Neuronal Ensembles with CANE Delineates a Hypothalamic Social-Fear Circuit." *Neuron* 92(4):739–53. doi: 10.1016/j.neuron.2016.10.015.

Satoh, K., and H. C. Fibiger. 1985. "Distribution of Central Cholinergic Neurons in the Baboon (Papio Papio). I. General Morphology." *The Journal of Comparative Neurology* 236(2):197–214. doi: 10.1002/cne.902360205.

Satoh, K., and H. C. Fibiger. 1986. "Cholinergic Neurons of the Laterodorsal Tegmental Nucleus: Efferent and Afferent Connections." *The Journal of Comparative Neurology* 253(3):277–302. doi: 10.1002/cne.902530302.

Saunders, Arpiar, Ian A. Oldenburg, Vladimir K. Berezovskii, Caroline A. Johnson, Nathan D. Kingery, Hunter L. Elliott, Tiao Xie, Charles R. Gerfen, and Bernardo L. Sabatini. 2015. "A Direct GABAergic Output from the Basal Ganglia to Frontal Cortex." *Nature* 521(7550):85–89. doi: 10.1038/nature14179.

Scheres, Anouk, Michael P. Milham, Brian Knutson, and Francisco Xavier Castellanos. 2007. "Ventral Striatal Hyporesponsiveness During Reward Anticipation in Attention-Deficit/Hyperactivity Disorder." *Biological Psychiatry* 61(5):720–24. doi: 10.1016/j.biopsych.2006.04.042.

Schindelin, Johannes, Ignacio Arganda-Carreras, Erwin Frise, Verena Kaynig, Mark Longair, Tobias Pietzsch, Stephan Preibisch, Curtis Rueden, Stephan Saalfeld, Benjamin Schmid, Jean-Yves Tinevez, Daniel James White, Volker Hartenstein, Kevin Eliceiri, Pavel Tomancak, and Albert Cardona. 2012. "Fiji - an Open Source Platform for Biological Image Analysis." *Nature Methods* 9(7):10.1038/nmeth.2019. doi: 10.1038/nmeth.2019.

Schlaepfer, Thomas E., Bettina H. Bewernick, Sarah Kayser, Rene Hurlemann, and Volker A. Coenen. 2014. "Deep Brain Stimulation of the Human Reward System for Major Depression—Rationale, Outcomes and Outlook." *Neuropsychopharmacology* 39(6):1303–14. doi: 10.1038/npp.2014.28.

Schmidt, Heath D., Katie R. Famous, and R. C. Pierce. 2009. "The Limbic Circuitry Underlying Cocaine Seeking Encompasses the PPTg/LDT." *European Journal of Neuroscience* 30(7):1358–69. doi:

10.1111/j.1460-9568.2009.06904.x.

Schoenbaum, Geoffrey, Andrea A. Chiba, and Michela Gallagher. 1999. "Neural Encoding in Orbitofrontal Cortex and Basolateral Amygdala during Olfactory Discrimination Learning." *The Journal of Neuroscience* 19(5):1876–84. doi: 10.1523/JNEUROSCI.19-05-01876.1999.

Schultz, Wolfram. 2013. "Updating Dopamine Reward Signals." *Current Opinion in Neurobiology* 23(2):229–38. doi: 10.1016/j.conb.2012.11.012.

Semba, K., and H. C. Fibiger. 1992. "Afferent Connections of the Laterodorsal and the Pedunculopontine Tegmental Nuclei in the Rat: A Retro- and Antero-Grade Transport and Immunohistochemical Study." *The Journal of Comparative Neurology* 323(3):387–410. doi: 10.1002/cne.903230307.

Shabani, S., R. Foster, N. Gubner, TJ Phillips, and GP Mark. 2010. "Muscarinic Type 2 Receptors in the Lateral Dorsal Tegmental Area Modulate Cocaine and Food Seeking Behavior in Rats." *Neuroscience* 170(2):559–69. doi: 10.1016/j.neuroscience.2010.07.028.

Shabel, Steven J., and Patricia H. Janak. 2009. "Substantial Similarity in Amygdala Neuronal Activity during Conditioned Appetitive and Aversive Emotional Arousal." *Proceedings of the National Academy of Sciences of the United States of America* 106(35):15031–36. doi: 10.1073/pnas.0905580106.

Shen, Li, Guang-Wei Zhang, Can Tao, Michelle B. Seo, Nicole K. Zhang, Junxiang J. Huang, Li I. Zhang, and Huizhong W. Tao. 2022. "A Bottom-up Reward Pathway Mediated by Somatostatin Neurons in the Medial Septum Complex Underlying Appetitive Learning." *Nature Communications* 13(1):1194. doi: 10.1038/s41467-022-28854-z.

Sheng, M., and M. E. Greenberg. 1990. "The Regulation and Function of C-Fos and Other Immediate Early Genes in the Nervous System." *Neuron* 4(4):477–85. doi: 10.1016/0896-6273(90)90106-p.

Sherafat, Yasmine, Malia Bautista, J. P. Fowler, Edison Chen, Amina Ahmed, and Christie D. Fowler. 2020. "The Interpeduncular-Ventral Hippocampus Pathway Mediates Active Stress Coping and Natural Reward." *ENeuro* 7(6). doi: 10.1523/ENEURO.0191-20.2020.

Shi, Xunbei, Haohua Wei, Zeka Chen, Jing Wang, Weimin Qu, Zhili Huang, and Chunfu Dai. 2021. "Whole-

Brain Monosynaptic Inputs and Outputs of Glutamatergic Neurons of the Vestibular Nuclei Complex in Mice." *Hearing Research* 401:108159. doi: 10.1016/j.heares.2020.108159.

Shinohara, Fumiya, Yuta Asaoka, Hironori Kamii, Masabumi Minami, and Katsuyuki Kaneda. 2019. "Stress Augments the Rewarding Memory of Cocaine via the Activation of Brainstem-Reward Circuitry." *Addiction Biology* 24(3):509–21. doi: 10.1111/adb.12617.

Shinohara, Fumiya, Yukari Kihara, Soichiro Ide, Masabumi Minami, and Katsuyuki Kaneda. 2014. "Critical Role of Cholinergic Transmission from the Laterodorsal Tegmental Nucleus to the Ventral Tegmental Area in Cocaine-Induced Place Preference." *Neuropharmacology* 79:573–79. doi: 10.1016/j.neuropharm.2014.01.019.

Shpokayte, Monika, Olivia McKissick, Xiaonan Guan, Bingbing Yuan, Bahar Rahsepar, Fernando R. Fernandez, Evan Ruesch, Stephanie L. Grella, John A. White, X. Shawn Liu, and Steve Ramirez. 2022. "Hippocampal Cells Segregate Positive and Negative Engrams." *Communications Biology* 5:1009. doi: 10.1038/s42003-022-03906-8.

da Silveira, Lenise Trito Garcia, Cristina Moraes Junta, Nadia Monesi, Gabriela Ravanelli de Oliveira-Pelegrin, Geraldo Aleixo Passos, and Maria José A. Rocha. 2007. "Time Course of C-Fos, Vasopressin and Oxytocin MRNA Expression in the Hypothalamus Following Long-Term Dehydration." *Cellular and Molecular Neurobiology* 27(5):575–84. doi: 10.1007/s10571-007-9144-2.

Singh, Kavita, Simone Cauzzo, María Guadalupe García-Gomar, Matthew Stauder, Nicola Vanello, Claudio Passino, and Marta Bianciardi. 2022. "Functional Connectome of Arousal and Motor Brainstem Nuclei in Living Humans by 7 Tesla Resting-State FMRI." *NeuroImage* 249:118865. doi: 10.1016/j.neuroimage.2021.118865.

Small, D. M., R. J. Zatorre, A. Dagher, A. C. Evans, and M. Jones-Gotman. 2001. "Changes in Brain Activity Related to Eating Chocolate: From Pleasure to Aversion." *Brain: A Journal of Neurology* 124(Pt 9):1720–33. doi: 10.1093/brain/124.9.1720.

Soares-Cunha, Carina, Ana Verónica Domingues, Raquel Correia, Bárbara Coimbra, Natacha Vieitas-Gaspar, Nivaldo A. P. de Vasconcelos, Luísa Pinto, Nuno Sousa, and Ana João Rodrigues. 2022. "Distinct Role of Nucleus Accumbens D2-MSN Projections to Ventral Pallidum in Different Phases

of Motivated Behavior." *Cell Reports* 38(7):110380. doi: 10.1016/j.celrep.2022.110380.

Soares-Cunha, Carina, Nivaldo A. P. de Vasconcelos, Bárbara Coimbra, Ana Verónica Domingues, Joana M. Silva, Eduardo Loureiro-Campos, Rita Gaspar, Ioannis Sotiropoulos, Nuno Sousa, and Ana João Rodrigues. 2020. "Nucleus Accumbens Medium Spiny Neurons Subtypes Signal Both Reward and Aversion." *Molecular Psychiatry* 25(12):3241–55. doi: 10.1038/s41380-019-0484-3.

Sonnenberg, J. L., F. J. Rauscher, J. I. Morgan, and T. Curran. 1989. "Regulation of Proenkephalin by Fos and Jun." *Science (New York, N.Y.)* 246(4937):1622–25. doi: 10.1126/science.2512642.

Souza, Rudieri, Debora Bueno, Leandro B. Lima, Maria J. Muchon, Luciano Gonçalves, Jose Donato, Sara J. Shammah-Lagnado, and Martin Metzger. 2022. "Top-down Projections of the Prefrontal Cortex to the Ventral Tegmental Area, Laterodorsal Tegmental Nucleus, and Median Raphe Nucleus." *Brain Structure and Function*. doi: 10.1007/s00429-022-02538-2.

Stamatakis, Alice M., and Garret D. Stuber. 2012. "Activation of Lateral Habenula Inputs to the Ventral Midbrain Promotes Behavioral Avoidance." *Nature Neuroscience* 15(8):1105–7. doi: 10.1038/nn.3145.

Steidl, Stephan, Katherine M. Cardiff, and Roy A. Wise. 2015. "Increased Latencies to Initiate Cocaine Self-Administration Following Laterodorsal Tegmental Nucleus Lesions." *Behavioural Brain Research* 287:82–88. doi: 10.1016/j.bbr.2015.02.049.

Steidl, Stephan, Shannon O'Sullivan, Dustin Pilat, Nancy Bubula, Jason Brown, and Paul Vezina. 2017. "Operant Responding for Optogenetic Excitation of LDTg Inputs to the VTA Requires D1 and D2 Dopamine Receptor Activation in the NAcc." *Behavioural Brain Research* 333:161–70. doi: 10.1016/j.bbr.2017.06.045.

Steidl, Stephan, and Kevin Veverka. 2015. "Optogenetic Excitation of LDTg Axons in the VTA Reinforces Operant Responding in Rats." *Brain Research* 1614:86–93. doi: 10.1016/j.brainres.2015.04.021.

Steidl, Stephan, Huiling Wang, Marco Ordonez, Shiliang Zhang, and Marisela Morales. 2017. "Optogenetic Excitation in the Ventral Tegmental Area of Glutamatergic or Cholinergic Inputs from the Laterodorsal Tegmental Area Drives Reward." *The European Journal of Neuroscience*

45(4):559–71. doi: 10.1111/ejn.13436.

Steinberg, Elizabeth E., Felicity Gore, Boris D. Heifets, Madison D. Taylor, Zane C. Norville, Kevin T. Beier, Csaba Földy, Talia N. Lerner, Liqun Luo, Karl Deisseroth, and Robert C. Malenka. 2020. "Amygdala-Midbrain Connections Modulate Appetitive and Aversive Learning." *Neuron* 106(6):1026-1043.e9. doi: 10.1016/j.neuron.2020.03.016.

Steinkellner, Thomas, Ji Hoon Yoo, and Thomas S. Hnasko. 2019. "Differential Expression of VGLUT2 in Mouse Mesopontine Cholinergic Neurons." *ENeuro* 6(4):ENEURO.0161-19.2019. doi: 10.1523/ENEURO.0161-19.2019.

Stephenson-Jones, Marcus, Christian Bravo-Rivera, Sandra Ahrens, Alessandro Furlan, Xiong Xiao, Carolina Fernandes-Henriques, and Bo Li. 2020. "Opposing Contributions of GABAergic and Glutamatergic Ventral Pallidal Neurons to Motivational Behaviors." *Neuron* 105(5):921-933.e5. doi: 10.1016/j.neuron.2019.12.006.

Steriade, M., S. Datta, D. Pare, G. Oakson, and RC Curro Dossi. 1990. "Neuronal Activities in Brain-Stem Cholinergic Nuclei Related to Tonic Activation Processes in Thalamocortical Systems." *Journal of Neuroscience* 10(8):2541–59. doi: 10.1523/JNEUROSCI.10-08-02541.1990.

Steriade, M., D. Paré, A. Parent, and Y. Smith. 1988. "Projections of Cholinergic and Non-Cholinergic Neurons of the Brainstem Core to Relay and Associational Thalamic Nuclei in the Cat and Macaque Monkey." *Neuroscience* 25(1):47–67. doi: 10.1016/0306-4522(88)90006-1.

Sternat, Tia, and Martin A. Katzman. 2016. "Neurobiology of Hedonic Tone: The Relationship between Treatment-Resistant Depression, Attention-Deficit Hyperactivity Disorder, and Substance Abuse." *Neuropsychiatric Disease and Treatment* 12:2149–64. doi: 10.2147/NDT.S111818.

Streefland, C., E. Farkas, F. W. Maes, and B. Bohus. 1996. "C-Fos Expression in the Brainstem after Voluntary Ingestion of Sucrose in the Rat." *Neurobiology (Budapest, Hungary)* 4(1–2):85–102.

Struthers, William M., Aimee DuPriest, and Jason Runyan. 2005. "Habituation Reduces Novelty-Induced FOS Expression in the Striatum and Cingulate Cortex." *Experimental Brain Research* 167(1):136–40. doi: 10.1007/s00221-005-0061-7.

Takagishi, Masamitsu, and Tanemichi Chiba. 1991. "Efferent Projections of the Infralimbic (Area 25)

Region of the Medial Prefrontal Cortex in the Rat: An Anterograde Tracer PHA-L Study." *Brain Research* 566(1):26–39. doi: 10.1016/0006-8993(91)91677-S.

Tan, Hwei-Ee, Alexander C. Sisti, Hao Jin, Martin Vignovich, Miguel Villavicencio, Katherine S. Tsang, Yossef Goffer, and Charles S. Zuker. 2020. "The Gut–Brain Axis Mediates Sugar Preference." *Nature* 580(7804):511–16. doi: 10.1038/s41586-020-2199-7.

Tan, Kelly R., Cédric Yvon, Marc Turiault, Julie J. Mirzabekov, Jana Doehner, Gwenaël Labouèbe, Karl Deisseroth, Kay M. Tye, and Christian Lüscher. 2012. "GABA Neurons of the VTA Drive Conditioned Place Aversion." *Neuron* 73(6):1173–83. doi: 10.1016/j.neuron.2012.02.015.

Tanaka, Daisuke H., Shusheng Li, Shiori Mukae, and Tsutomu Tanabe. 2021a. "Genetic Recombination in Disgust-Associated Bitter Taste-Responsive Neurons of the Central Nucleus of Amygdala in Male Mice." *Neuroscience Letters* 742:135456. doi: 10.1016/j.neulet.2020.135456.

Tanaka, Daisuke H., Shusheng Li, Shiori Mukae, and Tsutomu Tanabe. 2021b. "Trap." *Neuroscience Letters* 742:135456. doi: 10.1016/j.neulet.2020.135456.

Tang, Wenqi, Danqing Zhou, Siyu Wang, Sijia Hao, Xiaomeng Wang, Mohamed Helmy, Junming Zhu, and Hao Wang. 2021. "CRH Neurons in the Laterodorsal Tegmentum Mediate Acute Stress-Induced Anxiety." *Neuroscience Bulletin* 37(7):999–1004. doi: 10.1007/s12264-021-00684-x.

Terreberry, Robert R., and Edward J. Neafsey. 1987. "The Rat Medial Frontal Cortex Projects Directly to Autonomic Regions of the Brainstem." *Brain Research Bulletin* 19(6):639–49. doi: 10.1016/0361-9230(87)90050-5.

Tilley, Michael R., Barbara Cagniard, Xiaoxi Zhuang, Dawn D. Han, Narry Tiao, and Howard H. Gu. 2007. "Cocaine Reward and Locomotion Stimulation in Mice with Reduced Dopamine Transporter Expression." *BMC Neuroscience* 8(1):42. doi: 10.1186/1471-2202-8-42.

Tovote, Philip, Jonathan Paul Fadok, and Andreas Lüthi. 2015. "Neuronal Circuits for Fear and Anxiety." *Nature Reviews Neuroscience* 16(6):317–31. doi: 10.1038/nrn3945.

Travers, Susan P. 2002. "Quinine and Citric Acid Elicit Distinctive Fos-like Immunoreactivity in the Rat Nucleus of the Solitary Tract." *American Journal of Physiology-Regulatory, Integrative and Comparative Physiology* 282(6):R1798–1810. doi: 10.1152/ajpregu.00590.2001.

Tsai, Hsing-Chen, Feng Zhang, Antoine Adamantidis, Garret D. Stuber, Antonello Bonci, Luis de Lecea, and Karl Deisseroth. 2009. "Phasic Firing in Dopaminergic Neurons Is Sufficient for Behavioral Conditioning." *Science (New York, N.Y.)* 324(5930):1080–84. doi: 10.1126/science.1168878.

Tye, Kay M. 2018. "Neural Circuit Motifs in Valence Processing." *Neuron* 100(2):436–52. doi: 10.1016/j.neuron.2018.10.001.

Tzschentke, Thomas M. 2007. "Measuring Reward with the Conditioned Place Preference (CPP) Paradigm: Update of the Last Decade." *Addiction Biology* 12(3–4):227–462. doi: 10.1111/j.1369-1600.2007.00070.x.

Uddin, Lucina Q. 2015. "Salience Processing and Insular Cortical Function and Dysfunction." *Nature Reviews. Neuroscience* 16(1):55–61. doi: 10.1038/nrn3857.

Vallöf, Daniel, Aimilia Lydia Kalafateli, and Elisabet Jerlhag. 2019. "Brain Region Specific Glucagon-like Peptide-1 Receptors Regulate Alcohol-Induced Behaviors in Rodents." *Psychoneuroendocrinology* 103:284–95. doi: 10.1016/j.psyneuen.2019.02.006.

Vander Weele, Caitlin M., Cody A. Siciliano, Gillian A. Matthews, Praneeth Namburi, Ehsan M. Izadmehr, Isabella C. Espinel, Edward H. Nieh, Evelien H. S. Schut, Nancy Padilla-Coreano, Anthony Burgos-Robles, Chia-Jung Chang, Eyal Y. Kimchi, Anna Beyeler, Romy Wichmann, Craig P. Wildes, and Kay M. Tye. 2018. "Dopamine Enhances Signal-to-Noise Ratio in Cortical-Brainstem Encoding of Aversive Stimuli." *Nature* 563(7731):397–401. doi: 10.1038/s41586-018-0682-1.

Vertes, Robert P. 2004. "Differential Projections of the Infralimbic and Prelimbic Cortex in the Rat." *Synapse (New York, N.Y.)* 51(1):32–58. doi: 10.1002/syn.10279.

Vestlund, Jesper, and Elisabet Jerlhag. 2020. "The Glucagon-like Peptide-1 Receptor Agonist, Exendin-4, Reduces Sexual Interaction Behaviors in a Brain Site-Specific Manner in Sexually Naïve Male Mice." *Hormones and Behavior* 124:104778. doi: 10.1016/j.yhbeh.2020.104778.

Vincent, S. R., and P. B. Reiner. 1987. "The Immunohistochemical Localization of Choline Acetyltransferase in the Cat Brain." *Brain Research Bulletin* 18(3):371–415. doi: 10.1016/0361-9230(87)90015-3.

Volkow, Nora D., and Marisela Morales. 2015. "The Brain on Drugs: From Reward to Addiction." *Cell*

162(4):712–25. doi: 10.1016/j.cell.2015.07.046.

Wall, Nicholas R., Peter A. Neumann, Kevin T. Beier, Ava K. Mokhtari, Liqun Luo, and Robert C. Malenka. 2019. "Complementary Genetic Targeting and Monosynaptic Input Mapping Reveal Recruitment and Refinement of Distributed Corticostriatal Ensembles by Cocaine." *Neuron* 104(5):916-930.e5. doi: 10.1016/j.neuron.2019.10.032.

Wang, Hui-Ling, and Marisela Morales. 2009. "Pedunculopontine and Laterodorsal Tegmental Nuclei Contain Distinct Populations of Cholinergic, Glutamatergic and GABAergic Neurons in the Rat." *The European Journal of Neuroscience* 29(2):340–58. doi: 10.1111/j.1460-9568.2008.06576.x.

Wang, Shijing, Francesco Leri, and Sakina J. Rizvi. 2021. "Anhedonia as a Central Factor in Depression: Neural Mechanisms Revealed from Preclinical to Clinical Evidence." *Progress in Neuro-Psychopharmacology & Biological Psychiatry* 110:110289. doi: 10.1016/j.pnpbp.2021.110289.

Wang, Wenjing, Craig P. Wildes, Tanyaporn Pattarabanjird, Mateo I. Sanchez, Gordon F. Glober, Gillian A. Matthews, Kay M. Tye, and Alice Y. Ting. 2017. "A Light- and Calcium-Gated Transcription Factor for Imaging and Manipulating Activated Neurons." *Nature Biotechnology* 35(9):864–71. doi: 10.1038/nbt.3909.

Wang, Xiaomeng, Hongbin Yang, Libiao Pan, Sijia Hao, Xiaotong Wu, Li Zhan, Yijun Liu, Fan Meng, Huifang Lou, Ying Shen, Shumin Duan, and Hao Wang. 2019. "Brain-Wide Mapping of Mono-Synaptic Afferents to Different Cell Types in the Laterodorsal Tegmentum." *Neuroscience Bulletin* 35(5):781–90. doi: 10.1007/s12264-019-00397-2.

Whitaker, Leslie R., and Bruce T. Hope. 2018. "Chasing the Addicted Engram: Identifying Functional Alterations in Fos-Expressing Neuronal Ensembles That Mediate Drug-Related Learned Behavior." *Learning & Memory* 25(9):455–60. doi: 10.1101/lm.046698.117.

White, Norman M., Mark G. Packard, and Noboru Hiroi. 1991. "Place Conditioning with Dopamine D1 and D2 Agonists Injected Peripherally or into Nucleus Accumbens." *Psychopharmacology* 103(2):271–76. doi: 10.1007/BF02244216.

Williams, Victoria M., Adhil Bhagwandin, Jordan Swiegers, Mads F. Bertelsen, Therese Hård, Chet C. Sherwood, and Paul R. Manger. 2022. "Distribution of Cholinergic Neurons in the Brains of a Lar

Gibbon and a Chimpanzee." *Anatomical Record (Hoboken, N.J.: 2007)* 305(6):1516–35. doi: 10.1002/ar.24844.

Wise, Roy A. 2004. "Dopamine, Learning and Motivation." *Nature Reviews. Neuroscience* 5(6):483–94. doi: 10.1038/nrn1406.

Wolfman, Shannon L., Daniel F. Gill, Fili Bogdanic, Katie Long, Ream Al-Hasani, Jordan G. McCall, Michael R. Bruchas, and Daniel S. McGehee. 2018. "Nicotine Aversion Is Mediated by GABAergic Interpeduncular Nucleus Inputs to Laterodorsal Tegmentum." *Nature Communications* 9:2710. doi: 10.1038/s41467-018-04654-2.

Woolf, Nancy J., and Larry L. Butcher. 1986. "Cholinergic Systems in the Rat Brain: III. Projections from the Pontomesencephalic Tegmentum to the Thalamus, Tectum, Basal Ganglia, and Basal Forebrain." *Brain Research Bulletin* 16(5):603–37. doi: 10.1016/0361-9230(86)90134-6.

Wu, Ye Emily, Lin Pan, Yanning Zuo, Xinmin Li, and Weizhe Hong. 2017. "Detecting Activated Cell Populations Using Single-Cell RNA-Seq." *Neuron* 96(2):313-329.e6. doi: 10.1016/j.neuron.2017.09.026.

Xiao, Cheng, Jounhong Ryan Cho, Chunyi Zhou, Jennifer B. Treweek, Ken Chan, Sheri L. McKinney, Bin Yang, and Viviana Gradinaru. 2016. "Cholinergic Mesopontine Signals Govern Locomotion and Reward through Dissociable Midbrain Pathways." *Neuron* 90(2):333–47. doi: 10.1016/j.neuron.2016.03.028.

Xing, Bo, Nancy R. Mack, Kai-Ming Guo, Yu-Xiang Zhang, Billy Ramirez, Sha-Sha Yang, Li Lin, Dong V. Wang, Yan-Chun Li, and Wen-Jun Gao. 2021. "A Subpopulation of Prefrontal Cortical Neurons Is Required for Social Memory." *Biological Psychiatry* 89(5):521–31. doi: 10.1016/j.biopsych.2020.08.023.

Xiu, Jianbo, Qi Zhang, Tao Zhou, Ting-ting Zhou, Yang Chen, and Hailan Hu. 2014. "Visualizing an Emotional Valence Map in the Limbic Forebrain by TAI-FISH." *Nature Neuroscience* 17(11):1552–59. doi: 10.1038/nn.3813.

Xu, Mengsi, Zhiai Li, Cody Ding, Junhua Zhang, Lingxia Fan, Liuting Diao, and Dong Yang. 2015. "The Divergent Effects of Fear and Disgust on Inhibitory Control: An ERP Study." *PLOS ONE* 10(6):e0128932. doi: 10.1371/journal.pone.0128932.

Yang, Hongbin, Junhua Yang, Wang Xi, Sijia Hao, Benyan Luo, Xiaobin He, Liya Zhu, Huifang Lou, Yan-qin Yu, Fuqiang Xu, Shumin Duan, and Hao Wang. 2016. "Laterodorsal Tegmentum Interneuron Subtypes Oppositely Regulate Olfactory Cue-Induced Innate Fear." *Nature Neuroscience* 19(2):283–89. doi: 10.1038/nn.4208.

Ye, Li, William E. Allen, Kimberly R. Thompson, Qiyuan Tian, Brian Hsueh, Charu Ramakrishnan, Ai-Chi Wang, Joshua H. Jennings, Avishek Adhikari, Casey H. Halpern, Ilana B. Witten, Alison L. Barth, Liqun Luo, Jennifer A. McNab, and Karl Deisseroth. 2016. "Wiring and Molecular Features of Prefrontal Ensembles Representing Distinct Experiences." *Cell* 165(7):1776–88. doi: 10.1016/j.cell.2016.05.010.

Yokel, R. A., and R. A. Wise. 1975. "Increased Lever Pressing for Amphetamine after Pimozide in Rats: Implications for a Dopamine Theory of Reward." *Science (New York, N.Y.)* 187(4176):547–49. doi: 10.1126/science.1114313.

Zahm, Daniel S., Mary L. Becker, Alexander J. Freiman, Sara Strauch, Beth DeGarmo, Stefanie Geisler, Gloria E. Meredith, and Michela Marinelli. 2010. "Fos After Single and Repeated Self-Administration of Cocaine and Saline in the Rat: Emphasis on the Basal Forebrain and Recalibration of Expression." *Neuropsychopharmacology* 35(2):445–63. doi: 10.1038/npp.2009.149.

Zhang, Guang-Wei, Li Shen, Wen Zhong, Ying Xiong, Li I. Zhang, and Huizhong W. Tao. 2018. "Transforming Sensory Cues into Aversive Emotion via Septal-Habenular Pathway." *Neuron* 99(5):1016-1028.e5. doi: 10.1016/j.neuron.2018.07.023.

Zhang, Xian, Wuqiang Guan, Tao Yang, Alessandro Furlan, Xiong Xiao, Kai Yu, Xu An, William Galbavy, Charu Ramakrishnan, Karl Deisseroth, Kimberly Ritola, Adam Hantman, Miao He, Z. Josh Huang, and Bo Li. 2021. "Genetically Identified Amygdala-Striatal Circuits for Valence-Specific Behaviors." *Nature Neuroscience* 24(11):1586–1600. doi: 10.1038/s41593-021-00927-0.

Zhang, Xian, and Bo Li. 2018. "Population Coding of Valence in the Basolateral Amygdala." *Nature Communications* 9(1):5195. doi: 10.1038/s41467-018-07679-9.

Zhang, Yong, John R. Mantsch, Stefan D. Schlussman, Ann Ho, and Mary Jeanne Kreek. 2002. "Conditioned Place Preference after Single Doses or 'Binge' Cocaine in C57BL/6J and 129/J

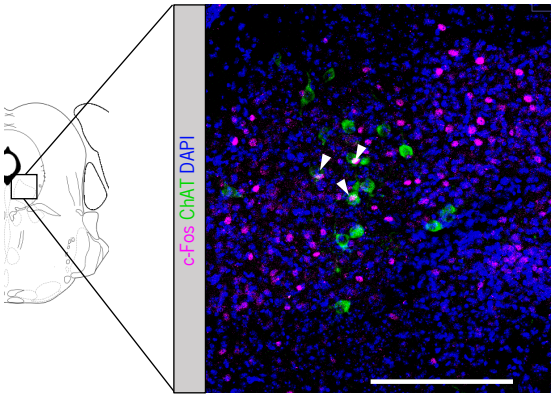
Mice." *Pharmacology, Biochemistry, and Behavior* 73(3):655–62. doi: 10.1016/s0091-3057(02)00859-6.

Zhao, Peilin, Huading Wang, Anan Li, Qingtao Sun, Tao Jiang, Xiangning Li, and Hui Gong. 2022. "The Mesoscopic Connectome of the Cholinergic Pontomesencephalic Tegmentum." *Frontiers in Neuroanatomy* 16.

Zweifel, Larry S., Emanuela Argilli, Antonello Bonci, and Richard D. Palmiter. 2008. "Role of NMDA Receptors in Dopamine Neurons for Plasticity and Addictive Behaviors." *Neuron* 59(3):486–96. doi: 10.1016/j.neuron.2008.05.028.

7. Annexes

Annex 1 – Representative image showing c-Fos and ChAT staining overlap. Arrows indicate double positive cells. Scale bar 200 μm.



Annex 2 – Representative image showing tdTomato expression in the LDT of tamoxifen-dependence recombination control group (NO-4OHT). Scale bar 200 μm.

